Commissariat à l'énergie atomique
Centre de Cadarache - 13108 St Paul lez Durance Cedex – France
Tél 33 (0)4 42 25 6222 - Fax 33 (0)4 42 25 6233
Email : dirsccp@cea.fr

Association EURATOM-CEA

Direction des sciences de la matière
Département de recherches sur la fusion contrôlée
Service chauffage et confinement du plasma

Activité	PHYSIQUE
Nature	**NOTE DE TRAVAIL**
Référence	**PHY/NTT-2008.001**
Titre	**METIS User's Guide**
Auteur(s)	J.F. Artaud
Résumé	This document provides the technical description of the METIS code. METIS is a fast integrated tokamak simulation tool for the CRONOS suite. This document includes the code description, physical models description, graphical user interface manual and data set description. METIS is an acronym for : **M**inute **E**mbedded **T**okamak **I**ntegrated **S**imulator.
Annexe (s)	
Destinataires :	

Visa Rédacteur	Visa Vérificateur	Visa Qualité, Structure	Visa émetteur
J.F. Artaud	G. Giruzzi		A. Becoulet
date :	date :	date :	date : signé le

Table of contents

1- Introduction

1.1- Preamble

This document provides the technical description of the METIS code. METIS is a fast integrated tokamak simulation tool for the CRONOS suite. This document includes description of the code, of the physical models used, of the data set, as well as the graphical user interface manual.

METIS is an acronym for : **M**inute **E**mbedded **T**okamak **I**ntegrated **S**imulator.

1.2- Motivation

The principal difficulties with the 1D½ simulation of tokamak plasma discharges (as made , e.g., with the CRONOS suite of codes *[Basiuk03]*) are related to:

- the lack of precise description of the transport coefficient in the presence of turbulence and MHD activity.
- the computing time necessary to perform the simulation , especially if the sources (current, heat, matter, momentum,...) are self-consistently evaluated.
- the numerical instabilities or poor convergence that often occur in complex simulations.

The METIS code has been developed to simulate tokamak plasma evolution using information coming from scaling laws coupled with simplified source models and using an almost always convergent computing scheme that allows to simulate a full plasma discharge in a time of the order of one minute.

1.3- Purpose

The METIS code is designed as a fast (cpu time < 1 minute per run) ,versatile tokamak simulator. It describes any time dependent scenario, including all current and heat sources. The fusion products and effects are described with a particular care. The METIS code includes a full fast current diffusion solver. It is a mix of 0 dimension laws and 1.5 dimension equations; it takes into account various non-linear couplings between physical quantities.
It is designed for :

- Fast shot analysis : the METIS code can provide a first shot simulation just after the end of the shot, when experimental data are available.
- Scenario design : during the preparation of the experiment, METIS can provide help to design the scheme of the shot and evaluate the effect of parameter change. It permits a great number of tries in a short time.
- CRONOS simulation preparation : METIS is useful during the preparation of CRONOS simulations. Since it can use directly the CRONOS data set to perform a run , it provides a way to check the data set before running the simulation
- CRONOS simulation verification : after a full 1,5 D simulation and especially if this is not the simulation of an existent tokamak shot, METIS allows to verify the coherence of results.
- Non existent tokamak projection : METIS allows to predict some key physical values for future tokamaks (it has already been used for SST1,ITER, EAST, FT3) . It is also useful for designing a new tokamak.
- METIS can be used for controllers development when it is used jointly with Simulink (http://www.mathworks.com/products/simulink/).

1.4- Basic Features

METIS includes a complete current diffusion solver (as in CRONOS but on a 21 points radial grid only). The MHD equilibrium is computed using a fast solver based on moments of the Grad-Shafranov equation *[Blank1, Blank2, Lao1]*. The bootstrap current and resistivity are computed using the Sauter formulation *[Sauter]*. The shapes of the current sources are based on simplified analytical formulations and efficiencies are given either by a scaling law (Fast Wave Current Drive), an analytical prescription (L*ower* H*ybrid*), analytical Fokker-Planck 0D integration (N*eutral* B*eam* I*njection* C*urrent* D*rive*), or simplified adjoint method solution (E*lectron* C*yclotron* C*urrent* D*rive*).

The density profile is described by means of a peaking factor that is given by a scaling law or prescribed. The line-averaged density is prescribed and the edge density is given by a scaling law.

The energy content of the plasma is given by a scaling law that depends on the scenario. The 0D solver takes into account the time evolution (equations are solved using an ODE solver). The temperature profiles are computed using time-independent transport equations. Transport coefficients have a simple analytical shape (1 + a * x ^ 2) and are normalized to retrieve the correct energy content. The ratio between ion heat diffusion coefficient and electron heat diffusion coefficient ($\frac{\kappa_i}{\kappa_e}$) is prescribed. Shapes of the sources are computed with the help of analytical formulation. The NBI and ICRH (I*on* C*yclotron Resonance* H*eating*) deposition repartition on ions and electrons are computed using an analytical Fokker-Planck 0D solution *[Stix]*. The D-T fusion power is computed using realistic cross-sections.

The plasma composition is deduced from prescribed line average effective charge (Z_{eff}) and prescribed minority ion fraction. The accumulation of He ashes is taken into account separately.

The line radiation is computed on the basis of coronal equilibrium (Post's formulation), the bremsstrahlung is corrected for relativistic effects and the cyclotron radiation is computed following the Albajar scaling [Albajar01,Albajar02].

1.5- Organisation of this document

The 2nd Section describes the computational aspects of METIS. The 3rd Section describes the physics models implemented in METIS. The 4th Section illustrates the use of METIS. The 5th Section gives the link between METIS and CRONOS definitions. The 6th Section is the user manual of the graphical user interface of METIS. The 7th Section explains how to use METIS with Simulink. The 8th Section describes the data set of METIS (input and output). The 9th Section is the list of files that compose the METIS code. The 10th and final Section describes the computational aspects of the combination between METIS and Simulink.

2- The METIS code – computational aspects

2.1- Foreword on computer capabilities

The typical present-day personal computer allows to perform a great amount of calculations in a short time. 1D Ordinary differential equations, integral and special functions can be used without any strong restriction. Only complex calculations and partial differential equations (2D or higher dimension problems, such as equilibrium equations, ray tracing , particles following, ...) require too much time and cannot be included in a fast tokamak simulator. Nevertheless, the internal magnetic configuration of the plasma plays a key role in plasma properties. For this reason,we have added to METIS an MHD equilibrium computed using moments and a complete fast solver for the current diffusion equation.

2.2- Integration in the CRONOS suite of codes

The METIS tool is integrated in the CRONOS suite *[Basiuk03]*, but it can be used on a stand-alone basis. METIS is written in Matlab. This language authorizes a fast development and prototyping. A graphical user interface is readily developed with Matlab, and it very easy to make various plot or work with the data in command line. METIS has a graphical user interface that permits to edit the data, change the parameters, plot the results, and save, load or export the data. The details of the graphical user interface (GUI) are described in Section 6

2.3- Data sources

The input data of METIS are the temporal reference values for geometry (major radius R_{ref} , minor radius a_{ref} , elongation K_{ref} and trianlugarity δ_{ref}) , additional power (Lower Hybrid $P_{LH,ref}$, Electron Cyclotron Resonance Heating $P_{ECRH,ref}$, Fast Wave Electron Heating & Ion Cyclotron Resonance Heating $P_{ICRH,ref}$, Neutral Beam Injection $P_{NBI,ref}$) , toroidal magnetic field B_{ref} measured at R_{ref} , line-averaged electron density $\bar{n}_{ref}$, isotopic ratio between tritium density and deuterium density in plasma η_{ref} and in neutral beam injection ϕ_{ref} , the line-averaged effective charge $Z_{eff,ref}$ and the position of maximum deposition of ECRH $x_{ece,ref}$.

Either the plasma current I_p or the poloidal flux at the edge Ψ_{ref} can be specified.

To complete these references, METIS uses scalar input that allow to choose internal options such as scaling laws, current drive scheme, plasma composition. These options are summarised in Section 6.5.

METIS can read its input data from various data sources. The input data can be prescribed by the user. By this way, any tokamak can be considered.

The already implemented data sources are :

- Tore Supra direct database access via the library TSLib
- JET database access via MDS+
- CRONOS data set

All the data can be edited with the graphical user interface at any moment. It is also possible to add access to other tokamak data bases.

2.4- Exportation of results

The results of the METIS simulation are available in the Matlab workspace and can be saved in a mat file. If METIS is run inside the CRONOS suite, the METIS data are saved together with the CRONOS data set.

From the METIS data set it is also possible to create an input data set for CRONOS. The profiles used in the data set are deduced from the internal description of METIS. The METIS data set is described in details in Section 8.

2.5- Algorithm and computing time

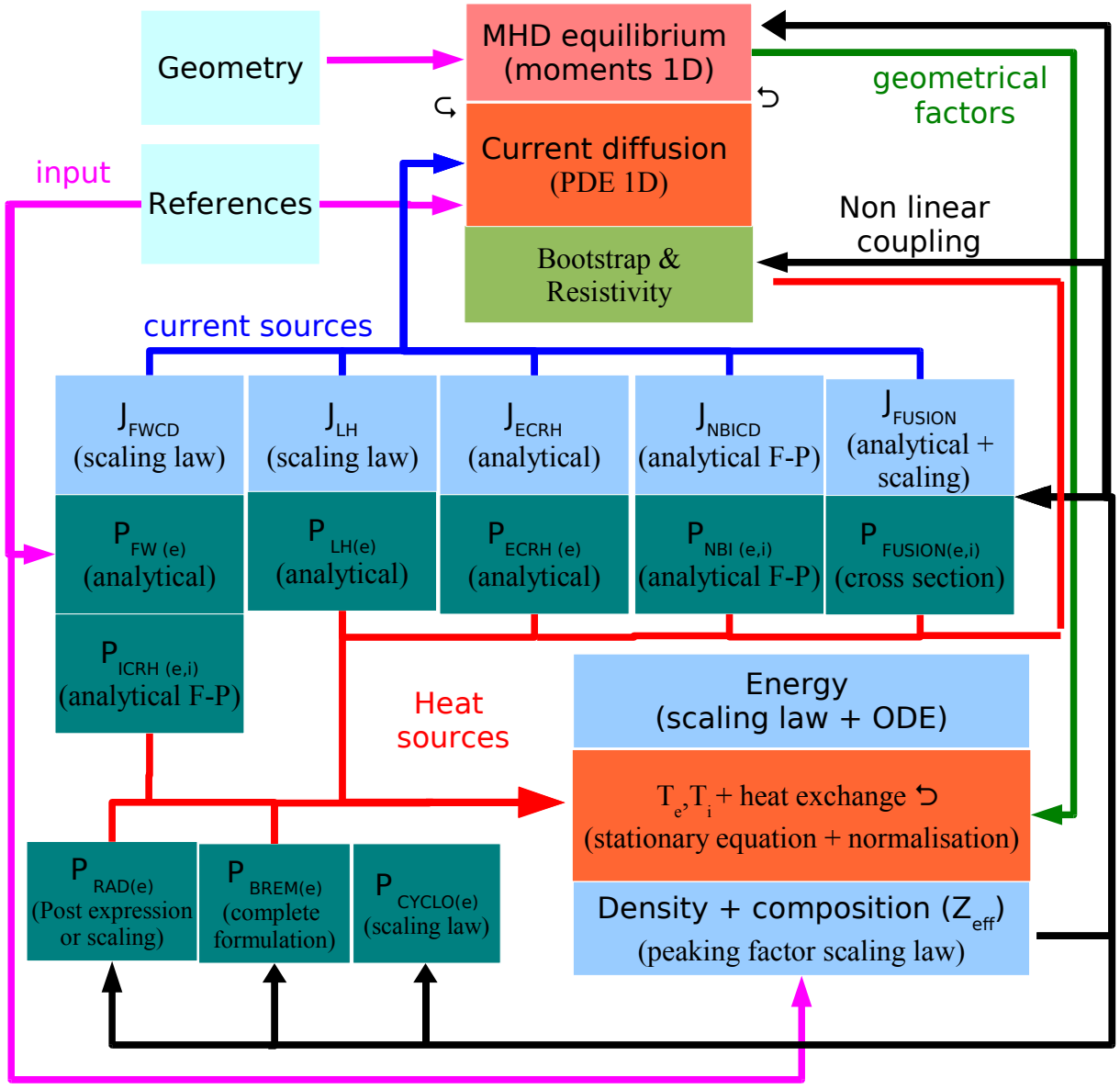

figure 1 : main connections and dependences between computing blocks in "zero1t.m" function.

In METIS, a "waveform relaxation" like algorithm is used for the main convergence loop and all the PDEs are solved by artificially separating time and space. Only the PDE for current diffusion is completely solved.

A METIS run begins by the initialisation of data structures (scalars and profiles). A first guess of the value is computed using very coarse approximations (see Section 3.20). This first guess allows to enter the main convergence loop.

The main convergence loop of successive guesses consists of the simple damping equation :
$g_{n+1}=\alpha_n F(g_n)+(1-\alpha_n)g_n$ where n is the loop index, F(g) is the central METIS function and

α is the damping factor. We have chosen : $\alpha_{n+1}=0.95\,\alpha_n$ for the 21 first loops and $\alpha_{n+1}=0.9\,\alpha_n$ later on. The maximum number of iterations is 31. The loop terminates when the relative change between $F(g_n)$ and g_n is smaller than a requested value (10^{-2} in fast computation mode and 10^{-3} in complete computation mode).

The central function of METIS "zero1t.m" computes from input parameters and from the previous guess a new guess of data for all the time slices. The figure 1 shows main connections and dependences between computing blocks. The order of evaluation is very important for numerical stability.

The computing order in "zero1t.m" function is the following :

1. geometry update (computes volume, surfaces and lengths with Last Closed Magnetic Surface parameters)
2. subtracts shinethrough and first orbit losses from NBI and ICRH references
3. computes ripple losses (if necessary) and subtracts from references
4. computes P_{loss} and P_{in}
5. computes supra-thermal energy contents of fast ions and integrates the slowing down ODE to compute thermal power sources.
6. computes ion thermal power sources for NBI, fast alphas and fast ions produced by ICRH.
7. scaling law computation for energy and L to H mode transition
8. confinement mode determination (L or H) and transition management
9. inclusion of ITB and internal inductance (l_i) effect on confinement time.
10. top pedestal pressure computation (including MHD pressure limitation).
11. energy contents computation (thermal and total) and energy time derivative computation.
12. electron density profile peaking factor computation
13. average electron density computation solving ODE with matter confinement time.
14. edge density evaluation
15. ashes accumulation computation
16. impurity average density determination
17. solution of the steady state heat transport equation (including $\frac{\chi_i}{\chi_e}$ determination and a convergence loop on equipartition term)
18. edge temperature computation
19. coarse estimation of limiter or divertor temperature and density
20. peak power on divertor coarse estimation with scaling
21. Z_{eff} scaling evaluation
22. current sources computation :

- LHCD (including synergy with parallel electric field and with ECCD)
- FWCD total current computation
- ECCD total current computation

23. NBI sources computation :
    - Beam damping computation
    - pseudo Fokker-Planck equation for ion/electron deposition and current sources estimation
24. density profile computation (with edge ionisation source and transport coefficients estimation)
25. W_{dia} computation
26. ρ_{max} time derivative calculation (see ρ_{max} definition in section 3)
27. impurities and Z_{eff} profiles computation
28. equilibrium moments computation (Shafranov shift, elongation and triangularity profiles)
29. effective trapped particle fraction computation
30. resistivity and boostrap current profiles computation
31. LHCD current profile shape estimation
32. ECCD and FWCD current profile estimation
33. Fast alpha particle “boostrap like” current profile estimation
34. runaway electron current profile estimation
35. flux surface shape computation (including morphing to LCMS)
36. flux average quantities computation (C2, C3, ...)
37. when required, initial Ψ profile computation (with given I_p and l_i)
38. Lao to toroidal flux coordinate transformation
39. resolution of current diffusion PDE.
40. computation of profiles link to Ψ , as safety factor , current density, ...
41. toroidal flux to Lao coordinate transformation
42. heat sources profiles computation
43. when required, ITB effect computation (on energy and transport coefficients shape)
44. disruption indicator calculation
45. DT fusion calculations (power, H_e source, neutron, ...) with, when required, TAE broadening effect simulation.
46. DD reaction computation (plasma-plasma, beam-plasma, beam-beam)
47. radiative powers calculation.
48. at the last call, plasma rotation estimation

49. at the last call, when required, reactor cost estimation

3- METIS equations

3.1- Introduction

In METIS, we may choose, for each feature or physical quantity, the expression that provides the right precision (not necessarily the best) compatible with the other choices and that allows to keep the computation time at the required level. The best precision is given by the full CRONOS suite code.

In this paper, the international system units are taken for all the physical quantities , excepted temperature, that is in eV. We note : c the speed of light in vacuum; e the proton charge; μ_0 the permeability of free space; ϵ_0 the permittivity of free space; k the Boltzmann constant ; m_e the electron mass; m_p the proton mass.

We use the following conventions : all quantities with index “ini”, are initial values used in the convergence loop; and all quantities with index “ref” are external references given to METIS by the user.

3.2- Geometry approximation

METIS can use a description of plasma geometry given by moments (radii, elongation, triangularity, Shafranov shift, etc.) or by prescribed LMCS given by points. In this case many internal computations use only moments that are recomputed; but global quantities are directly computed from LMCS, and the equilibrium mesh is corrected using a morphing function in such a way that the current diffusion equation is solved using corrected geometrical coefficients.

3.2.1- Moments description

This is a simplified geometry description compared to the full equilibrium calculations used in CRONOS . The plasma last close magnetic surface (LMCS) is given by the moment description. The plasma is supposed to have a symmetry between up and down (in this case the morphing function is turned off). The LMCS equation, in the plan (R,Z) is :

$$R_{LCMS}(t,\theta) = R_{ref}(t) + a_{ref}(t)\cos(\theta + \tau_d \sin(\theta))$$
$$Z_{LCMS}(t,\theta) = K_{ref}(t)\, a_{ref}(t)\sin(\theta)$$

where

$$\tau_d = \arcsin(\delta_{ref})$$

with R_{ref} the major radius , a_{ref} is the minor radius, K_{ref} is the elongation (ratio of semi axis) and δ_{ref} is the triangularity of the plasma. The moments depend on the time (t).

A vertical offset, Z_{ref} ,is defined and can be used in graphics.

3.2.2- LCMS given by points

In this case the LCMS is given by a list of points $(R,Z)_k$. These points are used to recompute the moments and the global geometric quantities as defined above.

The moments are defined as :

$$a_{ref}=\frac{max(R)-min(R)}{2}$$

$$R_{ref}=\frac{max(R)+min(R)}{2}$$

$$Z_{ref}=Z_{R=max(R)}$$

$$K_{ref}=\frac{S_p}{\pi a_{ref}^2}$$

$\delta_{ref}=\sin(\tau_d)$ with $\tau_d=\frac{\tau_{d,u}+\tau_{d,l}}{2}$ and

$\tau_{d,u}=\left|\frac{acos(\frac{R_{Z=max(Z)}-R_{ref}}{a_{ref}})-|U_u|}{\sin(U_u)}\right|$ and $\tau_{d,l}=\left|\frac{acos(\frac{R_{Z=min(Z)}-R_{ref}}{a_{ref}})-|U_l|}{\sin(U_l)}\right|$, and

$U_u=atan((R_{Z=max(Z)}-R_{ref})+i(max(Z)-Z_{ref}))$ and

$U_l=atan((R_{Z=min(Z)}-R_{ref})+i(min(Z)-Z_{ref}))$

3.2.3- Global deduced geometric quantities

From this definition, all the useful geometrical quantities are directly evaluated at the beginning of the METIS calculation (with negligible impact on the computation time):

- the plasma volume :

$$V_p=-2\,pi\int_0^{2\pi} R\,Z\frac{\partial R}{\partial\theta}d\theta$$

- the surface of the plasma cross-section :

$$S_p=-\int_0^{2\pi} Z\frac{\partial R}{\partial\theta}d\theta$$

- the plasma external surface :

$$S_{ext}=2\,pi\int_0^{2\pi} R\sqrt{\frac{dR}{d\theta}^2+\frac{dZ}{d\theta}^2}\,d\theta$$

- the LMCS length :

$$L_{LCMS}=\int_0^{2\pi}\sqrt{\frac{dR}{d\theta}^2+\frac{dZ}{d\theta}^2}\,d\theta$$

- the “area” elongation :

$$K_a=\frac{V_P}{2\pi^2 R_{ref}a_{ref}^2}$$

- The average plasma radius :

$$\rho_{ave}(t)=\frac{L_{LCMS}(t)}{2\pi}$$

3.3- METIS time-dependent quantities

3.3.1- Introduction

In this part, all the quantities that depend only on the time are defined . In the notation hereafter, the time dependence is implicit.

3.3.2- Energy and power 0D values

We define the total input power as :

$$P_{in} = P_{\alpha} + P_{\Omega} + P_{ICRH} + P_{LH} + P_{NBI} + P_{ECRH}$$

where P_{α} is the alpha particles power contribution, P_{Ω} is ohmic power, P_{ICRH} is the ion cyclotron resonance heating power (ICRH, any scheme), P_{LH} is the lower hybrid power (LH), P_{NBI} is the neutral beam injection power (NBI) and P_{ECRH} is the electron cyclotron resonance heating power (ECRH).

The loss power is defined *[ITER1]* as

$$P_{loss} = P_{in} - P_{brem} - P_{cyclo} - \lambda_{line} P_{line} - \frac{dW}{dt}$$

where P_{brem} is the bremsstrahlung radiative power, P_{cyclo} is the power lost by synchrotron radiation and P_{line} is the total radiative power due to line radiation. W is the total plasma energy content.

λ_{line} is the fraction of line radiation power coming from the core plasma. Generally $\lambda_{line} = \frac{1}{3}$ (this is the ITER FDR definition)

On the same way, we define P_{th} were additional powers are replaced by their thermal deposition (see chapter on supra-thermal content) :

$$P_{th} = P_{in,th} - P_{brem} - P_{cyclo} - \lambda_{line} P_{line} - \frac{dW_{th}}{dt}$$

3.3.3- Plasma composition

In the 0D part, the composition of the plasma is described by the volume-averaged density of the gas (considered as completely ionised). The plasma is composed of hydrogen isotopes of volume-averaged density respectively : $\langle n_H \rangle$ for hydrogen; $\langle n_D \rangle$ for deuterium and $\langle n_T \rangle$ for tritium. The sum of these densities is : $\langle n_1 \rangle = \langle n_H \rangle + \langle n_D \rangle + \langle n_T \rangle$. Depending of the “gas mode” the value of each isotope density is given by :

1. Hydrogen plasma :
   $\langle n_H \rangle = \langle n_1 \rangle$; $\langle n_D \rangle = 0$ & $\langle n_T \rangle = 0$
2. Deuterium plasma :
   if ICRH minority is hydrogen

$\langle n_D \rangle = \frac{\langle n_1 \rangle}{1 + C_{ref}}$; $\langle n_H \rangle = C_{ref} \langle n_D \rangle$ & $\langle n_T \rangle = 0$

otherwise

$\langle n_D \rangle = \langle n_1 \rangle$; $\langle n_H \rangle = 0$ & $\langle n_T \rangle = 0$

3. Deuterium & Tritium plasma :
   if ICRH minority is hydrogen

$\langle n_D \rangle = \frac{\langle n_1 \rangle}{1 + C_{ref} + \eta_{ref}}$; $\langle n_H \rangle = C_{ref} \langle n_D \rangle$ & $\langle n_T \rangle = \eta_{ref} \langle n_D \rangle$

   otherwise

$\langle n_D \rangle = \frac{\langle n_1 \rangle}{1 + \eta_{ref}}$; $\langle n_H \rangle = 0$ & $\langle n_T \rangle = \eta_{ref} \langle n_D \rangle$

4. Helium plasma :
   if ICRH minority is hydrogen

$\langle n_H \rangle = C_{ref} \langle n_{He} \rangle$; $\langle n_D \rangle = 0$ & $\langle n_T \rangle = 0$

   or if ICRH minority is deuterium

$\langle n_D \rangle = C_{ref} \langle n_{He} \rangle$; $\langle n_H \rangle = 0$ & $\langle n_T \rangle = 0$

   or if ICRH minority is tritium

$\langle n_T \rangle = C_{ref} \langle n_{He} \rangle$; $\langle n_D \rangle = 0$ & $\langle n_H \rangle = 0$

   otherwise

$\langle n_H \rangle = 0$; $\langle n_D \rangle = 0$ & $\langle n_T \rangle = 0$

where C_{ref} is the ratio between ICRH minority ion density and majority ion density and η_{ref} is the reference ratio between tritium and deuterium densities. The density of helium $\langle n_{He} \rangle$ does not distinguish H_{e3} and H_{e4} isotopes. Conversely, distinction is made between helium coming from deuterium/tritium reactions $\langle n_{He}^{ash} \rangle$ and coming from fuelling $\langle n_{He}^{fuel} \rangle$. We have $\langle n_{He} \rangle = \langle n_{He}^{ash} \rangle + \langle n_{He}^{fuel} \rangle$. The $\langle n_{He}^{ash} \rangle$ is computed with a 0D equation for ashes accumulation and $\langle n_{He}^{fuel} \rangle$ is defined by :
$\langle n_{He}^{fuel} \rangle = \eta_{He} \langle n_e \rangle$, where η_{He} is a prescribed parameter .

Additionally, the plasma contains two impurities of volume-averaged density $\langle n_{imp} \rangle$ (respectively $\langle n_{max} \rangle$) of number of charge Z_{imp} (respectively Z_{max})and of number of mass A_{imp} (respectively A_{max}). The density ratio between the two impurities is prescribed $\langle n_{max} \rangle = r_{imp} \langle n_{imp} \rangle$ and the mass number is computed with the simple rule

$A_x = \text{nearest integer of} (\frac{7}{3} Z_x)$.

The density ratio between impurities is prescribed : $\langle n_{max} \rangle = \eta_{imp} \langle n_{imp} \rangle$

The impurity density is computed to be consistent with effective charge Z_{eff} . In METIS the effective charge is given for a plasma without helium ashes. The effect of ashes is added to the prescribed effective charge .
Therefore we have, for a deuterium/tritium plasma:

1. when the prescribed effective charge is given as an input :

$$Z_{eff}=\frac{4\langle n_{He}^{ash}\rangle+\langle n_e\rangle Z_{eff,ref}}{\langle n_e\rangle}$$

2. when the prescribed effective charge is given by a scaling law :

$$Z_{eff}=\frac{4\langle n_{He}^{ash}\rangle+\langle n_e\rangle Z_{eff,sc}}{\langle n_e\rangle}$$

otherwise :

1. when the prescribed effective charge is given as an input :

$$Z_{eff}=Z_{eff,ref}$$

2. when the prescribed effective charge is given by a scaling law :

$$Z_{eff}=Z_{eff,sc}$$

with the neutrality equation

$$\langle n_e\rangle=\langle n_1\rangle+2\langle n_{He}\rangle+(Z_{imp}+\eta_{imp}Z_{max})\langle n_{imp}\rangle$$

and the effective charge equation

$$Z_{eff}\langle n_e\rangle=\langle n_1\rangle+4\langle n_{He}\rangle+(Z_{imp}^2+\eta_{imp}Z_{max}^2)\langle n_{imp}\rangle$$

we compute the volume-averaged density of each species.

3.3.4- Species profiles and impurities accumulation

In the METIS default mode, each species density profile is assumed to be proportional to the electron density profile, but we can also simulate an impurity neoclassical accumulation. In these case the shape of the heavier impurity follows the law *[Helander1]* :

$$\frac{n_{max}(t,x)}{n_{max}(t,x=0)}=\left(\frac{n_i(t,x)}{n_i(t,x=0)}\right)^{Z_{max}}\left(\frac{T_i(t,x=0)}{T_i(t,x)}\right)^{\frac{Z_{max}}{2}-1} \quad \text{where} \quad n_i(t,x)=\sum_{k\in\{\text{species}\}} n_k(t,x)$$

This law is computed for a cylindrical geometry, i,e., it does not included the curvature term.
To complete the equation set, we assume that $n_{imp}(t,x)\propto n_e(t,x)$ and $n_{he}(t,x)\propto n_e(t,x)$. Additionally, we maintain the volume-averaged density of impurities and helium unchanged compared to case without neoclassical accumulation. This allows to recompute the profile of the sum of the densities of hydrogen isotopes.

3.3.5- Scaling laws

METIS uses various scaling laws. This is an essential feature in order to ensure accurate

predictions.

The following definitions are used in the scaling laws :

$$n_{sc} = \frac{\bar{n}}{10^{19}}$$

$$\epsilon_{sc} = \frac{a_{ref}}{R_{ref}}$$

$$q_{cyl} = \frac{5 K_a a_{ref}^2 B_{ref}}{R_{ref} I_P}$$

$$F_q = \frac{q_{95}}{q_{cyl}}$$

$$B_{0,out} = B_{ref} \sqrt{\left(\frac{R_{ref}}{R_{ref} + a_{ref}}\right)^2 + \left(\frac{a_{ref}}{R_{ref} q_{95}}\right)^2}$$

$$f_a = 1 - \sqrt{\frac{2}{1 + m_{eff}}}$$

$$F_a = 0.1 \frac{m_{eff}}{f_a}$$

For m_{eff} the initial value is computed as

$m_{eff,ini} = 1$ for H plasma

$m_{eff,ini} = 2$ for D plasma

$m_{eff,ini} = 4$ for H_{e4} plasma

$m_{eff,ini} = (2 + 3 * \eta_{ref}) / (1 + \eta_{ref})$

where η_{ref} is the reference ratio between tritium and deuterium densities

For any other use, m_{eff} is computed as

$m_{eff} = \frac{\langle n_H \rangle + 2\langle n_D \rangle + 3\langle n_T \rangle}{\langle n_H \rangle + \langle n_D \rangle + \langle n_T \rangle}$ for hydrogen plasmas and $m_{eff} = 4$ for H_{e4} plasma.

The Hugill parameter :

$$H_g = \bar{n}\frac{\pi K a^2}{I_p}$$

The saturation density :

$$n_{sat} = 0.06 I_p R_{ref} \sqrt{A_{gaz}} K^{-1} a^{-2.5}$$

where A_{gaz} is the mass number of main plasma gas.

and we defined :

$$\mathring{n} = min(\bar{n}, n_{sat})$$

3.3.5.1- Energy

Scaling laws used for energy content prediction depend on the confinement regime (L mode or H mode), and on hypotheses for the fit of database quantities *[McDonald]*. The physicist can try different laws. In METIS the laws are paired (cf. figure 2): one for the L-mode and one for the H mode or one for the pedestal energy and one for the total H-mode energy. We use hereafter the energy confinement time, that is linked to the energy by $W_{sc,.} = \tau_{sc,.} P_{loss}$, where "." denotes any energy scaling.

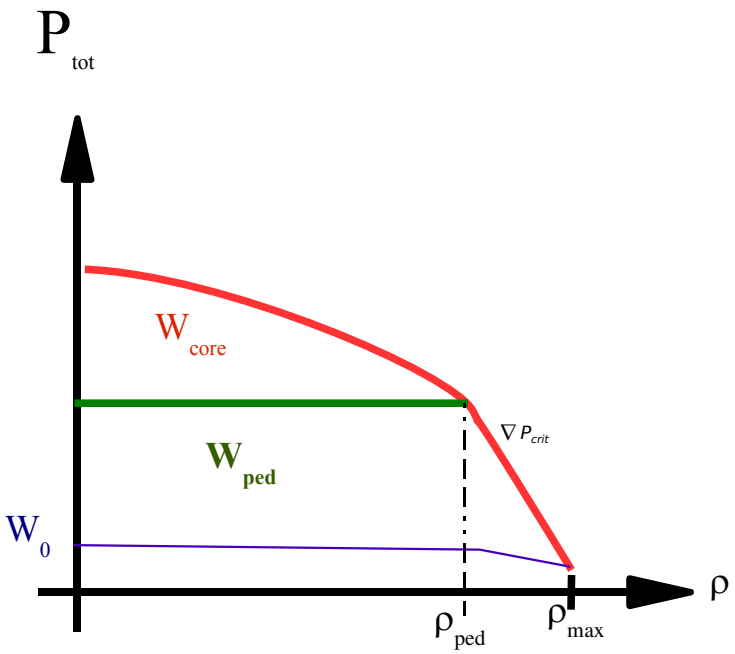

figure 2: plasma energy content ; the energy is decomposed between offset (W_0), pedestal (W_{ped}) and core (W_{core}).

The implemented scaling law for energy in the present version of the METIS code are:

1. Standard ITER scaling law *[ITER2]:*

in L mode, ITERL-96P(th): $\tau_{e,L} = 0.023\, I_p^{0.96} B_{ref}^{0.03} n_{sc}^{0.4} P_{in}^{-0.73} R_{ref}^{1.83} K_{ref}^{0.64} \epsilon_{sc}^{-0.06} m_{eff}^{0.2}$

in H mode, ITERH-98P(y,2): $\tau_{e,H} = 0.0562\, I_p^{0.93} B_{ref}^{0.15} n_{sc}^{0.41} P_{loss}^{-0.69} R_{ref}^{1.97} K_a^{0.78} \epsilon_{sc}^{0.58} m_{eff}^{0.19}$

and we take for the pedestal confinement time $\tau_{e,ped} = \frac{1}{2}(\tau_{e,H} - \tau_{e,L})$, that gives quite reasonable results.

2. Scaling optimized for the ohmic phase used by the ITER TEAM *[Lukash, Bracco]*:

$$\tau_{e,OH} = \frac{0.14\, a_{ref} R_{ref} H_g B_{ref}^{1.1}}{1 + 0.63\, B_{ref} H_g^2}$$

with a soft transition to standard ITER scaling law ITERL-96P(th) when additional power increases and :

$f_{rap} = min(1, max(0, \frac{I_p}{P_{loss}}))$ et $\tau_{e,L} = f_{rap}\tau_{e,OH} + (1 - f_{rap})\tau_{e,L96P(th)}$

if a H mode transition occurs, the standard ITER scaling law ITERH-98P(y,2) is used and the same pedestal confinement time as above is used.

3. Two-term scaling law as recommended by the IPTA group *[McDonald]*:

$\tau_{e,core} = 0.0693\, I_p^{0.62} P_{loss}^{-0.53} n_{sc}^{0.64} R_{ref}^{2.12} \epsilon_{sc}^{1.15} m$

$\tau_{e,ped} = 0.024\, I_p^{1.64} P_{loss}^{-0.44} n_{sc}^{-0.18} R_{ref}^{1.03} \epsilon_{sc}^{-0.39}$

and we have $\tau_{e,H} = \tau_{e,core} + \tau_{e,ped}$ and we take (just to complete, we do not use this for study in L mode) $\tau_{e,L} = \tau_{e,core}$.

4. scaling without beta dependence on total energy *[Petty, Joffrin1]* :

scaling law DS03 : $\tau_{e,H} = 0.028\, I_p^{0.83} B_{ref}^{0.07} n_{sc}^{0.49} P_{loss}^{-0.55} R_{ref}^{1.81} K_{ref}^{0.75} a_{ref}^{0.3} m_{eff}^{0.14}$

pedestal scaling : $\tau_{e,ped} = e^{-3.87} I_p^{1.6} n_{sc}^{-0.16} P_{loss}^{-0.4} R_{ref}^{1.03} \epsilon_{sc}^{-0.26}$

and we take for the L mode confinement time $\tau_{e,L} = \tau_{e,H} - \tau_{e,ped}$, which gives good results in Tore Supra simulations *[V. Basiuk, private communication]* and gives for ITER the same result as the standard ITERL-96P(th) scaling .

5. scaling obtained by applying the error-in-variable method recommended by the ITPA group *[McDonald]*:

in L mode the scaling ITERL-96P(th) it used and in H mode the scaling ITERH-EIV(y,2) :

$\tau_{e,H} = 0.0555\, I_p^{0.75} B_{ref}^{0.32} n_{sc}^{0.35} P_{loss}^{-0.62} R_{ref}^{2} K_a^{1.14} \epsilon_{sc}^{0.76} m_{eff}^{0.06}$

6. Scaling optimized for ohmic phase described in “Tokamak” by Wesson *[Wesson1]*:

$\tau_{e,OH} = 0.07\, \mathring{n}\, a\, R^2\, qcyl$

with a soft transition to standard ITER scaling law ITERL-96P(th) when additional power is increased and :

$$f_{rap}=min(1,max(0,\frac{I_p}{P_{loss}}))\quad \text{et}\quad \tau_{e,L}=f_{rap}\tau_{e,OH}+(1-f_{rap})\tau_{e,L96P(th)}$$

If a H mode transition occurs, the standard ITER scaling law ITERH-98P(y,2) is used and the same pedestal confinement time as above is used.

It very easy to add other scaling laws in METIS.

3.3.5.2- L-H threshold

The transition from L mode to H mode occurs in METIS whenever $P_{out} > P_{L2H}$ and the H mode to L mode transition occurs when $P_{in} < P_{L2H}$. We define :

$P_{L2H}=P_{L2H,scaling}+P_{L2H,offset}$ where $P_{L2H,offset}$ is a prescribed offset that is set to 0 by default and used to fit experimental data. and $P_{L2H,scaling}$ is one of scaling laws defined hereafter :

1. scaling ITER LH02noZeff *[Ryter]*:

$$P_{L2H,scaling}=0.042\,\bar{n}^{0.73}B_{0,out}^{0.74}S_{ext}^{0.98}$$

2. scaling ITER LH02Zeff *[Takizuka]*:

$$P_{L2H,scaling}=0.072\,\bar{n}^{0.7}B_{0,out}^{0.7}S_{ext}^{0.9}\left(\frac{Z_{eff}}{2}\right)^{0.7}F_a^{0.5}$$

3. scaling LH99(1) *[ITER3]*:

$$P_{L2H,scaling}=2.84\,\bar{n}^{0.58}B_{ref}^{0.82}SR_{ref}a_{ref}^{0.81}m_{eff}^{-1}$$

The transition from L mode to H mode is in fact softer. In fact, it is well known than the full H mode confinement is obtained only when the input power is well above the threshold. To simulate this effect, the key “l2hslope” can be used. In this case the confinement time becomes :

$$\tau_e=f_{L2H}\tau_H+(1-f_{L2H})\tau_{e,L}$$

with

$$f_{L2H}=min(1,max(0,\frac{\Delta P_{L2H}}{S_{L2H}}))\quad \text{and}\quad \Delta P_{L2H}=\frac{P_{in}-P_{L2H}}{P_{L2H}}$$

3.3.5.3- Effective charge scaling

Generally the line-averaged effective charge is prescribed. This reference is the value without ashes coming from DT reaction.

We can also use some scaling laws to predict its value. For Tore Supra, we use the scaling computed by P. Devynck for deuterium plasma [Devynck]:

$$Z_{eff,sc}=1+\frac{1079}{2}T_{ref}^{1.17}\langle n\rangle^{-0.17}+\frac{7.6810^9}{2}T_{ref}^{0.92}\langle n\rangle^{-0.51}$$

where $T_{ref}=\frac{\bar{T}_e^{\,2}}{\bar{T}_e}$

Other scaling laws can be easily implemented on demand.

remark: the Matthews scaling law is, generally, already used to predict the radiative power.

3.3.5.4- He confinement time scaling

The helium ash confinement time is usually prescribed as proportional to the energy confinement time

$\tau_{He}=\gamma_{He}\tau_E$, but can also be predicted using the following scaling law *[ITER4]* :

$\tau_{He}=0.74 V_p^{0.7} I_p^{0.31} \left(\frac{P_{in}}{\bar{n}}\right)^{-0.57} \left(\frac{\tau_E}{\tau_{E,L}}\right)$

3.4- Time dependent profiles in METIS

3.4.1- Profiles description

Two possible descriptions of profiles are implemented in METIS. The first one is used at the first call of the METIS solver, the second is used during the convergence loop (all others calls). In both descriptions, the space normalised variable x that labels the flux surfaces is used. This variable is exactly defined as :

$x=\Delta x(k-1), k\in\mathbb{N}, 1\leqslant k\leqslant 21, with\ \Delta x=0.05$

we note also :

$x_k=\Delta x(k-1)$

This x coordinate is the normalised Lao coordinate *[Lao1]*. All profiles are defined using this coordinate. The toroidal flux surface coordinate $\rho=\sqrt{\frac{\Phi}{\pi B_0}}$ is computed in METIS and named "rmx". Profiles that are used in the current diffusion solver are re-sampled on the toroidal flux surface coordinate.

The initial profiles are computed with the help of an analytical formulation and are described in Section 3.20. Otherwise, profiles are computed in various functions as, for example, the current diffusion solver. The list of profiles computed in METIS is given in Section 8.3. The profiles depend both of time and space.

We used the same definitions as in CRONOS for average quantities *[CRONOS]*.

The $\langle A\rangle$ denotes the volume average quantity of A. The $\langle A\rangle_S$ denotes the surface (on a poloidal section of the plasma) average quantity of A. The $\bar{A}$ denotes the line average quantity of A.

3.4.2- Pedestal description

In METIS, we compute the pressure P_{ped} at the top of the pedestal, using the energy content predicted by the scaling and modulated by a free coefficient f_{ped} :

$$P_{ped,sc}=\frac{2}{3}f_{ped}\frac{W_{ped,sc}}{V_P} \quad \text{with} \quad W_{ped,sc}=\tau_{E,ped}P_{th} \quad \text{and by default, we set} \quad f_{ped}=1$$

This value is limited by the maximal allowed pedestal pressure $P_{ped,max}$. This limit comes from an MHD stability criterion *[Onjun]* and from experimental considerations *[Maggi]* :

$$P_{ped}=f_{ped}\,min(P_{ped,sc},P_{ped,max})$$

$$P_{ped,max}=min(\frac{2}{3}P_{wth},max(\frac{1}{4}P_{wth},P_{ped,MHD})) \quad \text{with} \quad P_{wth}=\frac{2}{3}\frac{W_{th}}{V_P}$$

and $$P_{ped,MHD}=0.8\,\rho_{ped}F_{dia}(\rho_{ped})^2\langle\frac{1}{R}\rangle^3\frac{1+K(\rho_{ped})^2(1+5\,\delta(\rho_{ped})^2)}{4\mu_0 q(\rho_{ped})^3}(q(\rho_{edge})-q(\rho_{ped}))$$

where ρ_{ped} is the coordinate of the top of the pedestal and ρ_{edge} is the edge coordinate.

With this model, the pedestal width has a very weak influence on the pressure at the top of pedestal. Since in METIS the profiles have 21 radial points only, we always take the top of the pedestal at the nearest point after the edge (i.e., point 20 with x = 0.95).

3.4.3- Confinement modification

We define $W_{core}=\tau_{E,L}P_{th}$ in L mode $W_{core}=\tau_{E,H}P_{th}-W_{ped}$ in H mode

with $W_{ped}=0$ in L mode and $W_{ped}=\frac{3}{2}V_P P_{ped}$ in H mode.

The plasma confinement can be modified by various processes and in METIS we used finally :

$$W_{th}=H_{MHD}H_{li}H_{ref}\tau_{E,sc}P_{th}+W_{ITB} \quad \text{with} \quad W_{ITB}=(H_{ITB}-1)\tau_{E,sc}W_{core}$$

By default, all multiplicative factors are equal to 1. The energy confinement time is defined as $\tau_E=\frac{W_{th}}{P_{th}}$.

Factor definitions are:

- H_{ref} is a prescribed, time dependent, confinement factor
- H_{MHD} is a internally computed, time dependent, confinement factor that takes into account some confinement degradation due to MHD phenomena (see Section on MHD effects in METIS)
- H_{ITB} is a internally computed, time dependent, confinement factor that takes into account the enhancement of the confinement due to internal transport barrier formation (see chapter on ITB effect in METIS)
- H_{li} allows to take into account the effect of internal inductance on energy confinement. The li is not included in standard scaling laws. If this feature is used, we have *[Peeters]*:

  $H_{li}=(\frac{I_i}{I_{i,0}})^{\frac{2}{3}}$ where $I_{i,0}$ defines the neutral point.

3.5- Heat, fuelling and current sources description

3.5.1- Introduction

The description of the sources is very important in order to obtain a good precision on predicted values. We decomposed the sources in total power, total current drive, profile power source and current profile source. Each of these terms is computed with different formulations, depending on the best methods (in term of computing speed and precision) available.

3.5.2- ICRH in FWEH and FWCD scheme

In the fast wave electron heating and current drive scheme, it is assumed that the ICRH power heats only the electrons ; the power deposition is central and peaked, as computed by the ABSOR code *[Zerlauth]*. The current drive efficiency is determined by a fit of experimental data *[ITER5]*:

$$I_{fwcd}=s_{fwcd}\frac{P_{icrh}(t)\eta_{fwcd}(t)}{R_{ref}(t)\frac{n_e(t,x=0)}{10^{20}}} \quad \text{where}$$

$$\eta_{fwcd}(t)=(0.008\frac{T_e(t,x=0)}{10^3}+0.0021)\frac{6}{5+Z_{eff}(t)}$$

and where s_{fwcd} is related to the sign of the current :

$s_{eccd}=1$ for co-current (i.e. in the direction of toroidal plasma current), $s_{eccd}=-1$ for counter current and $s_{eccd}=0$ for FWEH scheme.

The shape of the power deposition profile is *[Meo]*:

$$p_{fw}\propto\frac{n_e(t,x)T_e(t,x)}{B_{out}(t,x)} \quad \text{where} \quad B_{out}(t,x)\simeq\frac{B_{ref}(t)}{R_{ref}(t)+a_{ref}(t)x}$$

with $\rho_m\int_0^1 p_{fw}(t,x)V'(t,x)dx=P_{ICRH}(t)$

The same shape is used for the current density profile $j_{fwcd}(t,x)$, that is normalised to the total current I_{FWCD} :

$$\rho_m\int_0^1 j_{fwcd}(t,x)S'(t,x)dx=I_{fwcd}(t)$$

3.5.3- ICRH in minority scheme

In this scheme, a fast ion population is generated and heats the plasma ions and electrons. This means that knowledge of the fast ion distribution function is essential. We use the analytical Stix formulation *[Stix]* that gives the steady state velocity distribution function $f(v)$ without space dependence. This distribution function is computed for each time in METIS. All parameters are taken at the resonance position $R_{res}(t)$ on the equatorial plane. The resonance position and the

harmonic is computed from the magnetic equilibrium, taking into account the prescribed frequency (f_{ICRH}) and minority ion mass, charge and concentration (C_{mino}). A key parameter is the volume occupied by the minority ions accelerated by the wave. The fraction of plasma volume involved is deduced from the resonance width and scaled on the PION code results *[Eriksson93]*. Once $f(v)$ is known, the supra-thermal content (cf. section about supra-thermals) and the power heating ions and electrons are deduced.

We also take into account the first orbit fast ion loss using the potato width of the orbit *[Eriksson01,Wesson2]*.

The shape of the power deposition is assumed to be a Gaussian curve centred on the resonance position with a width proportional to the resonance width scaled on the PION code results.

3.5.4- ICRH in 2nd harmonic (for He_3 or for T)

For these schemes at 2nd harmonic, we have no simple model to compute the distribution function, therefore we have used the same model as for the minority scheme. For tritium, we replace the concentration C_{mino} by the product of the minority concentration times the isotopic fraction η_{ref} divided by the square of the harmonic number. For other species, we replace the concentration C_{mino} by the minority concentration C_{mino} divided by the square of the harmonic number. This choice allows to fit the PION output to the ITER standard H-mode scenario.

3.5.5- LHCD

We have developed a simple model that will eventually be tuned on future results of the complete code LUKE. The LHCD effect is separated in two parts. The first one consists of the computation of the current source profile. The second part is the evaluation of the scaling law for LH current drive efficiency or of a simple law deduced from LUKE simulations *[Peysson]*. The power deposition is taken proportional to the current source and only electrons are heated.

The current shape source is determined on the basis of Landau absorption, accessibility and caustics *[R. Dumont, private communication ,and J. Decker , private communication]*. The wave spectrum is supposed to be composed of two Gaussian curves located at $n_{//0}$ and $-3n_{//0}$ and the initial width of the Gaussian curves is computed from the launcher toroidal width :

$\delta n_0 = \frac{c}{F_{LH}} W_{LH}$ for the positive part of the spectrum and $\delta n_0 = 3\frac{c}{F_{LH}} W_{LH}$ for the negative part of the spectrum; here F_{LH} is the LH wave frequency in Hz and W_{LH} is the toroidal width of the launcher (in m). The negative part provides no current and is computed only to get the complete power deposition shape. The directivity Δ_{LH} and $n_{//0}$ are prescribed (the relation between Δ_{LH} and $n_{//0}$ depends on the launcher geometry). The power in the positive part of the spectrum is proportional to Δ_{LH} .

The wave launched at the edge of the plasma is absorbed at the position where the distance between the line $n_{//} = n_{//0}$ and the Landau absorption curve is minimal; the point corresponds to $n_{//abs}$. The wave propagation and therefore the absorption is only possible in the domain enclosed by the upper and lower caustics. If the temperature is too low, the Landau absorption condition is modified to shift the curve in the domain enclosed by the caustics. If the line $n_{//} = n_{//0}$ does not intersect the domain enclosed by the caustics , the power is not absorbed by the plasma. If

$n_{//0} < \Upsilon_{LH}$ the current drive efficiency is decreased .

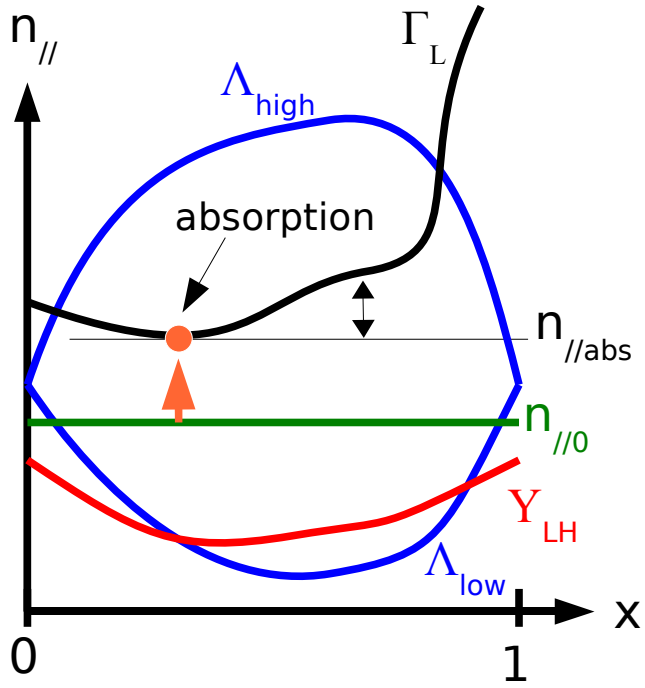

figure 3 : graph of absorption for Lower Hybrid; the absorption occurs at the location where the distance between the line $n_{//0}$ and Landau curve Γ_L is minimal.

We define :

$$\Lambda_{Low} = \frac{n_{//0}}{1 + \frac{\rho_m \sqrt{-\frac{P}{S}}}{qR_{axe}}}$$ the lower caustic

$$\Lambda_{Low} = \frac{n_{//0}}{1 - \frac{\rho_m \sqrt{-\frac{P}{S}}}{qR_{axe}}}$$ the higher caustic

$$\Upsilon_{LH} = \frac{\omega_{pe}}{\omega_{ce}} + \sqrt{1 + \frac{\omega_{pe}^2}{\omega_{ce}^2} - \frac{\omega_{pi}^2}{\omega^2}}$$ the accessibility limit

with

$$S = 1 + \frac{\omega_{pe}^2}{\omega_{ce}^2} - \frac{\omega_{pi}^2}{\omega^2} \quad , \quad P = 1 - \frac{\omega_{pe}^2}{\omega^2} - \frac{\omega_{pi}^2}{\omega^2} \quad \text{and} \quad D = \frac{\omega_{pe}^2}{\omega\,\omega_{ce}}$$

and with

$$\omega = 2\pi F_{LH} \quad , \quad \omega_{pe} = \sqrt{\frac{e^2 n_e}{m_e \epsilon_0}} \quad , \quad \omega_{pi} = \sqrt{\frac{e^2 Z_i n_e}{m_p A_i \epsilon_0}} \quad \text{and} \quad \omega_{ce} = \frac{eB}{m_e}$$

The absorption condition for the Landau absorption is :

$$\Gamma_L = \frac{(6.5 - 1.56\sqrt{\frac{2\rho_m}{R_{axe}+\rho_m}})}{\sqrt{\mu_{LH}\frac{T_e}{10^{-3}}}}$$ where the aspect ratio dependence is taken by a fit of LUKE simulations (and must be completed when more results for various devices will be obtained).

μ_{LH} is a free parameter that is taken equal to 1 when absorption is possible; but if the temperature is too low this parameter is adjusted in order to retrieve the absorption.

The source shape is defined as a Gaussian curve in a variable which is the difference between the Landau absorption curve and $n_{//\text{abs}}$:

$$P_{LH}, J_{LH} \propto e^{-\frac{1}{2}\left(\frac{n_{//\text{abs}} - \Gamma_L}{\delta n}\right)^2} \quad \text{with} \quad \delta n = \delta n_0 \frac{n_{//\,\text{abs}}}{n_{//0}}$$

We define also the parameter of modulation of current drive efficiency :

$$\zeta_{acc} = min\left(1, \frac{e^{n_{//0} - Y_{LH}(x=1)}}{\delta n_0}\right)$$

Once the absorption profile is computed, the driven current is determined from the current drive efficiency as follows.

In METIS the LH efficiency η_{LH} is defined as :

$$\eta_{LH} = \frac{I_{LH}\langle n_e \rangle R_{ref}}{P_{LH}} \quad \text{at} \quad V_{loop} = 0$$

The total current generated by the LH waves must take into account the synergy effect between the LH wave and the parallel electric field *[Giruzzi97]*.
We obtain the total current generated by Lower Hybrid, including the first order correction in the parallel electric field :

$$I_{LH} = \eta_{LH}\frac{P_{LH}}{\langle n_e \rangle R_{ref}} + \frac{V_{loop}}{R_{hot}} \quad \text{with} \quad R_{hot} = \frac{8 R_{ref}^2 \langle n_e \rangle^2}{P_{LH}\eta_{LH}^2}\frac{3 + Z_{eff}}{(5 + Z_{eff})^2}$$

The LH efficiency η_{LH} is given either by a scaling law or prescribed. In the absence of a universally accepted one, the following laws have been implemented :

1. The scaling law selected by the ITER team *[ITER6]*, at which we have added a limitation :

$$\eta_{LH} = S_{LH}\frac{2.4\,10^{20}}{5 + Z_{eff}}\tanh\left(\frac{T_e}{6\,10^3}\right)$$

2. The scaling law for Tore Supra and JET *[Goniche]*:

$$\eta_{LH}=2.7310^{19} D_{LH}^{0.3} \tau_E^{0.4} Z_{eff}^{-0.12} S_{LH} \zeta_{acc}$$

where D_{LH} is the directivity of LH launcher.

3. A scaling law for Tore Supra for vanishing loop voltage *[A. Becoulet, private communication]*:

$$\eta_{LH}=\frac{2.9510^{19}}{\sqrt{\frac{\bar{n}}{10^{19}}+3}} \frac{B_{ref}(1-\frac{\phi}{230})}{5+Z_{eff}} S_H$$

with $n_{//0}=\frac{(2.01-D_{LH})}{0.63}$ and $\phi=230(n_{//0}-1.8)$

4. A fit combining LUKE simulations and experimental data for Tore Supra and JET. This scaling development is in progress, and uses a theoretical expression for the current drive efficiency *[Fisch]* that is modified in order to take into account regimes at low temperature and poor accessibility *[J. Decker, private communication]*. This expression is also modified to take into account the effect of plasma elongation *[M. Goniche, private communication]* :

$$\eta_{LH}=\frac{6}{5+Z_{eff}} \zeta_{acc} \frac{\int_0^1 E_{LH} P_{LH} V' dx}{\int_0^1 P_{Lh} V' dx} \quad \text{with}$$

$$E_{LH}=f_1 \frac{(\omega_2^2-\omega_1^2)}{\ln(\frac{max(\omega_1,\omega_2)}{\omega_1})} min(1, e^{-f_2 \mu_{LH}(\frac{n_{//abs}}{n_{//0}}-K)}) \quad \text{where}$$

$$\omega_1=\frac{1}{max(n_{//0}, n_{//abs})} \quad \text{and} \quad \omega_2=\frac{1}{max(\Lambda_{low}, \Upsilon_{acc})}$$ and K is the plasma elongation.

At present, the best fit is obtained with : $f_1=410^{20}$ and $f_2=1$.

3.5.6- ECCD

Since in an ITER-like plasma the refraction is generally important, the determination of the power deposition of ECRH wave needs a ray tracing code. That is beyond the scope of a tool like METIS. Therefore, in METIS we prescribed the position (x_{eccd}) of the maximum of the power deposition profile. The shape of the power deposition is simply a Gaussian curve with a width (δ_{eccd}) determined from the width of the resonance *[Wesson3]*, with constants adjusted to fit the outputs of the REMA code *[Krivenski]* :

$$p_{eccd}(x,t)=p_{eccd,0} e^{\frac{(x-x_{eccd}(t))^2}{2\delta_{eccd}(t)}}$$

where $\delta_{eccd}(t)=\sqrt{\frac{1}{4}(\frac{v_{th}}{c})^4+\alpha_{eccd}\frac{I_{eccd}}{P_{eccd}}(\frac{v_{th}}{c})^2}$

with $v_{th}=\sqrt{\frac{2eT_e(t,x_{eccd})}{m_e}}$, $\alpha_{eccd}\simeq 1$

and $p_{eccd,0}$ satisfying $\rho_m\int_0^1 p_{eccd}(t,x)V'(t,x)dx=P_{eccd}(t)$

The current source profile $j_{eccd}(t,x)$ has the same shape as the power deposition. The total current is computed using a simple scaling *[Giruzzi87]*:

$$\rho_m\int_0^1 j_{eccd}(t,x)S'(t,x)dx=I_{eccd}(t) \quad \text{with} \quad I_{eccd}(t)=s_{eccd}\frac{\Gamma_{LH\in ECCD}\eta_{eccd}(t)P_{eccd}(t)}{n_e(t,x_{eccd}(t))R_{ref}(t)}$$

where s_{eccd} is the direction of the wave injection :

$s_{eccd}=1$ for co-current , $s_{eccd}=-1$ for counter current and $s_{eccd}=0$ for normal injection.

and where $\Gamma_{LH\in ECCD}$ is the synergy factor with lower hybrid (equal to 1 by default) and where :

$$\eta_{eccd}=\frac{1}{1+\frac{100}{\frac{T_e(t,x_{eccd})}{10^3}}}[1-(1+\frac{5+Z_{eff}}{3(1+Z_{eff})})(\sqrt{2}\mu_t)^{\frac{5+Z_{eff}}{1+Z_{eff}}}]\frac{6}{5+Z_{eff}} \quad \text{with}$$

$$\mu_t=\sqrt{\frac{a_{ref}x_{eccd}(1+\cos(\theta_{pol}))}{R_{ref}+a_{ref}x_{eccd}\cos(\theta_{pol})}} \quad .$$

3.5.7- Synergy between LH and ECCD

In some configurations, a synergy between ECCD and LHCD may increase the effect of the EC power on the total driven current. The factor $\Gamma_{LH\in ECCD}$ accounts for this effect. This factor must be prescribed. For Tore Supra *[Giruzzi04]*, the following law fits the experiment :

$$s_{eccd}\Gamma_{LH\in ECCD}=s_{eccd}+H_{MHD}\frac{min(\frac{2}{3}P_{LH},P_{ECCD})}{max(1,P_{ECCD})}\frac{s_{ECCD}+1}{2}max(0,\frac{\eta_{LH}}{\eta_{eccd}})\sqrt{\frac{(1-x_{eccd}^2)^{\nu_T}}{2}}$$

3.5.8- NBI Heating and CD

The neutral beam injection is described in METIS by a decay equation applied in a simplified geometry and an analytical solution of the Fokker-Planck equation.
The beam attenuation is computed for a few sub-beams. The beam intensity (Υ) damping equation along the beam path is :

$d\Upsilon\frac{(l)}{dl}=-n_e(l)\sigma_{eff}(l)\Upsilon(l)$ where l is the coordinate along the beam path

with the initial condition :

$\Upsilon(l=0)=\Upsilon_O$ at the entrance of the plasma

and

$\sigma_{eff}=\sigma_0(A_b,E_{b0},n_e(l),T_e(l),Z_{eff}(l))+\sigma_{bp}(A_b,E_{b0},n_e(l),T_e(l),\xi_b(l),S_{NBI}(l))$

where σ_0 is the stopping cross section *[Janev]* and σ_{bp} is the increment of the stopping cross section due to fast ions *[Okano]*. The stopping cross section along the neutral path depends on :

- the beam ion mass (A_b)
- the initial beam energy (E_{b0})
- the pitch angle at the point where the neutral particles are ionized (ξ_b)
- the fast ion source (S_{NBI})
- the electron density n_e and temperature T_e
- the plasma effective charge Z_{eff}

In METIS, the neutral beam path is taken in the equatorial plane of the plasma (at $Z = Z_0$) and the radius of tangency is prescribed $(R_{\tan})$. To insure a horizontal spread and prevent a point-like deposition, 3 sub-beams are computed at $\{R_{\tan}-\frac{a_{ext}}{6},R_{\tan},R_{\tan}+\frac{a_{ext}}{6}\}$. We used the average of the 3 sub-beams damping. From this, the power deposition $(p_b(x))$, mapped on the x coordinate, is computed. The vertical tilt is simulated by a final remapping : we substitute the coordinate x_T at x, then we perform a remapping on x with :

$x_T=z_T+x(1-z_T)$ where z_T is the intersection of the beam with the Z axes at $R_{\tan}$ converted in Lao coordinate. To take into account the vertical width of the beam, the effect is computed for 3 sub-beams with $Z_T\in\{Z_{ext}-0.05,Z_{ext}Z_{ext}+0.05\}$. The average of the 3 is taken as the power density deposition. Vertical and horizontal width of the beam is internally fixed in this version of METIS but they can be added as free parameters.

The final value of Υ gives the fraction of the power that is not deposited in the plasma (shinethrough).

From the power deposition $(p_b(x))$, we subtract the first orbit losses that are computed with a simplified model : we suppose that most of the fast ions are trapped near the plasma edge and we compute the orbit width ($\delta_o(x)$) *[formula 2.9 in reference : Eriksson01]*. The fast ions created at less than $\delta_o(x)$ from the edge are lost. In order to simulate the broadening of the deposition profile due to orbit width we convolve the profile by a step function of width $\delta_o(x)$.

From the power deposition $(p_b(x))$, we compute the fraction of the power that heats the main plasma ions using the formulae 5.4.12 in reference *[Wesson4]*. The supra-thermal content computation is detailed in Section 3.6.

The current source associated with NBI is computed by an analytical solution of the Fokker-Planck equation in which both trapping effects and energy diffusion are neglected *[Stix and L. G Eriksson, private communication]*:

$$J_{NBI}^{fast}=e\frac{p_b}{E_b}\tau_s\xi_b\left(\frac{v_0^3+v_c^3}{v_0^3}\right)^{\frac{2v_\gamma^3}{3v_c^3}}\int_0^{\frac{v_0}{v_c}}\left(\frac{z^3}{z^3+1}\right)^{\frac{2v_\gamma^3}{3v_c^3}+1}dz$$

where τ_s is the slowing down time, v_c ans v_γ are critical velocities and v_0 the fast ions initial velocity as they are defined in the Stix paper.

The electron back-current is computed with the Lin-Liu formulation *[Lin1]* and subtracted to the total NBI current.

3.5.9- Fusion products & associated sources

In METIS we take into account the fusion reactions between deuterium and tritium and between deuterium and deuterium or coming from thermal plasma, beam-plasma and beam-beam reactions.

Reactivities and and cross sections used in METIS are those of reference *[Bosch]*. Alternatively, METIS can use the reactivity given in reference *[Peres]*.

3.5.9.1- Thermal reactions

The fusion power source is simply computed using deuterium an tritium density profiles and ion temperature profile :

$S_{\alpha,th}=n_D(t,x)n_T(t,x)\langle\sigma\ v\rangle_{T(d,n)He4}(T_i(t,x))$ et $p_{\alpha,th}=eE_{\alpha,T(d,n)He4}S_{\alpha,th}$ where $E_{\alpha,T(d,n)He4}=3.56\ 10^6 eV$

For DD reactions there are two channels :

$$S_{p,DD,th}=\frac{1}{2}n_D(t,x)^2\langle\sigma\ v\rangle_{D(d,p)T}(T_i(t,x)) \quad \text{and}$$

$$S_{n,DD,th}=\frac{1}{2}n_D(t,x)^2\langle\sigma\ v\rangle_{D(d,n)He3}(T_i(t,x))$$

The associated power source in the plasma is :

$p_{DD,th}=e(E_{p,D(d,p)T}+E_{T,D(d,p)T})S_{p,DD,th}+eE_{He3,D(d,n)He3}S_{n,DD,th}$ where

$E_{p,D(d,p)T}=3.02\ 10^6 eV; E_{T,D(d,p)T}=1.01\ 10^6 eV$ and $E_{He3,D(d,n)He3}=0.82\ 10^6 eV$

The tritium-tritium reactions are neglected (in a tokamak the tritium is always mixed with deuterium and in this case the rate of T/T reactions is negligible compared to the rate of D/T reactions).

3.5.9.2- Beam-plasma and beam-beam interactions

Additional fusion reactions come from the interaction between the fast ions due to neutral beam injection and the plasma or the fast ions due to the beam itself. There are 5 types of reactions that must be considered :

- fast D ions on thermal T ions
- fast D ions on thermal D ions
- fast T ions on thermal D ions
- fast D ions with fast T ions
- fast D ions with fast D ions

The tritium-tritium reaction are neglected for the reasons given above.

The first case is the interaction between the beam and the plasma. From the cross section *[Bosch]* and using the formulation given by Mikkelsen *[Mikkelsen1]*, we compute the fusion reactivities by integrating the distribution function over velocity. We use in this case a simplified distribution function for the fast ions : we neglect anisotropy, taking into account only the slowing down *[Stix and L. G Eriksson, private communication]* and consider the stationary solution :

$$f(v)=\frac{P_b}{eE_b}\frac{\tau_s}{4\pi}\frac{\Theta(v-v_0)}{v^3+v_0^3}$$

To save computing time, we pre-compute the integral that appears in Mikkelsen formulation on a grid and we interpolate the results.

The second case is the interaction of fast ions with fast ions. The complete computation is too time-consuming for METIS. Therefore we used a coarse approximation that we scale on the complete formulation for a time slice only. This method gives a result close to the complete computation. The approximated method consists in using the formulation for beam-plasma interaction where the thermal temperature is replaced by the average fast ion energy. The complete formulation is described by Wolle *[Wolle]*. We used the method described in reference 13 of this report *[Cordey]* to compute the solution.

The fusion reaction due to interaction between fast ions generated by ICRH are not yet computed in METIS.

3.5.9.3- Fast alpha bootstrap-like current estimation

The fast alpha particles trapped in local magnetic field wells drive a bootstrap-like current. This current must be taken into account in the current diffusion equation. The complete calculation needs a code like SPOT *[Schneider]* and cannot be performed in METIS. We use a simplified scaling *[formula 9.4 in reference Eriksson01]* where we replace $n_f \Im(r)$ by

$\frac{\eta_{j,\alpha}}{\rho_m}\frac{dS_{\alpha,th}}{dx}$ where $\eta_{j,\alpha}=0.15$ is fixed to fit the results obtained with the SPOT code for the ITER standard H-mode scenario. In the future, this scaling must be completed for other plasma scenarios and configurations. The fraction of current driven by fast alpha particles in a reactor-like tokamak remains small (< 10% of the standard bootstrap current) but has an influence on current diffusion (since it is a central current).

The electron back-current is computed with the Lin-Liu formulation *[Lin1]* as for neutral beam injection.

3.5.9.4- Profile broadening due to Alfvénic instabilities

We have implemented in METIS the effect of Alfvénic instabilities on alpha particles to test the impact on fusion power in a reactor *[Vlad04, Vlad06]*. A simple model is implemented that broadens the fast alpha profile until the gradient of fast alpha pressure goes below the threshold at the position in the profile where the instability driven term is maximum *[Wesson5, Rosenbluth1]*. The threshold is given by equation 10 of reference *[Fu]* and the position where the instability driven term is maximum is given by the position where :

$-q^2\frac{d\beta_{alpha}}{dx}$ is maximum *[Pinches]*.

3.5.9.5- Neutron production rate

Neutron production rate for each nuclear reaction channel is directly deduced from the rate of fusion reactions in this channel. The profile shape of the neutron source is assumed to be identical to that of the fusion source for thermal reactions and proportional to the ion heat power for beam-plasma and beam-beam induced neutron sources.

3.6- Thermal power and supra-thermal stored energy calculation

The fast ions coming from heating (fusion, NBI and ICRH) contribute to the plasma pressure and plasma energy content. We can evaluate these quantities by solving a simplified version of the Fokker-Planck equation *[Stix, L. G Eriksson, private communication]*. If we neglect energy diffusion, trapping effect and pitch angle scattering, the Fokker-Planck equation for a mono-energetic ion source becomes:

$\frac{\partial f}{\partial t}=\frac{1}{v^2}\frac{\partial}{\partial v}(\frac{v^3+v_c^3}{\tau_s}f)+\frac{S_0}{4\pi v_0^2}\delta(v-v_0)$ where f is the distribution function, S_0 the fast ion source and v_0 the injection velocity, v_c is the critical velocity and τ_s the slowing down time as defined in reference *[Stix]*.

Temperature and density used in expression of v_c and τ_s are the power-weighted volume-averaged values :

$$A_w(t)=\frac{\int_0^1 p(t,x)V'(t,x)A(t,x)dx}{\int_0^1 p(t,x)V'(t,x)dx}$$

The steady state solution is :

$$f=\frac{S_0\tau_s}{4\pi}\frac{\sigma(v_0-v)}{v^3+v_c^3}$$

The stored energy can be written as :

$$W_{sup}=\int_0^\infty \frac{1}{2}mv^2 f\,4\pi v^2 dv=\int_0^\infty \frac{1}{2}m\frac{S}{0}\tau_s\frac{v^4}{v^3+v_c^3}dv$$

which yields finally :

$$W_{sup}=\frac{P_{inj}\tau_s}{2}(1-(\frac{v_c}{v_0})(\frac{1}{3}\ln(\frac{(v_0-v_c)^2+v_0v_c}{(v_0+v_c)v_c})+\frac{1}{\sqrt{3}}(atan(\frac{2v_0-v_c}{\sqrt{3}v_c})+atan(\frac{1}{\sqrt{3}}))))$$

where $P_{inj}=S_0\frac{1}{2}mv_0^2$ is the injected power.

We can now define the supra-thermal pressure associated with the stored energy. We simply take the shape of the power deposition defined for each heating source , named here p_{shape} , and we compute a proportional profile that satisfies :

$$p_{\sup}(t,x)=\eta_{\sup}(t)\,p_{shape}(t,x) \quad \text{and} \quad \frac{3}{2}\rho_m(t)\int_0^1 p_{\sup}(t,x)V'(t,x)dx=W_{\sup}(t) \qquad \forall t$$

Additionally, from simplified non steady state Fokker-Planck equation described above, we deduce the time evolution of the supra-thermal stored energy :

$\frac{dW_{\sup}}{dt}=\frac{-2W_{\sup}}{\tau_{eff}}+P_{inj}$ and the thermal power deposition is $P_{th}=\frac{2W_{\sup}}{\tau_{eff}}$ with

$$\tau_{eff}=\tau_s(t)\left(1-\left(\frac{v_c}{v_0}\right)\left(\frac{1}{3}\ln\left(\frac{(v_0-v_c)^2+v_0v_c}{(v_0+v_c)v_c}\right)+\frac{1}{\sqrt{3}}\left(atan\left(\frac{2v_0-v_c}{\sqrt{3}\,v_c}\right)+atan\left(\frac{1}{\sqrt{3}}\right)\right)\right)\right)$$

We can also compute the fraction of the power heating the electrons by splitting the above expression in electron collision and ion collision (this calculation is detailed in reference : *[Wesson6]*):

$$P_{th,el}=2\frac{W_{\sup}}{\tau_s} \quad \text{and by difference} \quad P_{th,ion}=P_{th}-P_{th,el}$$

For fast ions, the power deposited onto the main plasma ions can be easily computed with the help of the formulae 5.4.12, p 249 and gives the same result as the above formulation.

As an input for the equilibrium calculation,we define the total pressure :

$$p_{tot}(t,x)=p_{th}(t,x)+p_{\sup,\alpha}(t,x)+p_{\sup,NBI}(t,x)+p_{\sup,ICRH}(t,x)+p_{\sup,LH}(t,x)$$

with $p_{th}(t,x)=e\,n_e(t,x)T_e(t,x)+e\,n_i(t,x)T_i(t,x)$

We also define a thermal heating power :

$$P_{in,th}=P_{\alpha,th}+P_{\Omega}+P_{ICRH,th}+P_{LH,th}+P_{NBI,th}+P_{ECRH}$$

and the total energy content :

$$W=W_{th}+W_{\sup,\alpha}+W_{\sup,ICRH}+W_{\sup,NBI}+W_{\sup,LH}$$

where W_{th} is given by the scaling law.

Terms coming from LHCD are computed separately.

We finally define a synthetic W_{dia} :

$$W_{dia}=W_{th}+W_{\sup,\alpha}+\frac{3}{2}W_{\sup,ICRH}(1-f_{//,ICRH})+\frac{3}{2}W_{\sup,NBI}(1-f_{//,NBI})+\frac{1}{3}W_{\sup,LH}$$

with $f_{//,ICRH}=\frac{1}{3}\left(1+max\left(0,\tanh\left(\frac{E_{inj,ICRH}}{E_{c,ICRH}}\right)\right)\right)$

that gives consistent result for JET [ref: L.G. Eriksson, private communication]

and with $f_{//,NBI}=\frac{1}{3}+\frac{2}{3}\sin(\theta_{pitch})max\left(0,\tanh\left(\frac{E_{inj,NBI}}{E_{c,NBI}}\right)\right)$

that comes from a fit of the SINBAD *[Feng, Wolle]* code results in CRONOS.

The factor $\frac{1}{3}$ applied to LHCD is determined by simulations made with the LUKE code *[J. Decker, private communication]*.

3.7- Radiation

3.7.1- Introduction

The radiative losses play a key role in discharge prediction. The line radiation is always important. For ITER and other high-temperature devices, the Bremsstrahlung radiation becomes an important loss term and for a reactor the transport of heat by Cyclotron radiation can be a major heat transport mechanism. Additionally, in a reactor, the electron temperature is so high that the relativistic effects must be take into account for Bremsstrahlung radiation.

3.7.2- Line and Bremsstrahlung

The radiative power is computed from the temperature and density profiles of each species using the radiative collisional equilibrium *[Post]*. This gives an estimate of the profile of power radiated by line transition and thermal bremsstrahlung :

$$p_{rad}(t,x)=n_e(t,x)\sum_{k\in\{\text{species}\}} l(Z_k,T_e(t,x))n_k(t,x)$$

This radiative power profile is integrated over the plasma volume to compute the total radiated power $P_{rad}=\rho_m\int_0^1 V' p_{rad}\,dx$.

The total radiated power due to line radiation and bremsstrahlung can be normalized to the Matthews law *[Matthews97, Matthews99]*:

$$P_{rad,mat}=\frac{10^6}{4.5}(Z_{eff}-Z_{main})\left(\frac{\bar{n}}{10^{20}}\right)^{1.89}\frac{S^{0.94}}{Z_{max}^{0.12}}$$

where Z_{main} is the charge number of main plasma ions ($Z_{main}=1$ for hydrogen, deuterium or deuterium/tritium plasma and $Z_{main}=2$ for helium plasma).

Traditionally, a multiplicative factor f_{rad} can be prescribed. We introduce this factor in order to obtain a better match with experiments and to study the effect of radiated power on the fusion power. We notice that the previous expression can be quite inaccurate depending on the plasma scenario.

To calculate the P_{loss} value, we need to separate the bremsstrahlung radiation P_{brem} and the line radiation P_{line} . We use the following expression for the bremsstrahlung radiated power coming from volume integration of local expressions *[Dolan, Rybicki]*:

$$p_{brem}(t,x)=5.355\,10^3\frac{n_e(t,x)}{10^{20}}\sqrt{\frac{T_e(t,x)}{10^3}}\sum_{k\in\{\text{species}\}} Z_k^2\frac{n_k(t,x)}{10^{20}}$$

(with the Gaunt factor equal to 1.2, that gives an accuracy within about 20%)

and

$$P_{brem}=\rho_m\int_0^1 V' p_{brem}\,dx$$

We define :

$$P_{line} = P_{rad} - P_{brem}$$

We neglect here a small correction: low temperature finite Rydberg energy, electron-electron bremsstrahlung and re-absorption, but we introduce the high temperature corrections due to relativistic effects *[Stott]*:

$$P_{brem,rel} = P_{brem} X_{rel}(t,x) \quad \text{where}$$

$$X_{rel}(t,x) = (1+\frac{2T_e(t,x)}{511\ 10^3})(1+\frac{2}{Z_{eff}(t,x)}(1-\frac{1}{1+\frac{T_e(t,x)}{511\ 10^3}}))$$

With the same formulation, we estimate the total radiative loss in the SOL (P_{SOL}) taking an exponential decrease of the profile with a characteristic length of $max(\frac{a_{ref}}{100}, 0.01)$ in m.

3.7.3- Cyclotron radiation

The cyclotron radiation power loss is given by the Albajar scaling *[Albajar01,Albajar02]*:

$$P_{cyclo} = 3.84^{-2}(1-\omega_{ref})^{0.62} R_{ref} a_{ref}^{1.38} K^{0.79} B_{ref}^{2.62} n_{e,c}^{0.38} T_{e,c} (16+T_{e,c})^{2.61}$$
$$(1+0.12 T_{e,c}(\frac{(1-\omega_{ref})}{p_{a,c}})^{0.41\ -1.51}) \quad k_a g_a$$

with

$$g_a = 0.93(1+0.85 e^{-0.82\frac{R_{ref}}{a_{ref}}})$$

$$k_a = (\nu_n + 3.87\nu_T + 1.46)^{-0.79}(1.98+\nu_T)^{1.36}\beta_f^{2.14}(\beta_f^{1.53}+1.87\nu_T-0.16)^{-1.33}$$

and

$$n_{e,c} = n_e(t, x=0)/10^{20}$$

$$T_{e,c} = T_e(t, x=0)/10^3$$

$$p_{a,c} = 6.04\ 10^3 a_{ref} \frac{n_{e,c}}{B_{ref}}$$

where β_f is determined from the best fit of the electron temperature profile with the shape :

$T_{e,s} = T_{e,0}(1-x^{\beta_f})^{\nu_T}$ with $x \in [0, 0.9]$.

ω_{ref} is the effective wall reflection coefficient for cyclotron radiation.

3.8- Bootstrap and resistivity

The plasma neoclassical resistivity and bootstrap current profiles are computed with the help of the Sauter model *[Sauter]* . The total bootstrap current can be normalized to the Hoang scaling law *[Hoang1]*. This quantities are used by the current diffusion solver.

3.9- Moments equilibrium

A MHD equilibrium is mandatory to compute the geometrical coefficients used by the current diffusion solver. In METIS, the equilibrium is defined by moments *[Blank1, Blank2, Lao1]*, i.e., 3 moment equations :

1. the Shafranov shift equation ($\Delta(t,x)$).
2. the ellipticity equation ($K(t,x)$).
3. the triangularity equation $\delta(t,x)$.

The flux surfaces are internally described as :

$$R(t,x,\theta)=R_{ref}(t)+\Delta(t,x)+a_{ref}(t)x\cos(\theta+\arcsin(\delta(t,x))\sin(\theta))$$
$$Z(t,x,\theta)=Z_{ref}(t)+a_{ref}(t)K(t,x)x\sin(\theta)$$

where θ is a poloidal angle.

When the LCMS is given by points, a correction is applied on the shape of the flux surfaces. The morphing function use to correct the shape is

$$R_m=\rho_m\cos(\theta_m)+R_{axe}$$
$$Z_m=\rho_m\sin(\theta_m)+Z_{ref}$$

where

$$R_{axe}(t,x)=R_{ref}(t)+\Delta(t,x)$$

$$\rho_m=\rho_x f_m \quad \text{and} \quad f_m(t,x,\theta_m)=(1-x^{\alpha_m})+x^{\alpha_m}\frac{\rho_{DSMF}(t,\theta_m)}{\rho_s(t,\theta_m)}$$

and with

$$\rho_{DSMF}(t,\theta_m)=\sqrt{(R_{DSMF}(t,\theta_m)-R_{ref}(t))^2+(Z_{DSMF}(t,\theta_m)-Z_{ref}(t))^2}$$
$$\rho_s(t,\theta_m)=\sqrt{(R(t,x=1,\theta_m)-R_{ref}(t))^2+(Z(t,x=1,\theta_m)-Z_{ref}(t))^2}$$
$$\rho_x(t,x,\theta_m)=\sqrt{(R(t,x,\theta_m)-R_{axe}(t,x))^2+(Z(t,x,\theta_m)-Z_{ref}(t))^2}$$

The morphing exponent α_m is prescribed as a METIS parameter. Whenever the equilibrium computation does not converge, the equilibrium is recomputed with $\alpha_m=0$ and if globally the current diffusion does not converge, the value of α_m is decreased. The best value of α_m , that depends on the tokamak shape, can be determined by comparing the results with those of the HELENA code *[Huysmans1]* (using the function "z0dhelena.m").

When the flux surface shape is known, the flux-averaged quantities needed to solve the current diffusion equation are easily computed by direct numerical integration. For a greater numerical precision, the edge value of C2 is renormalized :

$$C2(\rho_m)=\frac{8\pi^3\mu_0 I_p}{R_{ref}B_{ref}V'(\rho_m)\langle\frac{1}{R^2}\rangle|_{\rho_m}}q_{eff}$$

using the following fit for q *[ITER2]*:

$$q_{eff}=\frac{5a^2B_{ref}}{I_P/1e6\,R_{ref}}\frac{(1+K_{ref}^2)}{2}[1+(\frac{a_{ref}}{R_{ref}})^2(1+\frac{(\beta_P+\frac{l_i}{2})^2}{2})]$$
$$(1.24-0.54\,K_{ref}+0.3(K_{ref}^2+d_{ref}^2)+0.13\,d_{ref})$$

The effective trapped fraction (f_{trap}) is computed with the help of Lin-Liu formulation [Lin2]. Magnetic field values are directly computed from equilibria.

3.10- Current diffusion

The most difficult quantity we have to evaluate in METIS is the safety factor. Many effects are related to the safety factor shape and value. To this end, a fast current diffusion solver has been implemented in METIS.

We solved the same current diffusion equation as in CRONOS *[CRONOS],* allowing to compute the poloidal flux evolution. The current sources are described in this document and the resistivity is given by the Sauter formulation. We use a finite difference solver that works either in the Crank-Nickolson mode or in a fully implicit mode (it is the same scheme as in CRONOS, but on a 21 points radial grid only). The evolution of the poloidal flux is computed time by time. Whenever the solver does not converge at a given time slice in the Crank-Nickolson mode, the evolution is re-computed in the fully implicit mode.

The mean effect of sawteeth can be simulated by a clamping of the poloidal flux :

$$\frac{\partial\Psi}{\partial x}|_{clamp}=max(\frac{\partial\Psi}{\partial x},\frac{\partial\Psi}{\partial x}|_{st})\quad\text{for}\quad x\in[0\,x_{trig}]\quad\text{with}$$
$$x_{trig}=max(\{x\in[0\,1]/\frac{\partial\Psi}{\partial x}<\frac{\partial\Psi}{\partial x}|_{st}\})$$

where $\frac{\partial\Psi}{\partial x}|_{st}=-\frac{FV'\langle\frac{1}{R^2}\rangle}{4\pi^2\rho_m q_{st}}$

q_{st} is the value of safety factor at which sawteeth occur , V' the volume element and F the diamagnetic function.

The plasma current cannot become negative in current hole due to an MHD instability*[Huysmans2]*. This feature is simulated by a modification of the poloidal flux. The current hole is associated with a very high safety factor. We used the following formulation :

$$\frac{\partial\Psi}{\partial x}|_{hole}=min(\frac{\partial\Psi}{\partial x},\frac{\partial\Psi}{\partial x}|_h)\quad\text{for}\quad x\in[0\,x_h]\quad\text{with}\quad x_h=max(\{x\in[0,1]/\frac{\partial\Psi}{\partial x}>\frac{\partial\Psi}{\partial x}|_h\})$$

where $\frac{\partial \Psi}{\partial x}|_h = -\frac{F V' \langle \frac{1}{R^2} \rangle}{4\pi^2 \rho_m q_{inf}}$ and we used $q_{inf} = 3\, q_{edge}$

The solver can work either with a given total plasma current or with an imposed loop voltage. The edge limit condition is chosen depending on the simulated mode.

From the poloidal flux, we compute the plasma current, the diamagnetic function and the parallel electric field. The formulas are the same as in CRONOS.

3.11- Loop voltage control

METIS can work either in prescribed current, prescribed loop voltage or prescribed edge flux. The free decay phase, corresponding to the free decay of current plasma at the end of the shot used on some tokamak, is not described in METIS *[Mikkelsen2]*. In the default mode the current is prescribed. When the key controlling the loop voltage mode is set to "prescribed loop voltage" or "zero loop voltage", the solver switches to the prescribed loop voltage when the loop voltage drops below the reference value and comes back to the prescribed current when the loop voltage is above 1.2 times the reference value. When the key controlling the loop voltage mode is set to "prescribed flux", the input reference Ψ_{ref} is used as a boundary condition in the current diffusion solver. The initial edge value of the flux profile is set to 0 the first time.

3.12- Runaway electron current

The purpose of the model included in METIS is not to describe the disruption but the influence of runaway electrons on current diffusion during the current ramp up *[Mineev]*. The model consists of two parts. The first part evaluates the total current carried by the runaway electrons. The second part gives a coarse estimate of the profile shape. This current is then treated as a source in the current diffusion equation.

The total current is computed using a simple model where the source is given by the first generation runaway electrons birth rate and the time evolution is given by the balance between the runaway electron confinement time and the second generation growth rate *[Jaspers]*:

$$\frac{d I_{run}}{dt} = (\Gamma_{run} - \frac{1}{\tau_{conf}}) I_{run} + S_{run}$$

where the source is :

$$S_{run} = e\, v_{e,crit} (\langle n_e \rangle - \langle n_{trap} \rangle)\, \nu_{ee} S_{//}$$

$S_{//}$ is given by the formula 4 of reference *[Jayakumar]* in which the correction proposed by Rosenbluth for toroidal plasma *[Rosenbluth2]* is included. We also assume that the average runaway creation velocity is the critical velocity ($v_{e,crit}$, formula 1 of reference *[Jaspers]*) and that only passing electrons carry the current (i.e. : $\langle n_{trap} \rangle = \langle n_e f_{trap} \rangle$).

The confinement time is assumed to be of the same order as the energy confinement time : $\tau_{conf} \approx \tau_E$. Moreover, the second generation growth rate (Γ_{run}) is given by the formula 18 in reference *[Rosenbluth2]*.

For the runaway current profile shape, we assume that the current density is proportional to the source S_{run} , computed using profiles instead of volume averaged values.

3.13- Transport equations

3.13.1- Introduction

METIS treats the heat transport, the density profile and the plasma rotation in different ways. The heat transport is split in 2 parts : a time dependent equation, that computes the energy content of the plasma, and the space dependent equation (scaled on the global plasma energy content) that gives temperature profiles. Edge and pedestal values are both deduced from scaling laws. The electron density profiles are completely deduced from prescribed line-average density, peaking factor and edge value scaling laws. Ion density profiles are all proportional to the electron density and deduced from prescribed effective charge, isotopic composition and ratio between densities of the various impurities (only when impurity accumulation is turned on, the density profile of the heaviest impurity is not assumed to be proportional to the electron density). The bulk plasma rotation velocity is given by a scaling law and its radial profile is assumed to be proportional to the ion temperature. In the next sections, the detailed models used in METIS for temperatures, densities and rotation computation are presented.

3.13.2- Heat transport and temperatures prediction (including T_i over T_e prediction)

The heat transport in METIS is solved by splitting the problem in two parts. The first part consists in deducing the energy content from a given scaling by solving the simple ODE :

$$\frac{dW_{th}}{dt} = -\frac{W_{th}}{\tau_E} + P_{loss}$$

The second part consists in solving the time independent transport equations :

$$\frac{\partial T_e}{\partial x} = \frac{-\int_0^x V' Q_e}{\kappa_e V' \langle |\nabla \rho|^2 \rangle} \quad \text{and} \quad \frac{\partial T_i}{\partial x} = \frac{-\int_0^x V' Q_i}{\kappa_i V' \langle |\nabla \rho|^2 \rangle}$$

where Q_e and Q_i are the sum of all the electron and ion heat source terms (as defined for CRONOS), including the equipartition term Q_{ei} that is proportional to $T_e - T_i$.

To this end, we have assumed :

$$\kappa_e = \kappa_0 (1 + K_E x^2) \quad \text{and} \quad \kappa_i = \mu_{e,i} \kappa_e$$

where $\mu_{e,i}$ is a scalar that is prescribed or that can be deduced from a simple model (described hereafter) and K_E is a shape scalar factor that is generally taken equal to 3 (as for ITER simulation *[ITER7]*).

The constant κ_0 is found from the solution of $\frac{3}{2} \rho_m \int_{x=0}^{1} (n_e T_e + n_i T_i) V' dx = W_{th}$

The equations for the temperatures are solved using the edge temperatures computed from the edge model described in next chapter. In H mode, the temperatures at the top of pedestal are computed in order to retrieve the predict pressure P_{ped} .

A convergence loop is performed to find the correct value of the equipartition term.

3.13.3- Balance between ion and electron transport

The transport balance between electron an ion heat transport channels is governed in METIS only by a scalar quantity ($\mu_{e,i}$) that is generally prescribed. A simple model *[Weiland, Asp1, Asp2]* can also be used, in which a profile-averaged value of this scalar is computed :

$$\mu_{e,i}=3.5\sqrt{\frac{T_i(t,x=0)}{T_e(t,x=0)}}\left(1+\tanh\left(\frac{\frac{R_{ref}}{L_{Ti}}-\frac{R_{ref}}{L_{Ti,th}}}{\frac{R_{ref}}{L_{Te}}}\right)\right) \quad \text{where}$$

$$\frac{R_{ref}}{L_{Ti,th}}=\frac{2}{3}\frac{R_{ref}}{L_{ne}}+\frac{20}{9}\frac{T_i(t,x=0)}{T_e(t,x=0)} \quad ,$$

$$K_t=\frac{f_{trap}(t,x=1)}{1-f_{trap}(t,x=1)} \quad , \quad L_{Ti}^{-1}=\frac{T_i(t,x=0)-T_i(t,x=x_{ped})}{\rho_m T_i(t,x=0)} \quad ,$$

$$L_{Te}^{-1}=\frac{T_e(t,x=0)-T_e(t,x=x_{ped})}{\rho_m T_e(t,x=0)} \quad \text{and} \quad L_{ne}^{-1}=\frac{n_e(t,x=0)-n_e(t,x=x_{ped})}{\rho_m n_e(t,x=0)} \quad .$$

The free coefficient 3.5 has been adjusted by comparison with JET and Tore Supra discharges. We assue that the electron turbulence in never stabilized when the ion turbulence in not stabilized (otherwise we can not define the ratio between ion and electron transport with a so simplified model, since the turbulence threshold for electron turbulence must be included). It is also assumed that the dependence of transport coefficients with respect to the safety factor profile is the same for electrons and ions.

3.13.4- Electron density profile

The shape of the density profile in METIS is simply described by three free parameters : the line-averaged density ($\bar{n}$) that is prescribed, the peaking factor (ν_n+1) that is prescribed or computed with the help of a scaling law and of the edge value ($n_{e,a}$) obtained from a simple model.

In L mode the shape of the profile is defined as :

$$n_e(t,x)=(n_{e,0}(t)-n_{e,a}(t))(1-x^2)^{\nu_n(t)}+n_{e,a}(t)$$

where $\nu_n=\frac{n_e(t,x=0)}{\langle n_e\rangle(t)}-1$.

In H mode, in order to ensure that the pedestal is also present in density profiles, the density profile is computed by another method. The density profile is constrained by the given volume averaged value, the peaking factor and the constraint of 0 derivative at the centre . The edge value is obtained separately. This information allows to define a unique density profile. We use a piecewise cubic Hermite polynomial interpolation to compute the other points.

The density peaking factor is computed from a scaling law or prescribed.

The first choice consists of directly giving the value. The 2nd choice consists of assuming a flat

profile. Others choices are based on fits of experimental data.

Two regimes are considered :

- In L mode, the observations show, depending on the tokamak and the discharge scenario, either a link with the safety factor [Hoang2] or a good correlation with the ratio between the so called saturation density *[Wesson7]* and the line-integrated density.
- In H mode, the experimental peaking factor can be well correlated with the Greenwald fraction *[Borrass, Wiesen1]* or with the normalised collisionality *[Weisen2]* .

Therefore, the choices in the METIS code are, in L-mode :

1. a given value $\nu_n = \nu_{ref}$
2. a peaking factor 0.01 , for a flat profile
3. a density profile proportional to the square root of the safety factor profile *[Isichenko, Boucher]* :
   $$\frac{\nabla n_e}{n_e} \propto \frac{\nabla q}{q} + O\left(\frac{\nabla T}{T}, ...\right)$$
   according to *[Weisen3],* the best approximation for the peaking factor is:
   $$\nu_n = \left(\frac{4}{3} l_i + \frac{1}{4}\right) - 1 \quad .$$
4. as a function of the ratio between the so called saturation density *[Wagner, Becker]*, and the line-integrated density :
   $$\nu_n = 0.5 \frac{n_{sat}}{\bar{n}}$$
   with $n_{sat} = 0.06\, 10^{20} \left(\frac{I_p}{10^6}\right) R \frac{\sqrt{A_{main}}}{K a^{(5/2)}}$ *[Wesson7]*

In H-mode :

1. a given value, typically the half of the L-mode value, α_n . It is usually observed that the density profile is flatter in H-mode than in L-mode. With the factor 2 , a quite good match of the density profiles modification between L-mode and H-mode phases in JET shots is obtained.
2. a peaking factor 0.01 , for a flat profile
3. as in L mode, related to l_i : $\nu_n = \left(\frac{4}{3} l_i + \frac{1}{4}\right) - 1$
4. depending on the ratio between the Greenwald density and the line-integrated density *[Wiesen1]* :

$$\nu_n \simeq 0.23 \frac{n_{Gr}}{\bar{n}}$$

with

$$n_{Gr} = 10^{20} \frac{I_p 10^{-6}}{\pi a^2}$$

5. depending on the normalized collisionality *[Weisen2]* :

$$\nu_n = 0.28 - 0.17 \ln \nu_{eff}$$

with

$$\nu_{eff} = 1\text{e-}14\, R\, Z_{eff} \frac{\langle n_e \rangle}{\langle T_e \rangle^2}$$

The edge electron density value $n_{e,a}$ computation is described in the section 3.13.5.

Another possibility, is to assume the density profile proportional to the ion temperature profile : $n_e(t,x) = C_e(t)(T_i(t,x) - T_i(t,x=1)) + n_{e,a}(t)$ where $C_e(t)$ is computed in order to retrieve the prescribed value of $\bar{n}$.

In order to take into account the time delay between gas injection and plasma response, the reference value of $\bar{n}$ is replaced by the solution of :

$$\frac{d\bar{n}}{dt} = -\frac{\bar{n}}{\tau_{ne}} + \frac{\bar{n}_{ref} + \frac{P_{NBI}}{E_{inj} \gamma_n V_P}}{\tau_{ne}}$$

where γ_n is a shape factor, precomputed from the density profile shape, defined as $\gamma_n \equiv \frac{\langle n_e \rangle}{\bar{n}}$.

We choose $\tau_{ne} = 2\tau_E$ which gives a good agreement for Tore Supra between the reference value $\bar{n}_{ref}$ and measurements by interferometry.

Additionally, the $\bar{n}_{ref}$ can be controlled in order to limit the radiative power fraction to, e.g., 80%.

3.13.5- Edge values estimation

3.13.5.1- Introduction

In order to close the system of equations, we must add a description of the edge (and Scrape-Off Layer). We use in METIS a simple model to predict the density and temperature at the edge (and also on the divertor / limiter). The configuration is described by a parameter that allows to choose the configuration in limiter or in divertor mode.

We define L_C as the connexion length and we have *[Tsitrone]*:

$L_C = \pi R_{ref} q_{edge}$ for a toroidal limiter

$L_C = \pi R_{ref}$ for a poloidal limiter

and

$L_C = \sqrt{L_{LCMS}^2 + (5\pi R_{ref} q_{edge})^2}$ with an X point

3.13.5.2- Edge density

The edge density is given by

1. an adapted multi – machine law in H mode and X point configuration *[Mahdavi]*:
   $n_{e,a} = C_n \bar{n}_l^2$ with $C_n = 5\,10^{-21} - 6.7\,10^{-24} T_{e,a}$ and $C_n \geq 10^{-21}$
   where $\bar{n}_l = min(\bar{n}, n_{Gr})$
2. in L mode in X point configuration by *[Porter]*:
   $n_{e,a} = 0.00236 \bar{n}_l^{1.08} K_{ref}^{1.11} B_{ref}^{0.78}$
3. in L mode with a toroidal limiter by the Tore Supra scaling law *[F. Clairet , private communication]*:
   $n_{e,a} = 1.0\ 10^{-21} \bar{n}_l^2 q_{edge} R_{ref}$
4. in L mode with a poloidal limiter by the multi-machine law *[Wesson8]*:
   $n_{e,a} = 5\ 10^{-21} \bar{n}^2$

3.13.5.3- Edge temperature

In H mode (supposed to be associated with a divertor configuration) , the following model is used *[Erents1, Erents2]*:

$T_{e,a} = 1.18\ 10^{-7} T_{e,d}^{0.2} [n_{e,a} L_c (1 - \frac{F_{SOL}}{2})]^{0.4}$ where $F_{SOL} = \frac{P_{rad,SOL}}{P_{loss}}$ is the fraction of radiative power loss in the SOL

and the "divertor temperature" [Kukushkin]:

$T_{e,d} = 15(1 + f_{Pellet})$ where f_{pellet} is the fraction of fuelling coming from pellet injection.

and the link between temperature and density is assumed to be *[Stangeby]*:

$$n_{e,d} = \frac{1}{2} n_{e,a} \frac{T_{e,a}}{T_{e,d}}$$

that gives an estimate of density on the divertor.

In L mode (supposed to be associated with a limiter), we used the following model *[Erents2, Cohen, Stangeby]*:

$T_{e,a} = (\frac{P_{LCMS}}{n_{e,a} \omega_{\lim} 2\gamma_{tr} \lambda_{SOL} e c_s})^{\frac{2}{3}}$ where $P_{LCMS} = P_{loss} - (1 - \lambda_{line}) P_{line}$ is the power convected to the separatrix and $c_s = \sqrt{\frac{e(\langle \frac{T_i}{T_e} \rangle + \langle Z_{eff} \rangle)}{m_{eff}}}$ is the speed of sound.

$\gamma_{tr}=7$ is the sheath heat transmission coefficient and we take $\lambda_{SOL}=\frac{a_{ref}}{100}$ as a characteristic SOL decay length and the characteristic wet length ($\omega_{\lim}$) is *[Stangeby]*:

1. for toroidal limiter : $\omega_{\lim}=\frac{2\pi R_{ref}}{q_{edge}}$
2. for poloidal limiter : $\omega_{\lim}=L_{LCMS}$

finally we take $T_{e,d}=T_{e,a}$ and $n_{e,d}=\frac{1}{2}n_{e,a}$

3.13.5.4- Estimation of peak power on divertor

For reactor studies we include a quite simple fit to estimate the peak power deposition on the divertor *[Pacher, and J. Johner , private communication]*:

$$P_{\text{peak,div}}=1.02\ 10^{30}\frac{q_{ped}^{0.52}R_{ref}^{0.33}}{n_{e,a}^{1.82}}\left(\frac{P_{\lim}}{S_{\text{ext}}}\right)^{2.37} \quad \text{with} \quad P_{\lim}=P_{\text{in}}-P_{line}-P_{brem}-P_{cyclo}-P_{SOL}$$

3.14- ITB and MHD effects

3.14.1- Introduction

To some extent, it is possible to simulate with METIS internal transport barriers (ITB) and some simple MHD effects.

3.14.2- Internal transport barriers

The effect of ITB in METIS is separated in two parts : the first is the increase of the plasma energy content by the modification of the H_{ITB} parameter and the second is the change in the transport coefficient shape. The two mechanisms must be consistent. The ITB mechanism in METIS is based on magnetic shear effect and Shafranov shift effect *[Garbet1]*. The effect of the toroidal rotation, density peaking and impurity content is not included so far. The effect of hot ions confinement enhancement is treated separately.

The standard transport coefficient shape , i.e. without ITB is

$\kappa=(1+K_E x^2)$

The transport coefficient shape with ITB become [Waltz, Maget]:

$$\kappa_{ITB}=\frac{f_s(q,\alpha(P,q))}{f_s(\bar{q},\alpha(P,\bar{q}))}(1+K_E x^2)$$

with :

$$f_s(q,\alpha)=\mathrm{e}^{\frac{-\left(s-\frac{3}{5}\alpha-\frac{1}{2}\right)^2}{2}} \quad \text{where} \quad s=\frac{x}{q}\frac{dq}{dx} \quad \text{and} \quad \alpha=-\frac{2\mu_0 R_{ref}q^2}{\rho_m B_{ref}^2}\frac{dP}{dx} \quad \text{,with} \quad P=e(n_e T_e+n_i T_i)$$

The effect of ITB is due to the difference in f_s for the true safety factor (q) and the monotonic

safety factor ($\bar{q}$). The monotonic safety factor is :

$\bar{q}=min(q)+x^{\upsilon_q}(q(x=1)-min(q))$ and υ_q is computed to minimize $\int_{x_{qmin}}^{1}(q-\bar{q})^2 dx$ with x_{min} is the most external position where $q=min(q)$.

The plasma energy content enhancement is computed by integrating the steady state transport equation for the cylindrical geometry and assuming that the density profile is flat, i.e.:

$$H_{ITB}=(\int_0^1 dx' \int_1^{x'} dx'' \frac{\int_0^{x''} dx''' (Q_e+Q_i)x'''}{\chi_{ITB}} x')/(\int_0^1 dx' \int_1^{x'} dx'' \frac{\int_0^{x''} dx''' (Q_e+Q_i)x'''}{\chi} x')$$

where Q_e and Q_i are the total heat sources respectively for electrons and ions, as defined in CRONOS *[CRONOS]*.

3.14.3- Hot ions confinement enhancement

In some tokamak experiments, when ion heating is dominant, the confinement is found to be enhanced *[Fonck, Bush]*. To simulate this effect, the following prescription is used :

$$H_{hot}=\tanh(\frac{P_{th,ion}}{3P_{\Omega}})\tanh(\frac{\langle T_i\rangle}{\langle T_e\rangle}\frac{(P_{th,ion}-P_{th,el}+P_{ei})}{(P_{th,ion}+P_{th,el})}) \quad \text{with} \quad P_{e,i}=\rho_m\int_0^1 Q_{ei}V'dx \ .$$

Generally, H_{hot} is added to H_{ITB} .

3.14.4- MHD beta limit

An empiric rule links the maximal sustainable value of β_n and the internal normalized inductance l_i *[Sabbagh]*. A limitation mechanism of β_n is implemented in METIS and can be turned on :

$$H_{MHD}=1-\tanh(3\frac{\beta_N-f_{MHD}l_i}{\beta_N}) \quad \text{for} \quad t\geq t_{MHD} \quad \text{,otherwise} \quad H_{MHD}=1$$

3.14.5- MHD q_0 instability

Various MHD instabilities, associated with reversed safety factor profile, reduce the plasma confinement. These instabilities are due to the double crossing of rational surfaces by the safety factor or by a strongly reversed q profile *[Zabiego]*. To mimic this behaviour, following prescriptions are available in METIS :

$$H_{MHD}=H_{MHD}(1-e^{-\frac{|q_0-q_{mn}|}{\delta_q}}x_{mn}^2) \quad \text{when} \quad q_0>1.1q_{min} \quad \text{for} \quad q_{mn}\in\{\frac{3}{2},2\}$$

with $q_0=q(x=0)$, $q_{min}=\min_{x\in[0,1]}(q(x))$ and $x_{mn}=\{x\in[0,1]/\,q(x)=q_{mn}\}$

and with $\delta_q=q_a\delta_x$ where δ_x is the step width of the radial grid.

For confinement decrease due to sawteeth :

$$H_{MHD}=H_{MHD}q_0x_1^2 \quad \text{when} \quad q_0<1$$

and for strongly negative shear :

$H_{MHD} = H_{MHD}(1 - \tanh(q_0 - q_{min} - 3)x_{qmin}^2)$ when $q_0 > (q_{min} + 3)$

with

$x_{qmin} = \{x \in [0,1] / q(x) = q_{min}\}$.

Remark : the effect is proportional to the volume of the plasma included within the radius of the selected value of the safety factor.

3.14.6- MHD rational surface confinement enhancement

ITB are often triggered when the ITB foot location corresponds to a low order rational safety factor value *[Garbet2, Joffrin2, Neudatchin]*. In order to get the correct time for ITB triggering, we need to help the transition by decreasing the transport when the minimum value of the safety factor crosses a low rational value. The mechanism implemented in METIS is the following :

$$\delta_H = \sum_{q_{mn} \in \{1, \frac{3}{2}, 2\}} \mathrm{e}^{-\frac{|q_{min} - q_{mn}|}{\delta_q}} x_{mn}^2$$

if $\delta_H < 0.1$ then $H_{ITB} = H_{ITB} + \delta_H$ else $H_{ITB} = H_{ITB} + 0.1$

3.14.7- Transport modification due to sawteeth

Sawteeth effect on the plasma energy content is generally already taken into account either in scaling laws or in the MHD confinement factor (H_{MHD}). We have to add the effect also of the transport coefficients shape on flattened pressure profiles:

$\kappa \to \kappa\{1 + \frac{1}{2}(K_{ST} - 1)[1 + \tanh(g(q_{ST} - q))]\}$, where K_{ST} is the flattening factor and g adjusts the sharpness of the transition (set to 30 by default).

3.15- Rotation

In this version of METIS, the toroidal rotation and the radial electric field have no coupling with the confinement of plasma and of fast ions. The rotation is computed out of the main loop of METIS. It is evaluated only to have an estimate to compare with experiments or code simulation results. Only the effect of neutral beam injection and of the spontaneous rotation are considered. Toroidal rotation due to ripple and fast ions losses and due to fast ion momentum transport are not taken into account. For these terms, no simple model is available, and the complete model is beyond the scope of a tool like METIS. The simple model implemented in METIS is sufficient for the study of NBI dominated plasmas, as well as for reactor studies, in which the fast alpha distribution is close to be isotropic and does not allow to transport a significant part of toroidal momentum (as seen in the simulations performed with SPOT *[Schneider]*). This simplified model does not allow to study plasma rotation when plasma is heated manly by ICRH,when ripple is significant and when the confinement of fast particles is poor (i.e. in small devices).

The computation of the rotation in METIS is separated in two parts. The first part consists in the evaluation of the volume-averaged toroidal momentum. The second part consists in the computation of the radial profiles of toroidal and poloidal rotation velocities and finally of the radial electric field.

The volume-averaged toroidal momentum computation is analogous to that of the energy contents.

The total momentum is :

$$\Re_{tot}=\int_0^1 \sum_{k\in\{species\}} m_p A_k n_k R v_{\phi,k} V' dx$$

where $v_{\phi,k}$ is the toroidal velocity of the species k.

The evolution equation of $\Re_{tot}$ is :

$$\frac{d\Re_{tot}}{dt}=-\frac{\Re_{tot}}{\tau_\phi}+S_{\phi,NBI}+S_{\phi,self}$$

where the confinement time of toroidal rotation , τ_ϕ , is taken proportional to the energy confinement time (τ_E). τ_ϕ includes the friction of the plasma with neutrals at the edge.

Momentum sources are due to :

1. Neutral beam injection toroidal moment source :

   $$S_{\phi,NBI}=R_{ref} m_p A_b \frac{P_{NBI}}{eE_{b0}}\sqrt{\frac{2eE_{b0}}{A_b m_p}}\frac{\langle p_{NBI}\zeta_b\rangle}{\langle p_{NBI}\rangle}$$

   this expression implies momentum conservation, which is true if fast ions losses are negligible.

2. the spontaneous plasma toroidal rotation :

   $S_{\phi,self}=\Gamma_\phi \tau_\phi v_{\phi,self}$ where Γ_ϕ is the conversion factor between velocity and momentum :

   $\Gamma_\phi=\frac{1}{\langle v_{\phi,shape}\rangle}\int_0^1 \sum_{k\in\{species\}} m_p A_k n_k R v_{\phi,shape} V' dx$ where $v_{\phi,shape}$ is assumed to be proportional to $T_i(x)$.

The spontaneous plasma rotation is given by a scaling law *[Rice]* :

$$v_{\phi,self}=0.46\,10^{11} B_{ref}^{1.1} P_\phi^{1.0} I_p^{-1.9} R_{ref}^{2.2}$$

where P_ϕ is the plasma pressure variation.

we choose for P_ϕ the following definition :

$$P_\phi=2\langle eT_i \sum_{k\in\{species\}} n_k\rangle+\frac{2}{3}\frac{(W-W_{th})}{V_p}$$

This expression takes into account the fact that for dominant electron heating *[Fenzi, Manini]*, the spontaneous toroidal rotation changes only because of ion pressure increased and on JET for NBI heated plasma, the thermal pressure is close to 2 times the ion pressure. The last term in P_ϕ takes into account the fast ion pressure that also drives toroidal rotation *[Eriksson03]*.

From $\Re_{tot}$ we deduce the volume-averaged plasma rotation $\omega_\phi=\frac{\Re_{tot}}{\Gamma_\phi R_{ref}}$.

The second part of this calculation consists in an estimation of the radial electric field $E_r(x)$ and poloidal ($V_{\theta,imp}$)and toroidal ($V_{\phi,imp}$) rotation of the main impurity, in the plasma

equatorial plane ($Z=Z_{ref}$) at the low field side. We use the formulation given in the reference *[Artaud]*, assuming that the rotation $\Omega_\phi(x)$ is homothetic to $T_i(x)$ and preserves $\Re_{tot}$. We neglect the friction between species in the computation of neoclassical poloidal rotation and use the following simplified expression *[Helander2]*:

$$V_{\theta,imp}=-\frac{k}{e Z_{imp} B}\nabla T_i$$

where the neoclassical coefficient k is given by the formula 1.31 in reference *[Rozhansky]*.

3.16- Ripple effect for Tore Supra

Since in Tore Supra the magnetic toroidal ripple is large and induces losses of fast particles, we have subtracted from LH and ICRH power (for minority scheme only) the ripple losses. The ripple losses are estimated using scaling laws specifically determined for Tore Supra *[Basiuk04 and V. Basiuk, private communication]*.

3.17- Cold edge neutral source/sink and density transport coefficients estimation

During the initial phase of tokamak discharges, the heat losses due to the ionization of neutrals at the edge of the plasma cannot be neglected.

The computation of the ionization source is separated in two parts. The first part consists in the evaluation of the recycling source (the gas puff is generally a correction to the recycling source and is included in it). The second part consists in the computation of the source shape.

As the density in METIS is prescribed, the recycling source, for a stationary state, is simply given by :

$N_0=\frac{\langle n_e\rangle V_p}{\tau_P}$ where τ_p is the particle confinement time, assumed to be equal to the energy confinement time τ_E (remark : in this case the effective particle confinement time, τ_P^* , is infinite).

We use in METIS a simple model of edge neutral source based on the model developed by P. Laporte for the transport of light neutrals *[Laporte]*. This computation uses tabulated cross sections and the charge exchange propagation is modelled using a diffusion coefficient *[Laporte, Beckurts]*. The source is composed of two terms : the first is associated with cold neutrals (S_0) that come from the wall and have a ballistic propagation before ionization or charge exchange. The second term is the diffusion of hot neutrals ($S_{0,m}$) generated by charge exchange. We superimposed a prescribed Gaussian curve (S_{pellet}) to simulate the effect of pellets. The source is normalized in order to retrieve the total incoming neutrals.

The ionization shrink sink is simply : $P_{ioniz}=E_{ioniz}(S_0+S_{0,m}+S_{pellet})$ with E_{ioniz} the average ionization energy that we take equal to 25 eV *[Stangeby]*.

Once the edge neutral source is computed, we can evaluate the particle transport coefficients. The electron flux can be written as *[CRONOS]*:

$$\Gamma_e = \frac{rh\hat{o}_m}{V'\langle|\nabla\rho|^2\rangle}\int_0^x [V'(S_{NBI}+S_0+S_{0,m}+S_{pellet}) - \frac{\partial V' n_e}{\partial t} + \frac{x'}{\rho_m}\frac{d\rho_m}{dt}\frac{dV' n_e}{dx'}]dx'$$

Then we can identify the pinch (V_e), using the closure relation :

$\Gamma_e = -D_e\frac{dn_e}{d\rho} - (V_e + V_{Ware})n_e$ where D_e is the diffusion coefficient, that we take equal to the electron heat diffusivity χ_e , and V_{Ware} is the Ware pinch *[Ware, Laporte]*.

Remark: These transport coefficients are a simple example of the possible choice for data analysis.

3.18- Reactor cost estimations

In view of optimising the cost of a reactor using the physics models implemented in METIS, we have added a post-processing function that scales the cost of main components using simple scaling arguments (as geometrical dimension , magnetic field etc. ...) *[Hertout]*. Scaling laws are determined in order to fit the projected price of ITER components.

The function gives the cost of components and of electricity using assumptions entered in METIS as parameters. Hereafter is an example of output for a DEMO-C like configuration without ECRH and ICRH system:

TFC_fab = 332.766 {toroidal field coil fabrication}
PFC_fab = 110.403 {poloidal field coil fabrication}
CS_fab = 79.4903 {central solenoid fabrication}
magn_struct = 486.733 {magnet structures}
conductors = 708.577 {conductors}
feeders = 44.7 {feeders}
[magn] = 1762.67

tokamak = 309.327 {tokamak building}
hotcell = 207.841 {hot cell building}
auxilliary = 115.495 {auxilliary building}
radwaste = 41.5682 {radwaset building}
personnel = 7.36022 {personnel building}
laboratory = 17.6645 {laboratory office building}
cryoplant = 44.1613 {cryoplant building}
control = 13.2484 {control building}
emergency = 19.1366 {emergency power supply building}
service = 10.3043 {site service building}
utility = 97.1548 {utility tunnels ans site improvements building}
engineering = 110.403 {engineering managments and others buildings}
[building] = 993.664

vacuum = 353.29 {vacuum vessel}
blanket = 375.965 {blanket}
divertor = 179.032 {divertor}
[vessel] = 908.288

coil = 319.433 {coil power supply system}
steadystate = 85.3785 {steady state power supply system}
[power] = 404.812

remote = 209.41 {remote handling}
assembly = 146.729 {machine assembly and tooling}
cooling = 577.473 {tokamak cooling system}
cryostat = 145.732 {cryostat and thermal shield}
cryoplant = 190.389 {cryoplant and cryodistribution}
balance = 1236.07 {balance of plant}
[machine] = 2505.8

ecrh = 0 {total of ECRH}
icrh = 0 {total of ICRH}
lhcd = 380 {total of LHCD}
nbi = 395.152 {total of NBICD}
[heating] = 775.152

system = 42.6892 {fuelling systems}
tritium = 523.759 {tritium plant}
pumping = 73.5784 {pumping and leaks detection system}
[fuelling] = 640.027

codac = 92.7387 {total of CODAC}
diagnostics = 388.619 {total of diagnostics}
computing = 102.745 {total of computer + simulation}
[control] = 584.103

[cost] = 8574.52 {MEuros @ 2000, +/- 20%}

Warning : following informations are coarse estimations for steady state !
[Electric power(GW)] = 1.09234
[Investment (euros/W)] = 7.84969
[Coe (euros/kWh)] = 0.150056

3.19- Experimental V_{loop} and energy fitting

METIS can adjust the Lower Hybrid current drive efficiency (η_{LH}) and the confinement improvement factor (H_{ref}) in order to fit the loop voltage measurement and the total energy measurement for a given time interval. The algorithm is a simple dichotomy search that performs the minimization of the χ^2 error. This algorithm is included in the main convergence loop.

We define the measured loop voltage as *[Ejima, Lloyd]*:

$$V_{meas} = V_{loop} + \frac{d\rho_m}{dt}\frac{R_{ref}\mu_0 I_p}{4\pi^2\rho_m^2} + \frac{1}{q_a}\frac{d\Phi_a}{dt} \quad \text{with} \quad \frac{d\Phi_a}{dt} = 2\pi\rho_m B_{ref}\frac{d\rho_m}{dt} + \pi\rho_m\frac{dB_{ref}}{dt}$$

3.20- Initial values

With the METIS algorithm, we must provide initial values for all the 0-dimensional variables and for all the profiles to start the simulation. We use various 0-dimensional expressions. These values are important for convergence but are quickly forgotten during the convergence loops. The only important values are the current profile and the loop voltage at the initial time.

3.20.1- Magnetic equilibrium 0D initial quantities

It is useful to remind the definitions of some scalar quantities related to the magnetic equilibrium. In general, we have used the ITER-FDR definitions *[ITER2]*. All input data are only time-dependant.

The poloidal beta is :

$$\beta_P = 8 \frac{W_{Th}}{3 \mu_0 I_P^2 R_{ref}} \frac{(1+K_{ref}^2)}{2 K_a}$$

where W_{Th} is the plasma thermal energy, I_p the plasma current

The effective safety factor at the edge is :

$$q_{eff} = \frac{5 a^2 B_{ref}}{I_P / 1e6 R_{ref}} \frac{(1+K_{ref}^2)}{2} [1 + (\frac{a_{ref}}{R_{ref}})^2 (1 + \frac{(\beta_P + \frac{l_i}{2})^2}{2})]$$
$$(1.24 - 0.54 K_{ref} + 0.3 (K_{ref}^2 + d_{ref}^2) + 0.13 d_{ref})$$

The safety factor at 95 % of the enclosed toroidal flux, in the presence of an X-point (otherwise q_{95} is not defined, q_{eff} is used instead in the formula) is :

$$q_{95} = min(5 a^2 \frac{B_{ref}}{I_P / 1e6 R_{ref}} \frac{1 + 0.95 K_{ref}^2 (1 + 1.9 d_{ref}^2 - 1.14 d_{ref}^3)}{2} \frac{1.17 - 0.65 \frac{a_{ref}}{R_{ref}}}{(1 - (\frac{a_{ref}}{R_{ref}})^2)^2}, \frac{q_{eff}}{1 + 0.25 h})$$

where h = 0 in L-mode and h = 1 in H mode.

For some computations, an initial value of the Shafranov shift is needed *[Lao1, Lao2]*:

$$\Delta = \Delta_0 (1 - x^2) \quad \text{with} \quad \Delta_0 = \frac{a_{ref}^2}{2 R_{ref}} [\frac{2(K_{ref}^2 + 1)}{3 K_{ref}^2 + 1} (\frac{W}{W_{th}} \beta_p + \frac{l_i}{2}) + \frac{1}{2} \frac{K_{ref}^2 - 1}{3 K_{ref}^2 + 1}] (1 - \frac{a_{ref}}{R_{ref}})$$

The initial value of effective trapped electron fraction *[Wesson8]*:

$$f_{trap} = 1 - \frac{(1-\epsilon)^2}{\sqrt{1-\epsilon^2} (1 + 1.46 \sqrt{\epsilon})} \quad \text{with} \quad \epsilon = \frac{a_{ref} x}{R_{ref} + \Delta}$$

3.20.2- Initial plasma current, safety factor and poloidal flux

In a simplified description [Wesson9], the plasma current density can be written as :

$$j_\phi (t, x) = j_0 (t) (1 - x^2)^{\nu_j (t)}$$

and the link with the self inductance l_i is given by :

$l_i = \log(1.65 + 0.89\,\nu_j)$

This formula can be used to compute the exponent knowing the internal self-inductance.

The link between the central safety factor q_0 and the effective edge safety factor q_{eff} is given by

$$\frac{q_{eff}}{q_0} = \nu_j + 1 = \frac{\pi a^2 j_0}{I_p}$$

In this description we have :

$$q_{ini}(t, x) = \frac{2\pi a^2 B_{ref}}{\mu_0 I_P R_{ref}} \frac{x^2}{1-(1-x^2)^{(\nu_j+1)}}$$

This is the initial value of the safety factor profile, computed by taking $l_i = l_{i\,ref}$.

The initial poloidal flux can be computed using the initial value of j_Φ and the first guess for the geometrical coefficients computed using Shafranov shift, constant elongation and triangularity: $\delta = \delta_{ref} x^3$.

3.20.3- Initial loop voltage

The first guess of V_{loop} is simply deduced from the ohmic power :

$V_{loop} = R_R I_\Omega$ where R_R is the plasma resistance defined as : $R_R = \frac{P_\Omega}{I_p}$ with :

$P_\Omega = \rho_m \int_0^1 \eta\, j_\Phi^2 V'\, dx$ where η is the plasma resistivity computed on the base of first guess profiles.

3.20.4- Initial description of temperature and density profile

A simplified description of the profiles is used at the first call of the METIS solver in order to initiate values. Afterwards, a more complete description is used (as described above).

The simplified initial description for the temperature is in L mode :

$$T_e(t, x_k) = (T_{e,0}(t) - T_{e,a}(t))(1 - x_k^2)^{\nu_T(t)} + T_{e,a}(t)$$

where $T_{e,0}$ is the central electron temperature and ν_T is a positive exponent (linked with the peaking factor).

and in H mode :

$$T_e(t, x_k) = (T_{e,0}(t) - T_{e,p}(t))(1 - x_k^2)^{\nu_T(t)} + T_{e,p}(t),\ for\ 1 \leqslant k \leqslant 20$$
$$T_e(t, x_k) = T_{e,a}(t),\ for\ k = 21$$

where $T_{e,a}$ is the edge electron temperature value (i.e., at the LCMS) and $T_{e,p}$ is the electron temperature at the top of the pedestal. For some purposes, it may be necessary to distinguish between the edge and the pedestal temperatures. The pedestal width is fixed at 0.05 of the minor

radius. The value of the pedestal width has no impact for the calculations in the METIS tool.

For the density :

$$n_e(t, x_k) = (n_{e,0}(t) - n_{e,a}(t))(1 - x_k^2)^{\nu_n(t)} + n_{e,a}(t)$$

where $n_{e,0}$ is the central electron temperature and ν_n is a positive exponent (linked with the peaking factor) and where $n_{e,a}$ is the edge electron density value (i.e., at the LCMS). The central values are obtained from the line-averaged reference. All the density and temperature profiles, for the first guess, are assumed to be proportional to the electron density and temperature profiles, respectively.

With this kind of profiles, we have a simple link between central and volume-averaged values :

$n_{e,0} = \langle n_e \rangle (1 + \nu_n)$ and $T_{e,0} = \langle T_e \rangle (1 + \nu_T)$, where $\langle\rangle$ denotes the volume average. The peaking factors are defined as $\frac{n_{e,0}}{\langle n_e \rangle} = (1 + \nu_n)$ for the density and as $\frac{T_{e,0}}{\langle T_e \rangle} = (1 + \nu_T)$ for the temperature.

The initial peaking factors are assumed to be :

$\nu_T = \frac{\tau_{E,Lmode}}{\tau_E} \nu_P - \nu_n$ where, for an initial ohmic plasma :

$$\nu_P = \frac{1}{3} \frac{1 + 4q_a^3 - (1 + 8\ln(q_a))q_a^2 - (4 - 2\ln(q_a))q_a}{(2\ln(q_a) - 3)q_a^2 + 4q_a - 1} + \tanh\left(\frac{\langle T_e \rangle}{\langle T_i \rangle}\right)$$

(Remark: this result is obtain with Maple and verified on measurements for some shots of Tore Supra and JET)

4- Applications

4.1- CRONOS companion tool

METIS is fully integrated in the CRONOS suite of codes. It is possible to :

1. create a METIS data set from a CRONOS data set
2. create a CRONOS input data set from a METIS data set
3. compare a METIS result to a CRONOS result (this can be done both in the METIS and in the CRONOS graphical output environments).
4. Plot any METIS data (0D and profile) with the data viewer of CRONOS (zdatatplot).

METIS is useful in CRONOS to prepare simulations of a new device and to test the consistency of CRONOS results whenever experimental data are not available.

4.2- Tore Supra

Like CRONOS, METIS is directly coupled with the Tore Supra data base and can read either experimental results or shot preparation parameters and references. METIS can be used as a pre-shot simulator or as an experimental analysis tool either on the fly or off-line. In the pre-shot mode, the simulation can be compared to the experimental results of a reference shot. Figures 4 to 9 illustrate the application of METIS to Tore Supra discharge # 33850.

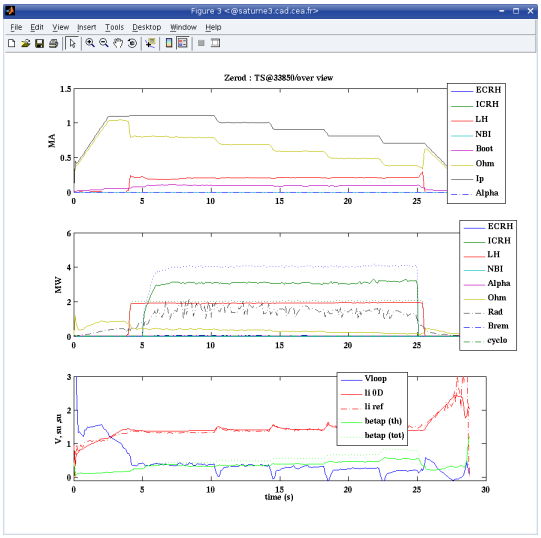

figure 4: Shot overview

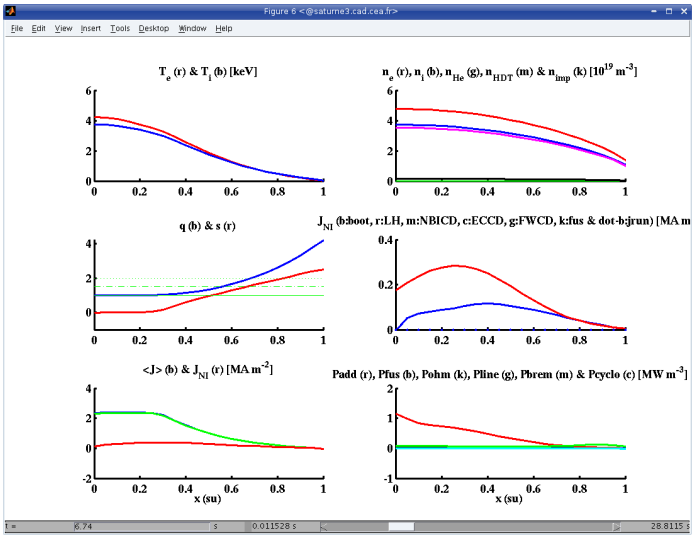

figure 5: main output profiles

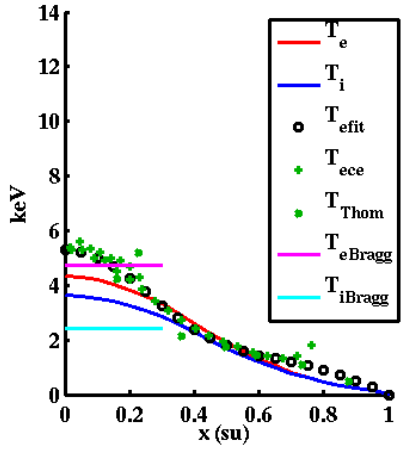

figure 6: comparison of METIS output temperature profiles with experimental data

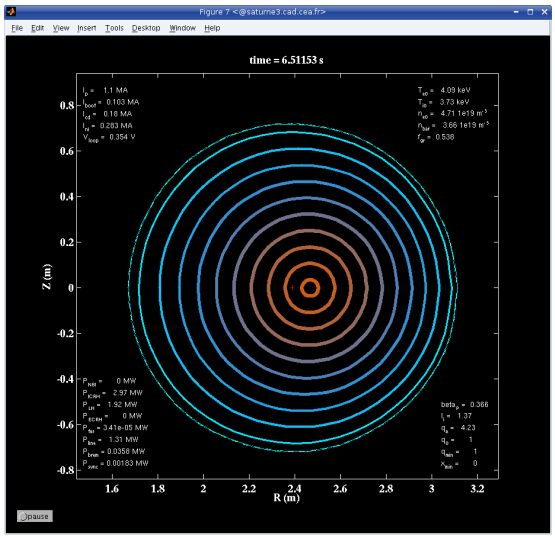

figure 7: METIS visualisation of 2D internal equilibrium

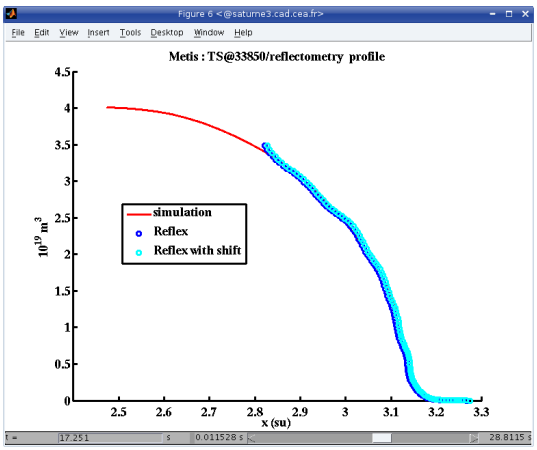

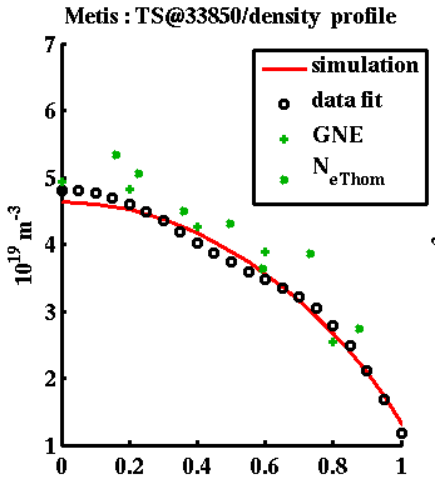

figure 8 and 9: comparison of METIS electron density profiles with experimental data (on left figure: with reflectometry and on right figure : with interferometry)

4.3- JET

METIS can directly read the data of JET through the MDS+ interface (illustrated in figures 10 and 11 for the shot 68413). Some quantities, such as the orientation of neutral beams, which are not read in the data base, must be entered manually. Results can be compared with experimental data through the METIS graphical output.

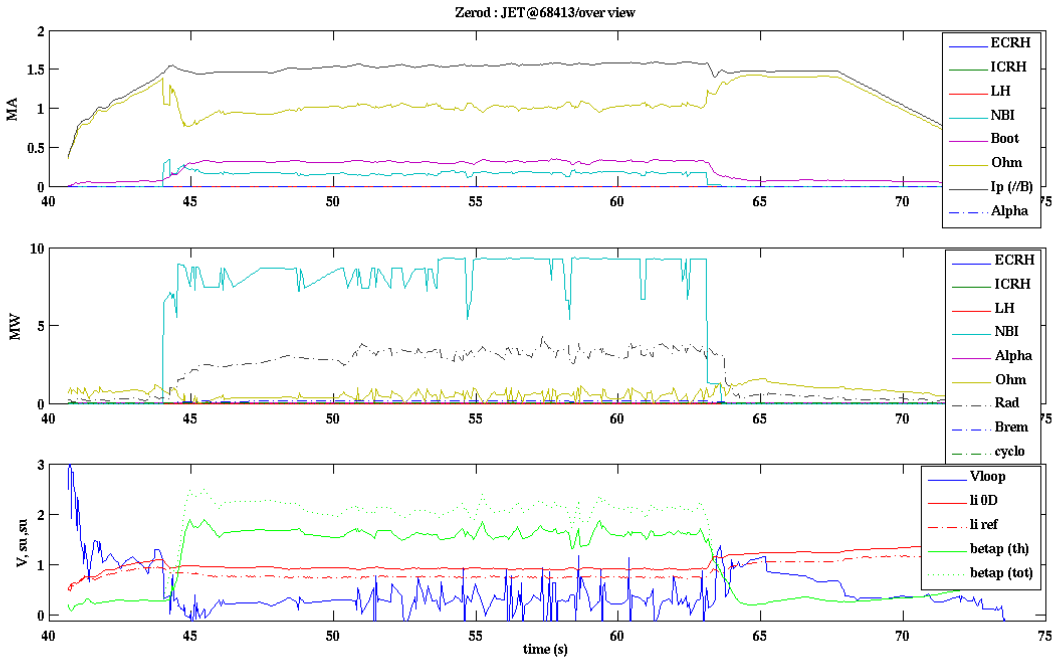

figure 10 : overview of METIS simulation of JET shot 68413

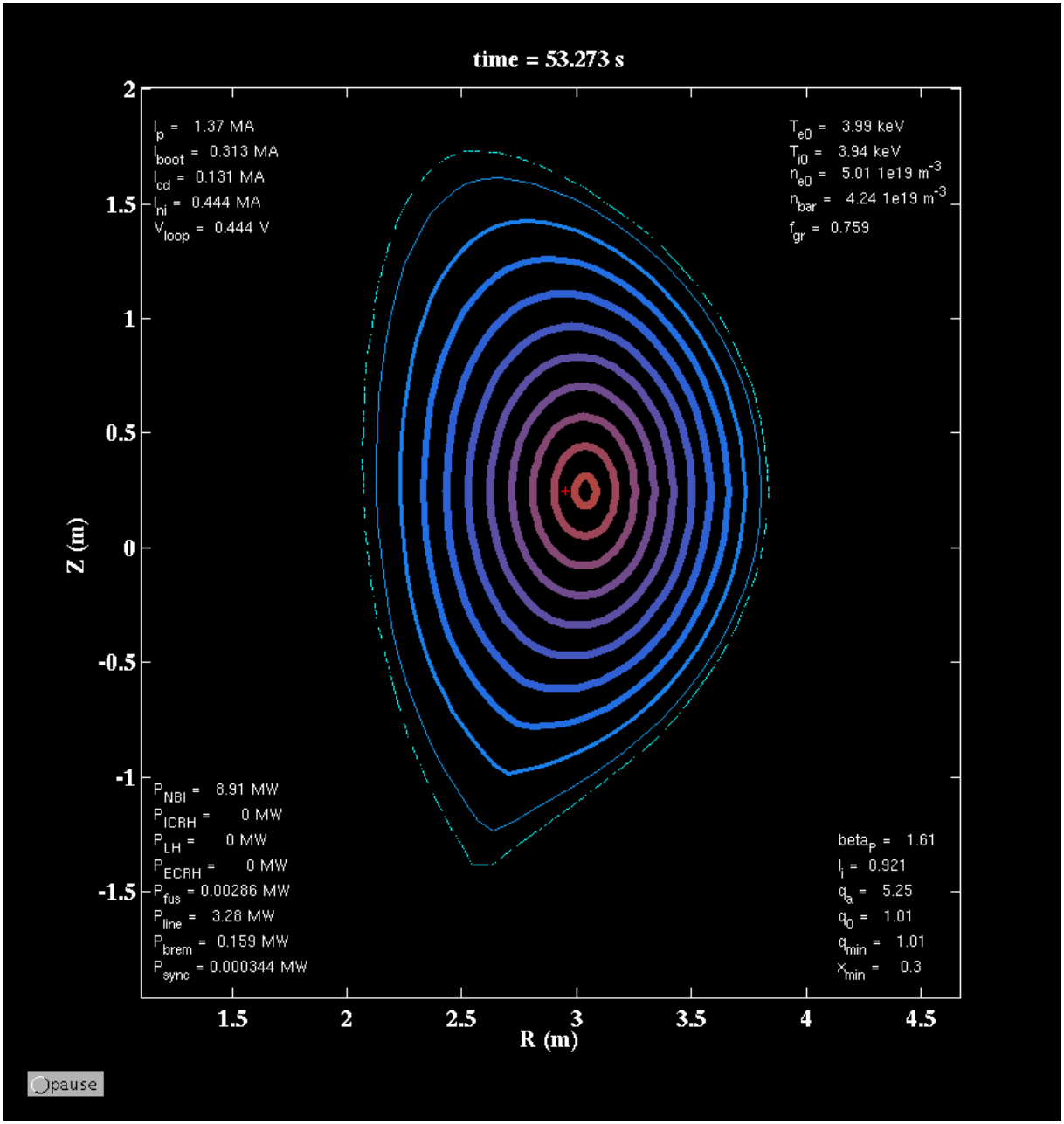

figure 11: equilibrium output at 53.273 s for the shot 68413 of JET

4.4- Designing new devices with METIS

METIS can be used to study scenarios of new devices such as ITER, DEMO, ...
METIS has successfully been used for JET upgrade studies *[Litaudon1]*, JT60-SA design, ITER ramp-up scenarios *[Kim]*, as well as for some reactor studies *[Litaudon2]*.

5- Useful definitions

5.1- CRONOS-inherited definitions

The definition of all quantities that are not defined in this documentation can be found in the technical documentation of CRONOS *[CRONOS]*.

5.2- Physical constants used in METIS

METIS uses the standard normalized physical constants of the IS *[Mohr]*.

name	value	tolerance	unity	comment
c	2.99792458 10^{8}	definition	m / s	vacuum light velocity
μ_0	4 π 10 $^{-7}$	definition	H / m	vacuum permeability
ε_0	$\frac{1}{c^2 \mu_0}$	definition	F / m	vacuum permittivity
h	6.62606876 10^{-34}	+/- 0.0000052 10^{-34}	J * s	Planck constant
α	7.297352533 10^{-3}	+/- 0.000000027 10^{-3}	none	fine structure constant
m_e	9.10938188 10^{-31}	+/- 0.00000079 10^{-31}	kg	electron rest mass
e	1.602176462 10^{-19}	+/- 0.000000063 10^{-19}	C	electron charge
m_p	1.6726485 10^{-27}	definition	kg	proton mass
u_a	1.66053873 10^{-27}	+/- 0.00000013 10^{-27}	kg	atomic unity
g	6.673 10^{-11}	+/- 0.010 10^{-11}	N * m^2 / kg^2	gravitational constant
k	1.3806503 10^{-23}	+/- 0.0000024 10^{-23}	J / K	Boltzmann constant
Д	6.02214199 10^{23}	+/- 0.00000047 10^{23}	mol^{-1}	Avogadro number
σ	5.670400 10^{-8}	+/- 0.000040 10^{-8}	W / m^2 / K ^{4}	Stephan constant

6- METIS user graphical interface

6.1- *Introduction*

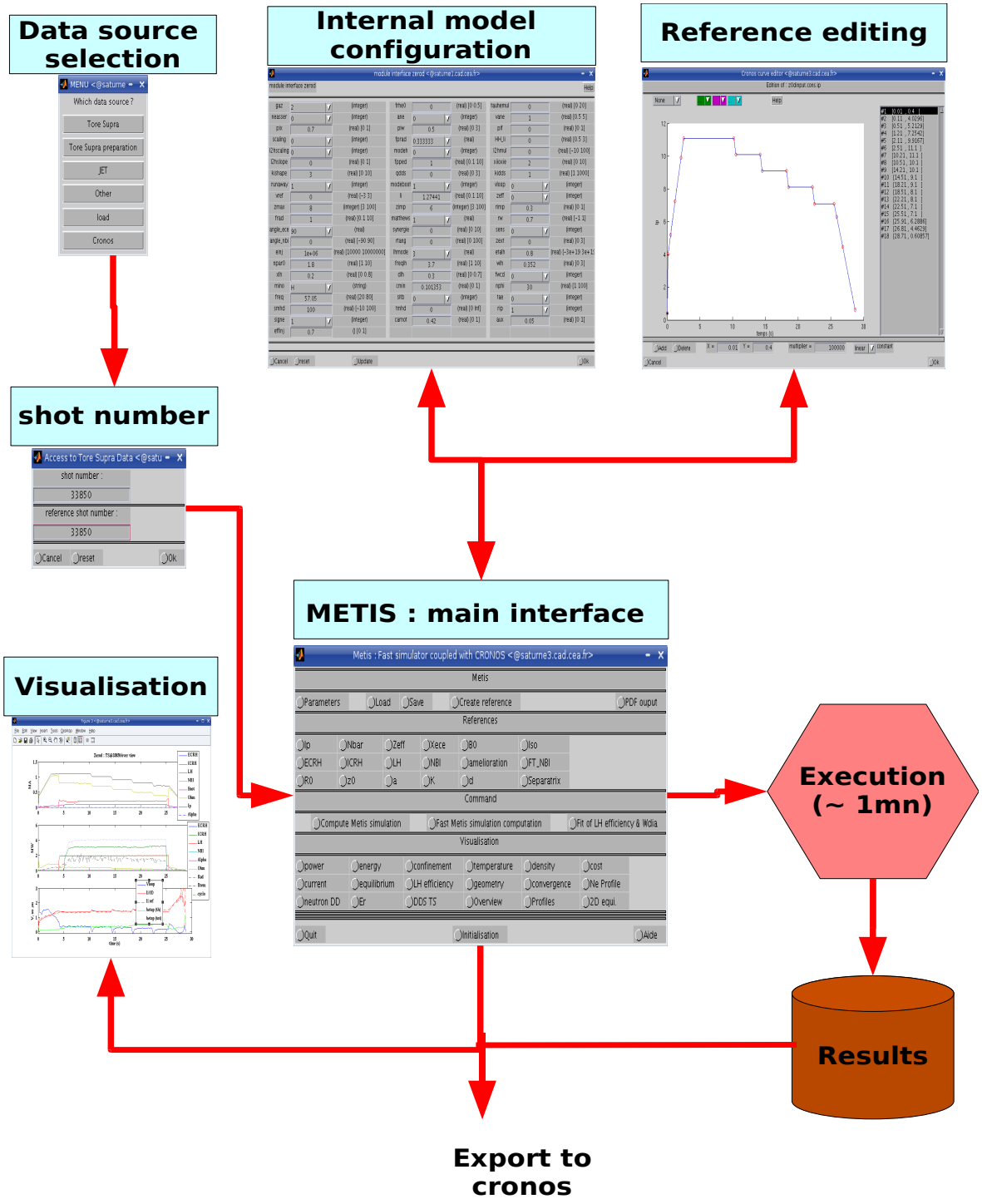

figure 12 : Milestones of a METIS simulation

METIS is completely controllable by its user graphical interface. The main steps of a METIS simulation are to:

1. select a data source
2. read data from a file or from a database
3. edit references
4. edit parameters
5. run simulation
6. visualise results
7. if necessary come back to 3 to adjust input
8. save data to file

Next paragraphs of this chapter give a detailed description of the use of the interface windows.

6.2- Main interface

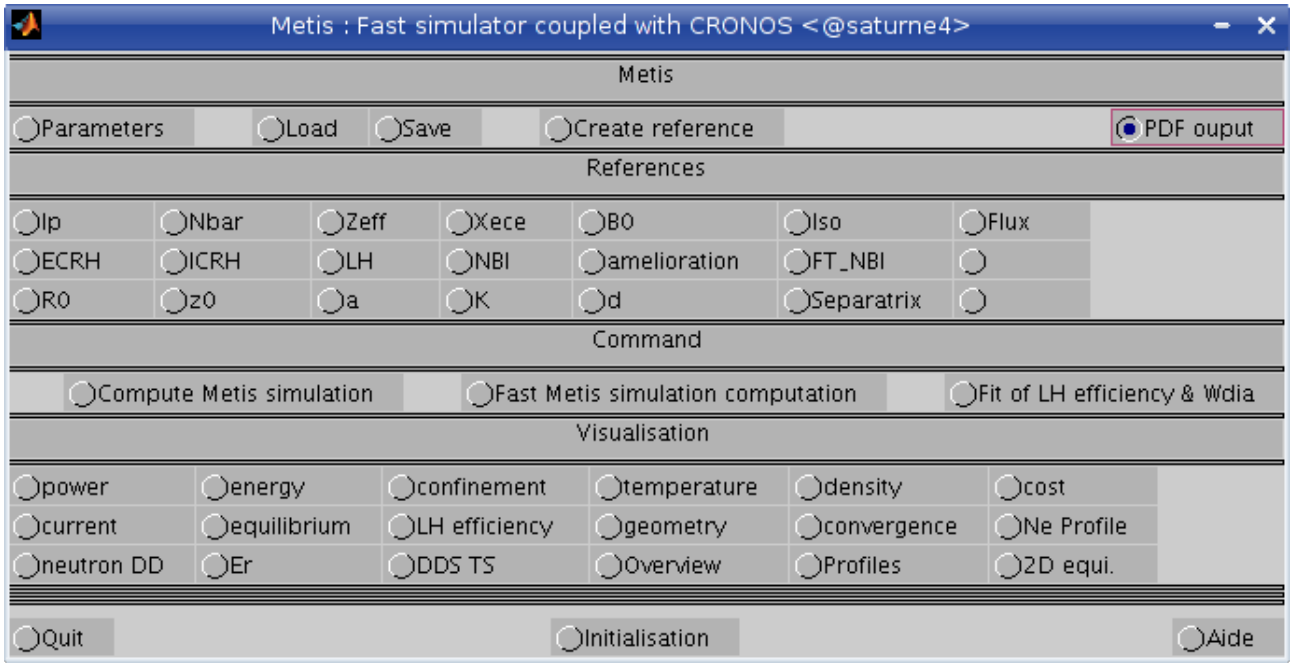

figure 13 : METIS main user graphical interface window

The figure 13 is a copy of the main window of the user graphical interface of METIS. The next paragraphs explain how to use this interface. The buttons of the top row are used to change scalar parameters (“Parameters”), load and save data, make a CRONOS data set for comparison (“Create reference”) and make a PDF document with all the 0D data plots. The second section allows to edit the temporal reference of the shot simulation. The third section commands the calculation. Each button of the fourth section opens a dedicated plot window. In the last section, the “quit” button closes METIS (but not Matlab and does not erase the data); the “help” button opens this document

and the “Initialisation” button creates a data set from the various sources.

6.2.1- METIS initialisation

The “initialisation” button opens a dialogue window that allows to choose the data source :

- “Tore Supra” : the METIS data set is initialised with data read in the Tore Supra data base (TsLib access).
- “Tore Supra preparation” : the METIS data set is initialised using data prepared by the tool “Top” and a reference shot can be used to have experimental data for comparison. If a reference shot is given, the LH source profile uses the Hard X-ray measurements from this shot. The current prepared shot can be accessed using the shot number 0 (Tore Supra standard convention).
- “JET” : the METIS data set is initialised with data read in the JET data base (MDS+ access).
- “Other” : the METIS data set is initialised with empty data. A dialogue window allows the user to specify the time base of the simulation. In this case, the user must edit all the references and enter the parameters.
- “Load” : load data from a previous METIS simulation saved on disk.
- if a CRONOS data set is loaded in the Matlab workspace, the “Cronos” button appears. It allows to initialise the METIS data set from a CRONOS data set stored in the Matlab workspace..

Remarks :

- ✔ If a METIS simulation is already loaded, the user can cancel the first initialisation. In this case, the METIS data set is not erased.
- ✔ The METIS data are in the Matlab workspace and can be handled and modified directly with Matlab commands in the Matlab command line window.

6.2.2- Input/output handle

The button “load” loads a Matlab file containing a METIS data set in the workspace. The “save” button saves the current METIS data set in a Matlab file. The button “Create reference” makes a CRONOS reference data set (in Matlab structure “jeux1”) used to compare a CRONOS simulation to a METIS simulation. The “PDF output” button creates a PDF report document containing all the 0D viewgraphs of METIS.

6.2.3- Reference modification

Each reference can be edited with the help of a dedicated interface (figure 14). This interface allows to add, suppress or modify any point of the curves with the mouse.

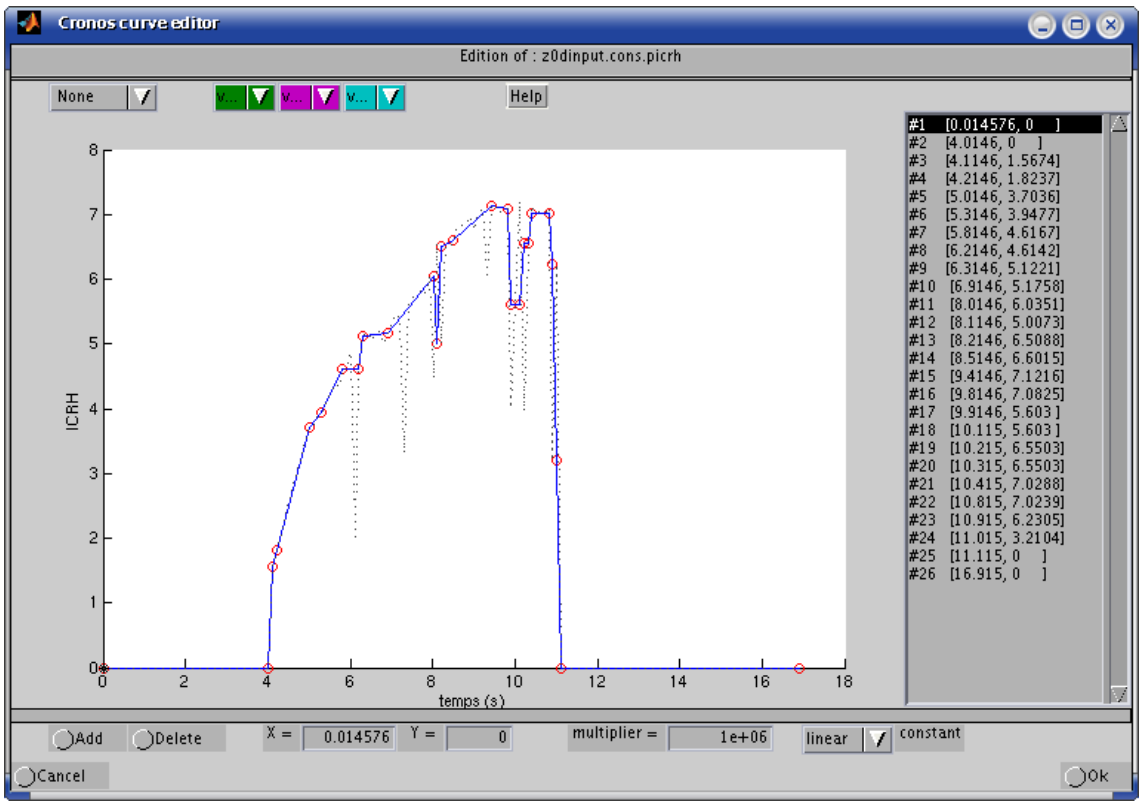

figure 14: example of GUI for reference edition.

The references to be edited are:

- "Ip" : plasma current reference (in A).
- "Flux" : edge poloidal flux (Wb)
- "Nbar" : line-averaged electron density (m^{-3}).
- "Zeff" : line-averaged effective charge.
- "xece" : position of the maximum power depostion for ECRH.
- "b0" : toroidal magnetic field (measured at "R0", in T).
- "iso" : ratio between tritium and deuterium densities.
- "ECRH" : power injected in the plasma by the electron cyclotron resonance heating system (W).
- "ICRH" : power injected in the plasma by the ion cyclotron resonance heating system (W).
- "LH" : power injected in the plasma by the lower hybrid electron heating system (W).
- "NBI" : power injected in the plasma by the neutral beam injection system (W).
- "Hmore" : improvement factor with respect to the selected scaling law.
- "FT_NBI" : ratio between tritium and deuterium fluxes in the injected neutral beam.

- “R0” : major radius of the plasma (m).
- “z0” : vertical position of the plasma (m).
- “a” : minor radius of the plasma (m).
- “K” : elongation of the plasma (ratio between the two axes of the ellipse).
- “d” : mean value of the upper and the lower triangularity of the plasma ($d = \frac{(R_{sepa}(Z = max(Z)) + R_{sepa}(Z = min(Z)) - 2R_0)}{2a}$).

6.2.4- Last closed magnetic surface creation

The button “Separatrix” allows to create an “ITER-like” last closed magnetic surface (LCMS) using an analytical formulation (figure 15) *[J Johner, private communication]*. This LCMS is given by a set of points. In this case, the moments (R0,a,K,d) are not used. A new edition of one of these moments erases the LCMS given by points .

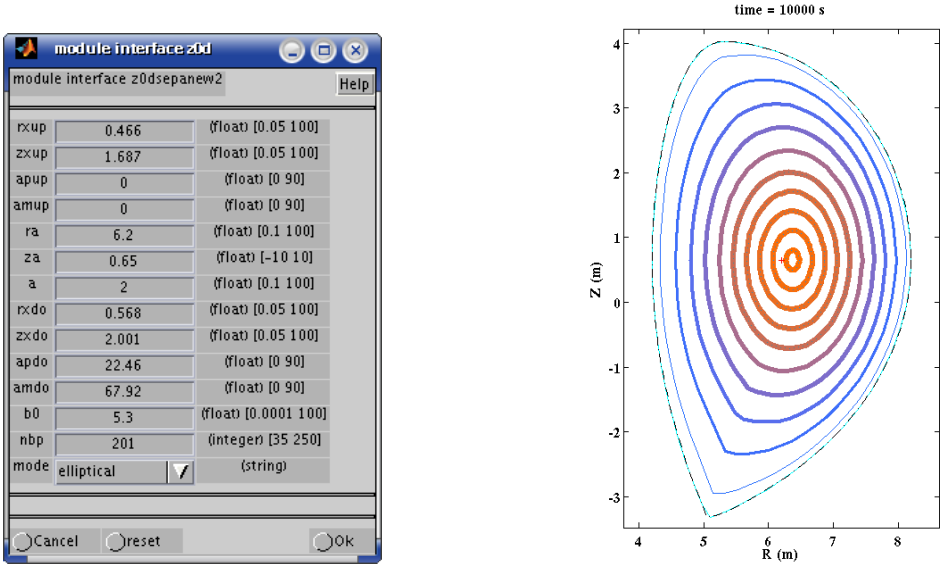

figure 15: GUI for separatrix parameters edition and results.

- rxup: upper triangularity (in minor radius unit), X point distance from magnetic axis
- zxup: upper elevation of the X point (in minor radius unit)
- apup: upper separatrix angle (R,X) (LFS, degrees)
- amup: upper separatrix angle (-R,X) (HFS, degrees)
- ra: major radius (m)
- za: elevation of the plasma (m)
- a: minor radius (m)
- rxdo: lower triangularity (minor radius unit), X point distance from magnetic axis
- zxdo: lower elevation X point (minor radius unit)
- apdo: lower separatrix angle (R,X) (LFS, degrees)
- amdo: lower separatrix angle (-R,X) (HFS, degrees)
- b0: maximal toroidal magnetic field on the conductor (T)
- delta: minimal distance between conductor and plasma (m)
- nbp : number of points for the separatrix (depends on the equilibrium module)
- mode: nature of the magnetic surface (*elliptical*, ellipse + hyperbola, hyperbola + ellipse, 2 semi-ellipses).

For more details on the LCMF generator, see technical documentation of the Helios code *[J. Johner, private communication]*.

6.3- Computation

In METIS, 3 modes of computation are implemented :

- the standard computation mode (button "Compute METIS simulation") : in this case the calculation is performed on the entire time base.
- the fast computation mode (button "Fast METIS simulation computation") : in this case the calculation is performed on a sub-sampling data set to ensure a smaller computation time (a function extracts the significant time steps of the shot).
- The fit computation mode (button "Fit of LH efficiency") : in this case the same calculation as in the standard mode is performed, but the lower hybrid current drive efficiency is chosen to fix the poloidal flux consumption. Moreover, the energy content is chosen in order to fit the measured one.

Furthermore, another computation mode is available : the evolution mode that allows to include METIS in a time loop (i.e. in a Simulink computation). The interface is the function "zerodevolution.m". Is this case METIS uses 4 time slices to allow accurate time derivative computations (at $[t_{k-2}, t_{k-1}, t_k, t_k+\tau_E]$) and only the 2 last time slices are computed ($[t_k, t_k+\tau_E]$) since the 2 previous ($[t_{k-2}, t_{k-1}]$) are already computed.

6.3.1- Information displayed during the run

During the run, for each convergence loop a dot is written on the screen. Other symbols give some information on convergences :

- B : toroidal flux inconsistency or bad value in B_{ref}
- E : non convergence of heat transport solver for some time slices
- I : $I_P > 2 I_{P,ref}$ in mode V_{loop} given or 0
- M : plasma separatrix shape incompatible with equilibrium
- S : ODE integration problem for computation of supra-thermal ions energy
- ! : solver switch to implicit mode at one time slice
- x : non-convergence in current diffusion solver at one time slice
- X : major convergence problem in current diffusion solver
- # : decrease of step change in fit algorithm
- ^ : increase of LH efficiency
- v : decrease of LH efficiency
- @ : METIS initialisation phase
- ~ : slow convergence, convergence is forced.
- E INIT -> : mode evolution, initialisation phase
- E x.yz -> : mode evolution (x.yz is the final time in s)

- R : time regression during evolution with Simulink
- Z : replay same time slice during evolution with Simulink

Symbols that are associated with a convergence problem may appear during first convergence loops, but not at the end of the run. If the non-convergence symbols persist during the whole evolution, the result must be analysed carefully in order to understand the nature of the problem.

6.4- Standard METIS viewgraphs

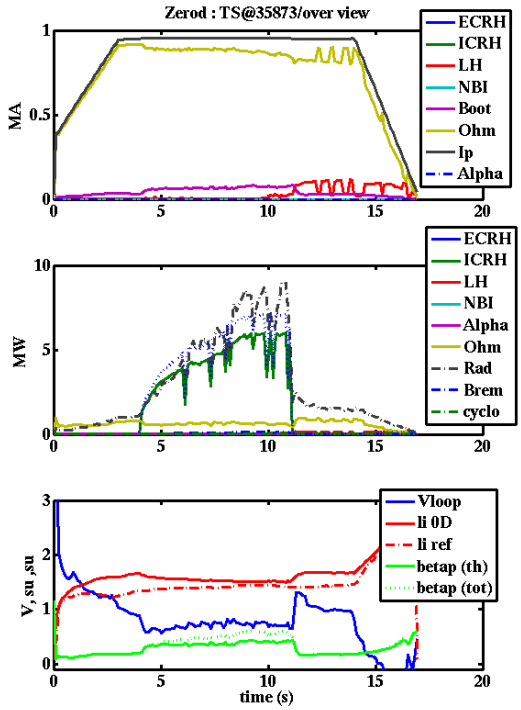

figure 16 : example of standard viewgraph ; here is the "overview" graph.

- "Power" : plots of 0D power sources and comparison with CRONOS or experimental data.
- "Energy" : plots of 0D energy contents and comparison with CRONOS or experimental data.
- "Confinement" : plots of 0D confinement times and comparison with CRONOS or experimental data.
- "Temperature" : plots of 0D temperatures and comparison with CRONOS or experimental data.
- "Density" : plots of 0D densities and comparison with CRONOS or experimental data.
- "Cost" : compute the electric power provided by a reactor, the cost of the reactor and the electricity.
- "Current" : plots of 0D current sources and comparison with CRONOS or experimental data.
- "Equilibrium" : plots of 0D equilibrium and comparison with CRONOS or experimental data.

- "LH efficiency" : plots of 0D LH current drive efficiency and poloidal flux consumption, and comparison with CRONOS or experimental data.
- "Geometry" : plots of 0D geometry moments, volume, surfaces and comparison with CRONOS or experimental data.
- "Convergence" : plots convergence indicator of METIS.
- "Ne Profile" : For a Tore Supra shot, plot of the density profile and comparison with measurements; plot of the cold neutral source and associated transport diffusivity and pinch.
- "neutron DD" : plots the neutron flux and central ion temperature and comparison with experimental data (this graph works only for Tore Supra and JET shots).
- "Er" : plots a coarse estimation of radial electric field and of the toroidal rotation.
- "DDS TS": viewgraph reserved for Tore Supra shots; it plots the central temperature (ECE) and the central safety factor to compare the time at which sawteeth appear and the time where q = 1 is predicted to be in the plasma.
- "Overview" : plots an Overview and the scenario of the shot (time history).
- "Profiles" : plots the main profiles used in METIS.
- "2D equilibrium" : plots the 2D flux surface equilibrium as used in METIS.

Some other viewgraphs are available from the Matlab command line :

- "z0plotnbi" : compare METIS sources for neutral beam injection to PENCIL prediction (for JET only)
- "z0plotshine" : plots time evolution of the Neutral Beam shinethrough.

6.5- METIS parameters

The METIS code is fully configurable with the keys available in the graphical interface (figure17). Hereafter, the keys are grouped by subject.

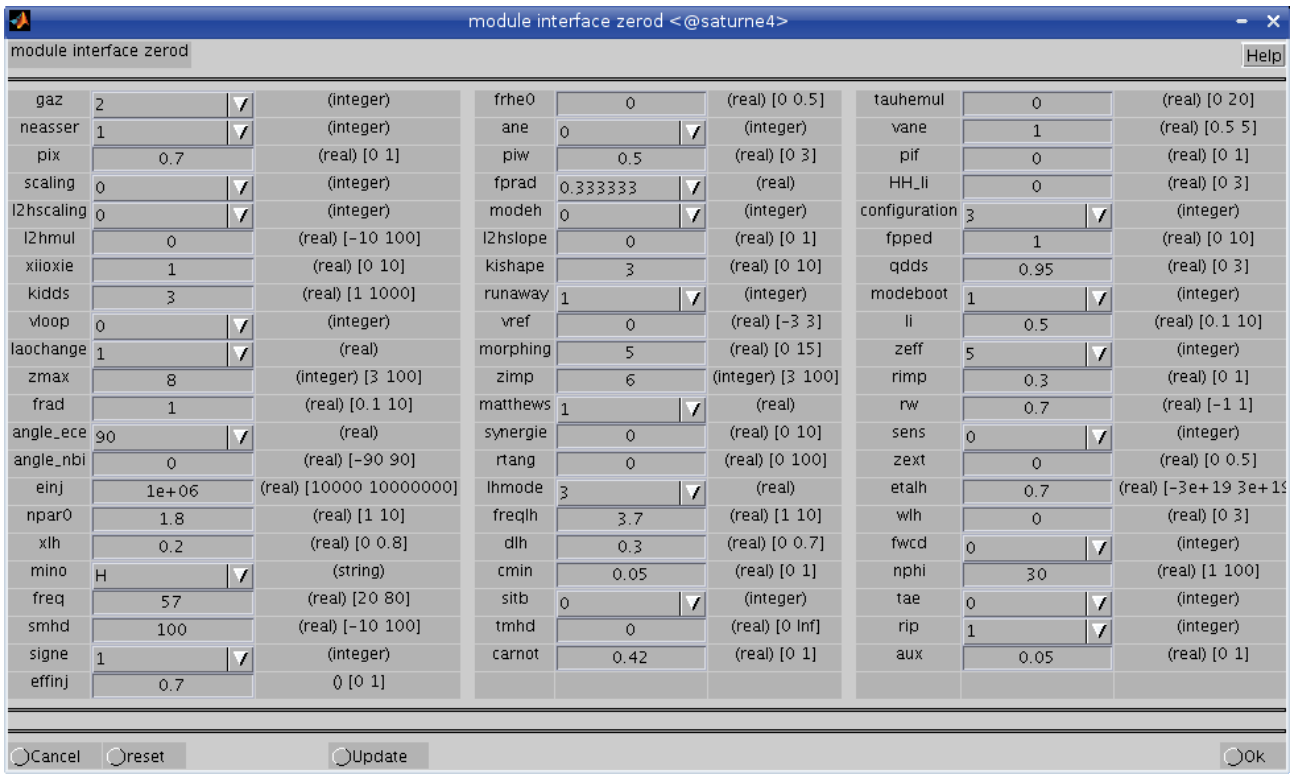

figure 17: METIS parameters graphical user interface window

6.5.1- Plasma composition:

- "gas" : this key allows to choose the main plasma composition. The valid values are :

Key value	*Description*
1	main plasma ion is hydrogen
2	main plasma ion is deuterium
3	burning deuterium and tritium plasma
4	main plasma ion is helium

- "zimp" : atomic charge number of "light" plasma impurity
- "zmax" : atomic charge number of "heavy" impurity, used to compute radiative power in Matthews scaling law
-

- “rimp” : ratio between densities of heavy impurity (zmax) and density of light impurity (zmin)
- “zeff “ : choice of the method to handle and compute the profile of effective charge. In all the cases, the value of the computed profile is the value without the helium ashes coming from DT fusion reactions. This contribution is added to the Zeff profile after having computed Zeff without ashes, but the contribution of helium is taken into account in the calculation of the impurity accumulation.

Key value	***Description of the method***
0	Zeff is given by the reference name “zeff” and the profile is flat
1	The profile is computed taking into account the neoclassical impurity accumulation (of charge zmax) and the line-averaged value is renormalized on the reference name Z_{eff}
2	The profile is computed taking into account the neoclassical impurity accumulation (of charge zmax) and the line-averaged value is renormalized to retrieve the scaling law for carbon main impurity.
3	The profile is computed taking into account the neoclassical impurity accumulation (of charge zmax) and the line-averaged value is renormalized to retrieve the scaling law for beryllium main impurity.
4	The profile is computed taking into account the neoclassical impurity accumulation (of charge zmax) and the line-averaged value is renormalized to retrieve the scaling law for tungsten main impurity.
5	Z_{eff} is given by the Tore Supra scaling law *[Devynck]* and the profile is flat.

Remark : the scaling laws for Z_{eff} may change between various METIS implementation.

- “frhe0” : ratio of helium ions density over electrons density that is injected into the plasma and that does not come from ashes of DT fusion reactions.

6.5.2- Plasma confinement :

- “scaling” : this key allows to select the two scaling laws used for the simulation. Depending of the choice, a scaling law gives the thermal energy content of the plasma in L-mode and the second one in H-mode or,alternatively, the first one gives the thermal energy content of the core plasma and the second one the thermal energy content of the pedestal. A special value allows to fit experimental measurements.

Key value	***description***
0	ITERL-96P(th) & ITERH-98P(y,2)
1	OH scaling *[Lukash, Bracco]* with soft transition to ITERL-96P(th) or ITERH-98P(y,2)
2	2 terms ITPA recommendation *[McDonald]*

Key value	*description*
3	2 terms, no beta dependence *[Petty, Joffrin1]*
4	Fit of the experimental measurements
5	EIV ITPA *[McDonald]*
6	OH (Wesson) with soft transition to ITERL-96P(th) or ITERH-98P(y,2)

- "modeh" : this key authorizes or forbids the transition from L mode to H mode during the simulation.

Key value	*description*
0	forbids L to H mode transition
1	authorizes L to H mode transition
2	forces H mode

- "configuration" : this allows to choose the configuration of the plasma between limiter and divertor in L and H mode

Key value	*L mode configuration*	*H mode configuration*
0	poloidal limiter	poloidal limiter
1	toroidal limiter	toroidal limiter
2	poloidal limiter	divertor with one X point
3	toroidal limiter	divertor with one X point
4	divertor with one X point	divertor with one X point

- "l2hscaling" : this key allows to select the scaling law used during the simulation to compute the power threshold for the L to H mode transition.

Key value	*description*
0	LH99(1)
1	LH2002 *[Ryter]*
2	LH2002 with Zeff effect *[Takizuka]*

- "l2hmul" : this key authorizes to add an offset to the power threshold for the L to H mode transition computed with the scaling law. The value is in MW. This feature is used to reproduce the experimental transition with better accuracy.
- "l2hslope" : if is not 0, allows a soft transition from L to H confinement . The transition is complete when the difference between the power crossing the separatrix and the threshold is above or equal to l2hslope * $P_{threshold}$.

- "fpped" : this is a multiplier of the pedestal pressure (~ energy content). The pedestal pressure is deduced from the difference between H mode and L mode energy content (given by scaling laws) when it is not given directly by a pedestal scaling law. The pedestal pressure is limited by MHD phenomena and by some experimental limitation (pedestal maximal energy content is between 1/4 and 2/3 of thermal energy content *[Maggi]*). if fpped is equal to 0, then the pedestal pressure has exactly the value given by the scaling law.
- "tauhemul" : this key is the ratio between the effective helium confinement time and the energy confinement time. If this key is set to 0, a scaling law is used *[ITER4]*.
- "taurotmul": this key is the ratio between the toroidal momentum confinement time and the energy confinement time. By default, its value is set to 0.3.
- "fprad" : this key selects the method used to compute the loss power that is used in the scaling law.

Key Value	***description***
0	No line radiation power is subtracted from the calculation of P_{loss}
1/3	1/3 of line radiation power is subtracted from the calculation of P_{loss}
2/3	2/3 of line radiation power is subtracted from the calculation of P_{loss}
1	line radiation power is subtracted from the calculation of P_{loss}

- "rip" : This key turns on or off the magnetic ripple contribution to the power losses computation (for the Tore Supra tokamak). The calculation uses a scaling law (deduced from measurements) to compute the power lost in the ripple by the ICRH heating (in minority scheme) and by the Lower Hybrid heating. These losses are subtracted from the additional power and by this way from the loss power.

Key Value	***description***
0	Ripple effect is not computed
1	Ripple effect is taken into account

- "HH_li" : if not equal to 0, the plasma energy content is corrected using the normalised internal inductance variation : $W = W_{sc}(\frac{l_i}{l_{i,0}})^{\frac{2}{3}}$ where $l_{i,0}$ is the value of internal inductance for which the plasma energy content is the one given by the scaling law [Peeters].

6.5.3- Electron density shape and evolution

- "ane" : this key allows to choose the law that gives the electron density peaking factor (see

description of electron density profile in the text, the peaking factor is defined as the ratio between the central value and the volume-averaged one).

Key value	***description***
0	The peaking factor varies like $1+0.5\frac{n_{sat}}{\bar{n}}$ in L mode *[Weisen1-Weisen3]* and $1+0.23\frac{n_{Greenwald}}{\bar{n}}$ in H mode *[Borrass]*.
1	The electron density profile is flat (i.e., the peaking factor is 1).
2	The peaking factor is a linear function of the internal inductance (li), in other words of the safety factor *[Weisen1-Weisen3]*.
3	The peaking factor is a linear function of the effective collisionality in H mode and is a linear function of the internal inductance in L mode *[Weisen1-Weisen3]*. if the key "modeh" is set to 0, the peaking factor is a linear function of the effective collisionality in L mode.
4	The peaking factor is given as a parameter.

- "vane" : this key gives the value of the peaking factor of the electron density profile when the key ane is set to 4.
- "neasser": this key selects the mode of evolution of the electron density.

Key value	***description***
0	The electron line density is equal to the reference "nbar" at any time
1	The electron line-averaged density is computed with a 0-D evolution equation ($\frac{d\bar{n}}{dt}=\frac{-\bar{n}}{\tau_n}+\frac{\bar{n}_{reference}}{\tau_n}+\frac{S_{nbi}}{V_{plasma}}$), using the particle confinement time ($\tau_n=2\tau_E$ in METIS).
2	Same as case 1, but a control on radiative power is added. The density is controlled to limit the radiative fraction to 0.8.

- "pix" : position of maximum of pellet deposition profile (su, [0,1])
- "piw" : width of pellet deposition profile (gaussian, su)
- "pif" : fraction of fuelling due to pellet injection

6.5.4- Temperature profile shape

The METIS code solves the stationary heat transport equation. Main effects on temperature profiles come from the shape of the heat sources and sinks and from the ratio T_i over T_e, owing to equipartition. Furthermore, the shape of the transport coefficients can change details of the profiles.

- "xiioxie" : this key tunes the ratio of ion over electron heat diffusivity. The value, usually, is in the interval 0.5 to 2. If this key is set to 0, METIS computes this ratio with the help of ITG/TEM fluid stability analysis *[Asp1, Asp2]*.
- "kishape" : this key allows to change the shape of the heat diffusivity ($\kappa_{e,i} \propto (1 + \kappa_{shape} x^2)$). If this key is set to 0, the shape is given by the shear function ($f(s, \alpha)$).

6.5.5- Current diffusion

- "vloop" : this key allows to choose the edge condition of the poloidal flux diffusion equation.

Key value	***description***
0	The plasma current follows the current reference "Ip"
1	The edge poloidal flux is constant (Vloop =0 and the plasma current is free)
2	The edge time derivative of the poloidal flux is constant (Vloop = given value and the plasma current is free)
3	The edge poloidal flux is constant (Vloop =0) and the lower hybrid current drive power is adjusted in order to keep the plasma current at the reference value.
4	The edge poloidal flux is prescribed

- "vref" : this key gives the value below which the control on loop voltage is turned on (case of control at Vloop = 0) and gives the value of loop voltage when this value is fixed.

- "breakdown" : electric field at the break-down time in unit of Dreicer electric field; tune the shape of runaway source and the value of Vloop at the first time step

- "runaway" : this key turns on or off the computation of the runaway electron current when the parallel electric field is near the runaway creation threshold. This mechanism tends to limit the parallel electric field and can be seen as a modification of the plasma resistivity.

Key value	***description***
0	The runaway electron current is set to 0
1	The runaway electron current is computed

- "modeboot" : this key is used to choose the law that gives the total bootstrap current. The shape of the bootstrap current density is always given by the Sauter law *[Sauter]*.

Key value	***description***
0	The total bootstrap current is normalised to Hoang's scaling law *[Hoang1]*

Key value	*description*
1	The bootstrap current is given by the Sauter formula without re-normalization

- "li" : this key gives the value of internal inductance at the first time of the simulation. It is used to compute the initial plasma current profile.
- "laochange" : this key turns on or off the internal coordinate change between Lao coordinate and toroidal flux coordinate for current diffusion. This coordinate change can be turned off for circular tokamaks at low β in order to accelerate the computation.

Key value	*description*
0	turn off coordinate change
1	turn on coordinate change (default value, always valid)

- "morphing" : exponent of morphing curve for the matching of the separatrix. If = 0, the morphing function is not used.

6.5.6- MHD effects

- "sitb" : This key allows to take into account the effect on energy confinement of the magnetic shear, of the normalised pressure gradient and of the enhancement of confinement with majority ion heating ("hot ion mode"). The effect of rational surfaces with negative shear can also be simulated.

Key value	*description*
0	No effect taken into account
1	The effect of $f(s,\alpha)$ is taken into account
2	As option 1, but additionally the enhancement of confinement with majority ion heating ("hot ion mode") is taken into account
3	As option 2, but additionally the effect of rational surfaces with negative shear is simulated.

- "smhd" : this key allows to limit the normalised pressure β_N . The limit can be either a multiple of internal inductance l_i or an absolute level.

Key value	*description*
> 0	Limit fixed at this value, expressed in %. A great value is equivalent to have no limit.
0	Standard limit at $4 l_i$
< 0	Limit fixed at $\|\text{value}\| * l_i$

- "tmhd" : this key gives the time (in s) at which the β_N limitation is turned on.
- "tae" : this key allows to turn on the effects of TAE on fast alpha deposition. A broadening of the profile is computed to ensure to be below the instabilities threshold.

Key value	*description*
0	The TAE effects are not taken into account
1	The TAE effects are taken into account

- "qdds" : this allow to simulate the mean effect, in time, of the sawteeth on the current diffusion. This key gives the value of the safety profile below which the safety factor is clamped at the "qdds" value.
- "kidds" : this key allows to simulate the flattening of temperature profiles in the area where the safety factor profile is clamped. This key is a multiplier of the transport coefficient.

6.5.7- Radiative power

- "rw" : this key gives the effective wall reflection coefficient of the cyclotron radiation. The value must be between 0 and 1.
- "frad" : This key is a multiplicative constant applied to the line radiated power .
- "matthews" : this key allow to choose how the total line radiative losses are computed. The shape of the line radiation is always computed with the help of the Post radiative coefficients *[Matthews97, Matthews99].*

Key value	*description*
0	The line radiative power is computed with the help of the Post radiative coefficients.
1	The line radiative power is computed with the help of the Post radiative coefficients and renormalized on the Matthews scaling law.

6.5.8- ICRH and FWCD

- "fwcd" : this key selects the heating scheme.

Key value	*description*
-1	Fast wave counter current drive
0	Minority heating scheme
1	Fast wave current drive
2	Fast wave electron heating

- "cmin" : this key gives the ratio between minority species density and the main ion plasma density. In the case of DT plasma, if the minority is tritium, the ratio is given by the reference name "iso" time the value of the key "cmin"; otherwise it is the ratio of minority density over the sum of deuterium and tritium density. The value of this key is taken into account for the calculation of the plasma composition and is used to compute the supra-thermal ions pressure in the case of minority heating. If this key is set to 0, the computation of the supra-thermal ions pressure is bypassed (for ICRH).
- "mino" : this key selects the minority species.

Key value	*description*
H	first harmonic hydrogen minority scheme
He3	first harmonic He3 minority scheme
He4	first harmonic He4 minority scheme
T	second harmonic tritium minority scheme

- "freq" : this key gives the central frequency (in MHz) of ICRH waves. This parameter is used to compute the position of the ICRH resonance.
- "nphi" : this key gives the main toroidal number of ICRH waves. This parameter is used to compute the width of the ICRH power deposition.

6.5.9- ECRH and ECCD

- "angle_ece" : this key gives the location, in poloidal angle, of the ECCD power deposition. The angle is given in degrees (0° for the low field side, 90° for the plasma center and 180° for the high field side) .
- "synergie" : this key is used to tune the synergy effect between lower hybrid current drive and the electron cyclotron current drive. When this key is set to 1, there no effect. If this key is set to 0, the synergy is computed on the basis of formula given in section 3.5.7.
- "sens" : this key selects the heating scheme.

Key value	*description*
-1	Electron cyclotron counter current drive
0	Electron cyclotron heating
1	Electron cyclotron co-current drive

6.5.10- NBCD

- "angle_nbi" : this key gives the effective angle, in degrees, between neutral beam and the poloidal plane at the tangent point. The value must be positive for co-current drive and negative for counter-current drive. A zero value corresponds to perpendicular injection without any direct current drive.
- "einj" : this key fixes the energy of neutral beam injection for monoatomic neutrals. The energy is given in eV. The composition of the injected beam in DT plasma is assumed to be deuterium and tritium (the ratio is given by the reference "ftnbi"). The injected species is assumed to be deuterium in a deuterium plasma and to be hydrogen in helium and hydrogen plasmas.
- "rtang" : this key allows to choose the radius (in m) where the beam is tangent to the flux surface. This key is not used in perpendicular injection. If the key is set to 0, the program computes R_{tan} using "angle_nbi" between toroidal direction and beam at plasma edge.
- "zext" : vertical shift of the beam in normalized coordinate.

6.5.11- LHCD

- "lhmode" : this key allows to choose the scaling law used to compute the lower hybrid current drive efficiency. The effect of parallel electric field is added to the direct lower hybrid current drive by computing the hot resistivity.

Key value	***description***
0	If the LH shape deposition is computed (wlh key >0) , efficiency is computed with a "Fisch" like law, otherwise with the ITER physics basis like scaling $\eta_{LH}=\frac{2.4\,10^{20}}{Z_{eff}+5}\tanh(\frac{T_e[eV]}{6\,10^3})$
1	Computed to fit experimental poloidal flux consumption
2	Given value
3	Goniche's scaling law depending of energy confinement time
4	SimulTS scaling (used for "CIMES" project design on Tore Supra)

- "etalh" : this key gives, when the "lhmode" key is set to 2, the lower hybrid current drive efficiency (in A/W/m^2) ,otherwise, the launcher directivity. The launcher directivity is used in the scaling law.
- "xlh" : this key fixes the center of the Gaussian describing the lower hybrid deposition, when the deposition is given by a Gaussian. The value is expressed in normalized square root of the toroidal flux.
- "dlh": this key gives the width of the Gaussian describing the lower hybrid deposition, when the deposition is given by a Gaussian. The value is expressed in normalized square root of the toroidal flux. If this key is set to 0 , for Tore Supra use, the deposition is taken proportional to the hard X-ray profiles.
- "wlh" : when this key is strictly positive, the deposition profile is computed with the help of

the propagation diagram. In this case wlh is the toroidal width of the active part of the launcher (0.352 m for Tore Supra and JET, and 0.539 m for ITER).

- "npar0" : this key gives the parallel indices of the maximum of the positive part of the launched spectra.
- "freqlh" : this key fixes the frequency (in GHz) of the lower hybrid wave.

6.5.12- Device configuration

- "signe" : sign of toroidal magnetic field, defined as $sign(\vec{B}_\phi . \vec{J}_\phi)$
- "machine" : normalised name of the device (not editable from GUI , set at initialisation)

6.5.13- Reactor performance

- "carnot" : thermodynamic duty for power plant heat to electricity efficiency conversion.
- "aux" : fraction of electric power produced by the reactor which is recirculated in auxiliary systems (cooler, pumping, magnet, ...)
- "effinj" : efficiency of additional heating source (W of heating power in plasma by W of electric power used by the heating source)

7- METIS Evolution & Simulink

“Simulink® is an environment for multidomain simulation and Model-Based Design for dynamic and embedded systems. It provides an interactive graphical environment and a customizable set of block libraries that let you design, simulate, implement, and test a variety of time-varying systems, including communications, controls, signal processing, video processing, and image processing” [Simulink1].

METIS can be used together with SIMULINK. This allows to test various controllers. The controllers are implemented in SIMULINK and METIS simulates the plasma response.

The link between METIS and Simulink is provided by a S-function [Simulink2] that calls the METIS evolution interface “zerodevolution.m” (figure 18). An example of S-function is “simmetis.m”. The S-function is used in METIS through the model “interface_simmetis.mdl”, a component of “library_simmetis.mdl”. This S-function can be tested with “flux_control_example.mdl” that implements a simple controller for the poloidal edge flux. “Simmetis” uses a standard METIS data set stored in the workspace of Matlab, in such a way that the METIS parameters and references can be handled directly from the METIS interface. At the end of the simulation, results can be plotted using the standard METIS tools.

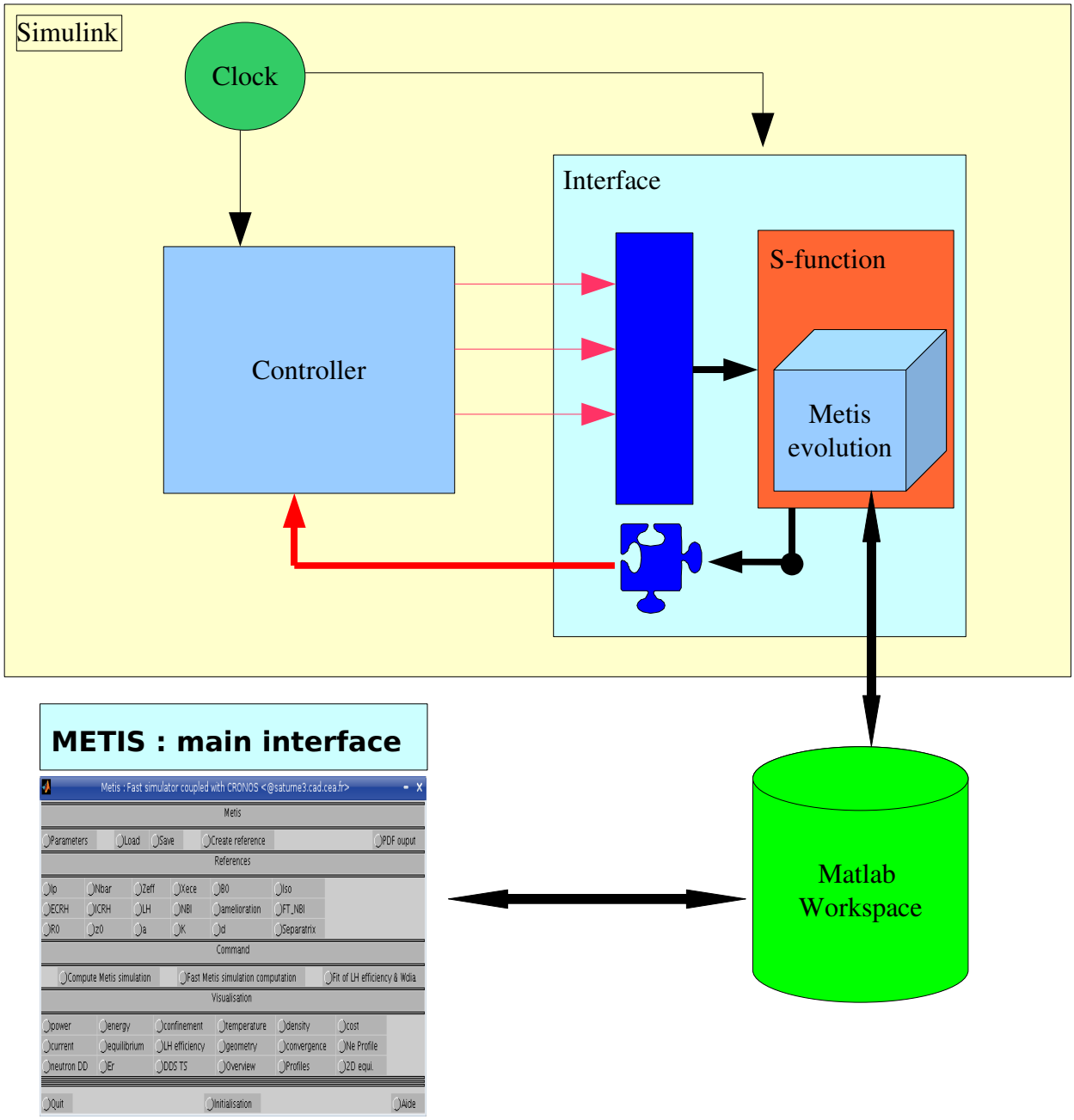

figure 18 : Principle of link between METIS and Simulink

When the METIS data set is saved, the Simulink system is saved in the same file. When a METIS data set is loaded, if METIS had be used in connection with Simulink, the system is re-opened. When the “simmetis” function is called at the initialisation the Simulink, system is saved.

The figures 19 gives an example of METIS and Simulink coupling.

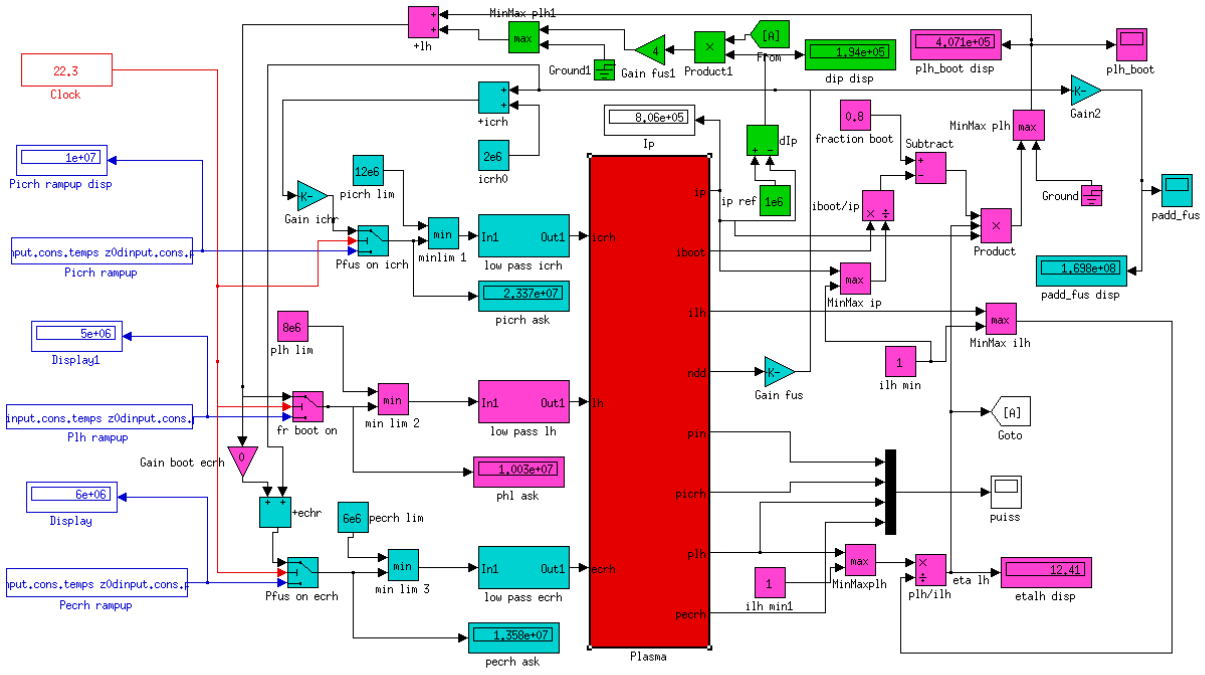

figure 19 : example of coupling between METIS and Simulink.

8- METIS data set

8.1- Introduction

The METIS data set is composed of two Matlab structures, containing the input and the output data, respectively (plus a copy of the parameters used for the simulation)

The input data structure is called “z0dinput”. It is composed of several sub-structures :

- z0dinput.option: this substructure contains METIS scalar parameters.
- z0dinput.info : this substructure contains METIS scalar parameters descriptions.
- z0dinput.zsinfo : this substructure contains METIS 0D data descriptions.
- z0dinput.profinfo : this substructure contains METIS profile descriptions.
- z0dinput.exp0d : this substructure contains 0D data coming from measurements or from a CRONOS data set. These data are used in viewgraphs for comparison with METIS results.
- z0dinput.cons: this substructure contains references for the simulation.
- z0dinput.geo: this substructure contains the geometrical parameters of the plasma and the vacuum magnetic field.
- z0dinput.machine: this field contains the name of the tokamak .
- z0dinputshot: this field contains the shot number in the case of real shot simulation .

When METIS is used with Simulink, the substructure z0dinput.system contains the name of the Simulink system, the location of the .mdl file and the XML structure describing the system. Additionally, the z0dinput structure used for the simulation is duplicated (to keep in memory initial values of references; the new ones contain the value computed by controllers).

Other data in “z0dinput” structure are reserved for program internal use.

The output data are stored in substructures of the CRONOS data structure “post”:

- post.z0dinput : this is a copy of the input structure, made after the METIS run (that splits data between “edition” data and simulation data).
- post.zerod : this substructure contains the 0D, time-dependent data of METIS
- post.profil0d : this substructure contains the profile data of METIS

Remark : the time base of the data stored in “post.zerod” is not the same as the time base of profiles stored in “post.profil0d”.

8.2- METIS 0D data description

The data stored in the “post.zerod” substructure are :

- RR : plasma resistivity (Ω)
- aitb : effect of ITB on temperature peaking factor
- ane : exponent of electron density profile ($\frac{n_{e0}}{\langle n_e \rangle} = 1 + a_{ne}$)

- ape : exponent of electron pressure profile ($\frac{P_{e0}}{\langle P_e \rangle} = 1 + a_{pe}$)
- asser : if = 1, feedback on V_{loop} is turned on
- ate : exponent of electron temperature profile ($\frac{T_{e0}}{\langle T_e \rangle} = 1 + a_{Te}$)
- betan : normalized total beta of the plasma
- betap : poloidal normalized pressure of the plasma (thermal)
- betaptot : poloidal normalized pressure of the plasma (total)
- d0 : central value of Shafranov shift (m)
- diboot : relative error on Iboot, at the end of convergence
- difcurconv : current diffusion solver convergence state (solver converges if greater than 0)
- dini : relative error on Ini, at the end of convergence
- disrup : if =1, radiative disruption flag
- dlh : LH deposition width
- dpfus : relative error on pfus, at the end of convergence
- drmdt : time derivative of the average minor radius rm (m/s)
- dw : relative error on w, at the end of convergence
- dwbpdt : time derivative of plasma stored poloidal energy (W)
- dwdt : time derivative of total plasma energy (W)
- dwthdt : time derivative of thermal plasma energy (W)
- ecrit_he : alpha critical energy (eV)
- ecrit_icrh : critical energy for ICRH (eV)
- ecrit_nbi : critical energy for NBI (eV)
- efficiency: Lower Hybrid current drive efficiency from Fisch's theory (A/W/m2)
- einj_icrh : mean energy of fast ion produced by ICRH in minority scheme (eV)
- einj_lh : mean LH electron energy, only defined if rip = 1 (eV)
- esup_fus : D-T fusion fast alpha supra-thermal energy (J)
- esup_icrh : ICRH fast ions supra-thermal energy (J)
- esup_lh : LH fast ions supra-thermal energy (J)
- esup_nbi : NBI fast ions supra-thermal energy (J)
- etalh : LH current drive efficiency (A /W/m^2)
- etalh0 : LH current drive efficiency @ vloop = 0 (A /W/m^2)
- etalh1 : LH current drive efficiency correction due to hot conductivity (A/W/m^2)

- fracmino: minority fraction accelerated by ICRH ($\frac{\langle n_{mino} \rangle}{\langle n_e \rangle}$)
- frloss_icrh : fraction of ICRH power lost due to fast ions losses
- frnbi : fraction of NBI absorbed in the plasma
- fwcorr : internal reserved data
- hitb : improvement factor of energy content due to ITB
- hmhd : deterioration factor of energy content due to MHD (β_N limit)
- iboot : bootstrap current (A)
- icd : total current driven (A)
- ieccd : ECCD driven current (A)
- ifus : fast alpha (fusion) bootstrap current (A)
- ifwcd : FWCD driven current (A)
- ilh : LH driven current (A)
- inbicd : NBI driven current (A)
- ini : total non-inductive current (A)
- iohm : ohmic current (A)
- ip : plasma current in toroidal direction (A)
- ipar : plasma current // B (A)
- irun: runaway electron current (A)
- j0fus : data reserved to an internal use
- jxfus : data reserved to an internal use
- li : internal self inductance (formula 3 of ITER FDR)
- meff : effective mass (number of atomic mass, HDT ions)
- modeh : confinement mode versus time: 0 = L et 1 = H
- mu0_nbi: initial value of pitch angle for NBI ($\frac{v_{//}}{v}$)
- n0a : number of cold neutrals entering the plasma at the edge every second (coming from recycling and gas puff, s^{-1})
- n1m : volume-averaged density of H + D + T ions (m^{-3})
- nDm : volume-averaged density of deuterium ions (m^{-3})
- nTm : volume-averaged density of tritium ions (m^{-3})
- nb : number of convergence loops carried out
- nbar : line-averaged electron density (m^{-2})
- ndd: total DD neutrons per second (s^{-1})
- ndd_nbi_nbi: beam/beam DD neutrons per second (s-1)

- ndd_nbi_th: beam/plasma DD neutrons per second (s-1)
- ndd_th: plasma/plasma thermal DD neutrons (s-1)
- ne0 : central electron density (m-3)
- nebord : plasma edge electron density (m^{-3})
- negr : Greenwald limit density (m^{-3})
- nelim : plasma electron density near the divertor (m^{-3})
- nem : volume-averaged electron density (m^{-3})
- nhem : volume-averaged helium density(m^{-3})
- ni0 : central ion density (m^{-3})
- nim : sum of volume averaged ion densities (m^{-3})
- nimpm : volume-averaged density of impurities (other than helium, m^{-3})
- nsat : saturation electron density, used for the calculation of the density peaking factor (m^{-3})
- pbrem : Bremsstrahlung radiation losses (W)
- pcyclo : cyclotron radiation losses (W)
- pddfus: fusion power from DD reactions (W)
- peakdiv: divertor peak power density estimate (W/m^2)
- pecrh : ECRH power (W)
- pei : equipartition power (W)
- pel : total thermal electron power deposition, used in the calculation of T_i/T_e (W)
- pel_fus : Alpha power deposited on electrons (W)
- pel_icrh : ICRH power deposited on electrons (W)
- pel_nbi : NBI power deposited on electrons (W)
- pelec: reactor electric power provided to the network (W)
- peri : length of the LCMS (m)
- pfus : total D-T fusion power carried by alpha particles (W)
- pfus_loss : fast alpha power losses due to first-orbit losses (estimate, W)
- pfus_nbi : NBI induced D-T fusion power (W)
- pfus_th : thermal power deposition of fast alpha particles (W)
- picrh : ICRH power, decreased of ripple losses in the case of Tore Supra shot simulation (W)
- picrh_th : ICRH thermal power deposition (W)
- pin : total additional heating power (W)
- pion : total thermal ion power deposition, used in the calculation of T_i/T_e (W)

- pion_fus : Alpha power deposited on ions (W)
- pion_icrh : ICRH power deposited on ions (W)
- pion_nbi : NBI power deposited on ions (W)
- pioniz: power losses due to cold neutral ionization(W)
- piqj: peaking factor of current profile
- piqnbi : peaking factor of the NBI power deposition profile
- plh : LH power, decreased of ripple losses in the case of Tore Supra shot simulation (W)
- plh_th : LH thermal power deposition (W)
- plhrip : Lower Hybrid power loss due to ripple for Tore Supra (W)
- plhthr : flux power at the LCMS; must be compared with L->H threshold power
- plim: divertor power flux estimate (W)
- ploss : plasma loss power, as defined in ITER Physics Basis (W)
- plossl2h : switch-on power for transition from L mode to H mode (W)
- pnbi : NBI heating power (W)
- pnbi_th : NBI thermal power deposition (W)
- pohm : ohmic power (W)
- pped : pressure at the top of pedestal (Pa)
- ppedmax: maximum allowed total pressure at the pedestal top (Pa)
- prad: impurity radiation losses, without Bremsstrahlung (W)
- pradsol: radiation losses in the SOL (W)
- priptherm : Tore Supra ripple losses, thermal part (W)
- pth : thermal input power, defined as tau_L * Pth = Wth (W)
- pw : effective power, define as taue * pw = W (W)
- q0 : estimate of central value of the safety factor
- q95 : safety factor @ 95% of poloidal flux
- qa : edge safety factor
- qeff : effective safety factor at the edge (computed with ITER formula given section 3.20.1)
- qmin : estimate of minimal value of the safety factor
- rm: average minor radius : sqrt(PHI/pi/B0) of LCMS (m)
- rres: radial position of the ICRF resonance layer (m)
- salpha : total number of alpha particles produced by D-T reactions per second (s-1)
- sext : external plasma surface (m^2)
- sp : poloidal section plasma surface (m^2)

- stf : number of wrong data in zs containing NaN or Imag
- taue : energy confinement time (s)
- tauee : electron energy confinement time (s)
- tauei : electron/ion heat exchange time (s)
- tauh : energy confinement time in H mode (s)
- tauhe : confinement time of helium ashes (s)
- tauhe_h : confinement time of helium ashes in H mode (s)
- tauhe_l : confinement time of helium ashes in L mode (s)
- tauii :ion energy confinement time (s)
- tauip : characteristic time of current decrease in term of R/L (s)
- tauj : characteristic diffusion time of current ($\tau_j = \mu_0 .* \rho_{max}^2 \frac{\int_0^{\rho_{max}} \frac{S'}{\eta} d\rho}{\int_0^{\rho_{max}} S' d\rho}$,s)
- taus_he : characteristic slowing down time for fast alpha particles (s)
- taus_icrh : characteristic slowing down time for ICRH fast ions (s)
- taus_nbi : characteristic slowing down time for NBI fast ions (s)
- tauthl : energy confinement time in L mode
- te0 : central electron temperature (eV)
- tebord : plasma edge electron temperature (eV)
- telim : plasma electron temperature near the divertor (eV)
- tem : volume-averaged electron temperature (eV)
- temps : time base vector
- tite : volume-averaged ratio T_i / T_e
- vloop : loop voltage at the edge of the plasma (V)
- vmes: loop voltage as measured on a fixed magnetic loop (V)
- vp : plasma volume (m^3)
- w : total plasma energy (J)
- wbp : poloidal magnetic field energy stored in the plasma (J)
- wdia: 3/2 perpendicular plasma energy (J)
- wrad : estimate of volume-averaged toroidal rotation velocity of the bulk plasma (rad/s)
- wrlw : plasma energy from RLW scaling law (J)
- wth : thermal plasma energy (J)

- xeccd : ECCD maximum deposition location
- xfus : fast alpha maximum deposition location
- xitb : radius of ITB (estimate)
- xlh : LH maximum deposition location
- xnbi : NBI maximum deposition location
- xpoint : flag set to 1 if the plasma is diverted (used to compute edge values)
- xres : ICRF resonance layer normalized radius location
- zeff : plasma effective charge with helium ashes
- zeffsc : zeff value, as given by the scaling law
- zmszl : ratio between volume-averaged zeff and line-averaged zeff

8.3- METIS profiles description

The data stored in the "post.profil0d" substructure are :

- C2 : C2 geometrical coefficient (see CRONOS technical document)
- C3 : C3 geometrical coefficient (see CRONOS technical document)
- Raxe : major radius of the centre of each flux surface (m)
- Rsepa : radial coordinate of the LCMS points (m)
- Zsepa : vertical coordinate of the LCMS points (m)
- bpol : averaged poloidal magnetic field (T)
- dn : density diffusivity estimate (m^2/s)
- dphidx: toroidal flux space derivative ($\frac{d\Phi}{dx}$,Wb)
- dpsidt : time derivative of poloidal flux (V)
- dx: flux surface geometrical triangularity
- ej: ohmic power density (W/m^3)
- epar : parallel electric field (V/m)
- epsi : inverse aspect ratio ($\frac{a_{ref}\,x}{R_{axe}(x)}$, m)
- er : neoclassical radial electric field (, V/m)
- eta : neoclassical resistivity (Ω m)
- fdia : diamagnetic function (Tm)
- fprad : line radiative power shape; reserved to an internal use only
- ftrap : effective trapped electron fraction profile
- ge : electron flux ($m^{-2}s^{-1}$)
- grho : $\langle|\nabla\rho|\rangle$ (see CRONOS technical document)

- grho2 : $\langle |\nabla \rho|^2 \rangle$ (see CRONOS technical document)
- grho2r2 : $\langle \frac{|\nabla \rho|^2}{R^2} \rangle$ (see CRONOS technical document)
- jboot : bootstrap current density (A/m^2)
- jeccd : parallel current density source due to ECCD ($j_{ECCD} = \frac{\langle \boldsymbol{J}_{\boldsymbol{ECCD}} . \boldsymbol{B} \rangle}{B_{ref}}$, A/m^2)
- jeff: $j = \frac{\langle \boldsymbol{J} . \boldsymbol{B} \rangle}{B_{ref}}$ (A/m^2)
- jfus : fast alpha bootstrap current density (A/m^2)
- jfusshape : alpha particles bootstrap current density shape; reserved to an internal use only
- jfwcd : parallel current density source due to FWCD ($j_{FWCD} = \frac{\langle \boldsymbol{J}_{\boldsymbol{FWCD}} . \boldsymbol{B} \rangle}{B_{ref}}$, A/m^2)
- jlh : parallel current density source due to LHCD ($j_{LH} = \frac{\langle \boldsymbol{J}_{\boldsymbol{LH}} . \boldsymbol{B} \rangle}{B_{ref}}$, A/m^2)
- jli : average current density, equivalent at jmoy in CRONOS (A/m^2)
- jnbicd : parallel current density source due to NBICD ($j_{NBICD} = \frac{\langle \boldsymbol{J}_{\boldsymbol{NBICD}} . \boldsymbol{B} \rangle}{B_{ref}}$, A/m^2)
- jnbishape : NBICD current density shape; reserved to an internal use only
- jni : total current density source (A/m^2)
- jrun : runaway current density (A/m^2)
- kx : flux surface elongation s
- n0 : neutral density coming from the edge, hot neutrals (m^{-3})
- n0m: neutral density coming from edge, cold neutrals (m^{-3})
- n1p : density of HDT ions (m^{-3})
- nbishape_el : NBI power deposition on electron profile; reserved to an internal use only
- nbishape_ion : NBI power deposition on ion profile; reserved to an internal use only
- nep : electron density (m^{-3})
- nhep : density of helium (m^{-3})
- nip : ion density (m^{-3})
- nzp : density of main impurity (m^{-3})
- omega : toroidal plasma rotation frequency ($\frac{\sum_{k \in \{species\}} n_k m_k \langle V_{\phi,k} R \rangle}{\sum_{k \in \{species\}} n_k m_k}$,rad/s)
- palf : alpha power source (W/m^{-3})
- pbrem : profile of bremsstrahlung radiation power losses source (W/m^3)

- pcyclo : cyclotron radiation power source (W/m^3)
- pecrh : power density due to ECRH (W/m^3)
- pfus : power density due to fusion reactions (W/m^3)
- pfus_ion : power density due to fusion reactions, coupled to ions (W/m^3)
- pfweh : power density due to FWEH (W/m^3)
- phi : toroidal flux (Wb)
- picrh : power density due to ICRH minority heating (W/m^3)
- picrh_ion : power density due to ICRH minority heating, coupled to ions (W/m^3)
- pioniz : loss power due to cold neutral ionization (W m-3)
- pitch : pitch angle profile for NBI (cos(beam,B))
- plh : power density due to LH (W/m3)
- pnbi : power density due to NBI (W/m^3)
- pnbi_ion : power density due to NBI, coupled to ions (W/m^3)
- pohm : ohmic power deposition (W/m^3)
- prad : radiated power sink (W/m^3)
- psi : poloidal flux (Wb)
- ptot : total pressure profile (Pa)
- qjli : safety factor
- r2i : $\left\langle \frac{1}{R^2} \right\rangle$ (see CRONOS technical document)
- ri : $\left\langle \frac{1}{R} \right\rangle$ (see CRONOS technical document)
- rmx : averaged radius of each flux surface ($\sqrt{\frac{\Phi}{\pi B_0}}$,m)
- s0 : ionisation sources coming from edge, hot neutrals ($m^{-3}\,s^{-1}$)
- s0m : ionisation sources coming from edge, cold neutrals ($m^{-3}\,s^{-1}$)
- salf : alpha particle source (m^{-3})
- source_el : total heating power density coupled to electrons (W/m^3)
- source_ion : total heating power density coupled to ions (W/m^3)
- spellet : equivalent continuous particle source due to pellet injection (m^{-3}/s)
- spr : surface element (m^2, int(spr,x= 0..1) = plasma poloidal section surface)
- temps : time vector associated to the profiles (only times, at which the profiles are computed, are stored)
- tep : electron temperature (eV)

- tip : ion temperature (eV)
- utheta : neoclassical poloidal rotation speed ($\frac{\langle V_{k,\theta} \rangle}{\langle B_p \rangle}$,m/s/T), for main impurity
- vn : anomalous particle convection velocity estimate (m^2/s)
- vpr : volume element (m^3, $\int_0^1 V' dx = \text{plasma volume}$)
- vpr_tor : volume element, reserved for internal use (m^2, $\rho_m \int_0^1 V'_{tor} dx = \text{plasma volume}$)
- vtheta : fluid velocity, theta component , at R = Rmax of each flux surface, for main impurity (m/s)
- vtor : toroidal rotation speed , at R = Rmax of each flux surface, for main impurity (m/s)
- ware : Ware pinch estimate (m/s)
- xie : electron diffusivity estimate (m^2/s)
- xieshape : heat transport coefficient shape without ITB effect
- xieshape_itb : heat transport coefficient shape with ITB effect
- xii : ion diffusivity estimate (m^2/s)
- xli : radial normalized coordinate (as in CRONOS, square root of toroidal flux, normalized to 1 at the edge).
- zeff : effective charge number

9- METIS main files description :

1. calibreifus.m: this file is used to calibrate the 0D formula giving the fast alpha “bootstrap” current with the help of SPOT simulations
2. close_0plot.m: close all the METIS figures
3. demo0d.m: script used to call METIS for some DEMO simulations
4. ermax.m: this function computes the threshold value of the parallel electric field above which runaway electrons are created.
5. formene.m : this function computes the shape of the density profile in H mode
6. FT3_metis.m : script for FT3 simulations
7. gg0d.m: this function computes the geometrical coefficients as V', using the separatrix description, the Shafranov shift profile and the elongation profile.
8. iter_rampup_lh.m : script for ITER ramp-up simulation with LH
9. iter_rampup.m : script for ITER ramp-up simulation
10. iter_rampup_sunhee.m : script for ITER ramp-up simulation compatible with DINA simulation
11. JTC_SU0d.m : script for JTC simulation
12. lit_profne.m : function used to read and use measured electron density (for TS only)
13. piqpe.m : computed transport coefficient shape taking into account ITB.
14. scenarzerodfci.m: this function computes the most probable scheme for ICRH (minority, FWEH, ...) with the help of input parameters.
15. sigmavnbitplasmad.m : this function pre-computes the matrix “sigmav_nbi_t_plasma_d.mat” of fusion reactivity for a deuterium (or tritium) neutral beam and the bulk plasma.
16. sigmav_nbi_t_plasma_d.mat : matrix of reactivity for beam/plasma fusion reactions
17. sigmav_nbi_t_plasma_d_1000x100.mat : matrix of reactivity for beam/plasma fusion reactions
18. sigmav_nbi_t_plasma_d_1e6.mat : matrix of reactivity for beam/plasma fusion reactions
19. sigmavnbitplasmad.m : this function pre-computes the matrix
20. “sigmav_nbi_t_plasma_d.mat” of fusion reactivity for a tritium neutral beam and the bulk plasma.
21. svb2int.m: cross section for beam/plasma fusion reactions
22. z0beambeam.m : this function computes beam/beam interaction effects
23. z0csdd.m : fusion cross-sections and thermal reactivities DD
24. z0csdt.m: fusion cross-sections and thermal reactivities DD
25. z0csdt.m : auxiliary function used to compute the matrix of reactivity for beam/plasma fusion reactions
26. z0curdiff.m : fast solver for the complete current diffusion equation
27. z0dacces.m : this function creates a full CRONOS data set using the results of the METIS

simulator.

28. z0densview.m : this function plots density transport coefficients and sources (TS only)
29. z0dfitlheta.m : this script performs the fit of LH current drive efficiency in order to reproduce experimental poloidal flux consumption.
30. z0dhelena.m : this script is used to benchmark the results of the analytical equilibrium of METIS against the complete and precise results of the Helena equilibrium solver. Additionally, this script benchmarks the Sauter law results against Nclass results.
31. z0dmovie.m : this script makes a 2 D movie of a poloidal section of the plasma. Ten flux surfaces are drawn with a code of colour.
32. z0dnanimag.m: function used to detect NaN of Inf in METIS results.
33. z0dprofinfo.m : this function returns the description of every profile data.
34. z0dsepanew2.m: function computing an analytical separatrix using the method of J. Johner
35. z0dtsneutron.m: this script draws a graph allowing to compare the experimental neutron flux and the central ion temperature to the METIS results for Tore Supra.
36. z0dtsticxs.m : this script plots METIS results versus Ticxs measurements (TS only)
37. z0dxdt.m : time derivative operator with second order continuity prolongation .
38. z0ex.m : this function extracts mean weighting value from a signal.
39. z0expote.m : this function computes exponents used in the Albajar cyclotron radiation scaling.
40. z0icrh.m: this function computes the heat source for ICRH in the minority scheme at the first harmonic.
41. z0irun.m : this function computes runaway electron current with the help of model detailed section 3.12 .
42. z0j3.m: this function gives the profile of fast alpha bootstrap current with the help of a parametric formulation.
43. z0lhacc2lobes.m : this function calls z0lhacc for the positive and negative part of LH spectrum.
44. z0lhacc.m: this function computes the lower hybrid deposition with the help of the propagation diagrams in the plan ($r,n_{//}$).
45. z0loglin.m : function that commutes plots from lin/lin to lin/log representation.
46. z0maxpped.m : function that computes the maximum pressure at the top of the pedestal with the help of a simplified expression of the ballooning limit.
47. z0morph.m : this function computes the morphing function to transform geometry coefficient from moment representation to real geometry .
48. z0nbi_fvmu.m : analytical distribution function for NBI.
49. z0nbipath.m : this function computes the path of the center of the neutral beam and deduces the heat deposition profile.
50. z0nbistop.m : this function computes the Janev stopping cross section for NBI
51. z0nbistoptot.m : this function computes the total stopping cross section for NBI
52. z0nbistopfast.m: this function computes the increment of stopping cross section due to fast

ions for NBI

53. z0neutron_dd.m : function computing the neutron flux due to DD reactions.
54. z0neutron_profil.m : this function computes a rough estimate of neutron DD shape
55. z0ode.m : this function implements a fast algorithm for solving on discrete times the equation $\frac{du}{dt} = \frac{-u}{\tau(t)} + S(t)$ where $\tau(t) \in \tau_k$ and $S(t) \in S_k$ for $t \in t_k$.
56. z0piqpe.m : this function computes the improvement factor due to ITB. This function solves the stationary heat transport equation with and without ITB mechanism.
57. z0plotc.m : this function plots the graphs of different quantities related to confinement.
58. z0plotconv.m: this function plots the graphs related to the convergence of METIS.
59. z0plotctrl.m : script for scaling law benchmark between METIS and CRONOS
60. z0plotdds.m: this function plots the graphs related to the sawteeth for Tore Supra.
61. z0plote.m: this function plots the graphs related to energy contents.
62. z0ploteq.m: this function plots the graphs related to MHD equilibrium.
63. z0ploter.m: this function plots the graphs related to radial electric field.
64. z0plot_FT3.m : script to plot FT3 simulations.
65. z0plotgeo.m: this function plots the graphs related to the last closed magnetic surface geometry.
66. z0plotj.m: this function plots the graphs related to the plasma current and current sources.
67. z0plot_JTC_SU.m : script to plot JT60_SA specific simulations results about neutron rates.
68. z0plotlh.m: this function plots the graphs related to lower hybrid current drive.
69. z0plotn.m: this function plots the graphs related to densities.
70. z0plotnbi.m : compare METIS NBI profiles and Pencil output for JET
71. z0plotp.m: this function plots the graphs related to power sources an sinks.
72. z0plotsc.m: this function plots the scenario of the simulated shot
73. z0plotshine.m : this function plots the NBI shinethrough time evolution
74. z0plott.m: this function plots the graphs related to temperatures.
75. z0profne.m : computes n_e profile , associated sources and transport coefficients.
76. z0profview.m: this function plots the main profiles used in METIS.
77. z0qp.m : this function computes an analytical shape for the safety factor, it is used for initialisation.
78. z0rapport.m : this function makes a PDF document with all the possible graphs of METIS
79. z0rot2.m : this function computes the toroidal rotation of the plasma induced by neutral beam injection, pressure, ICRH, LH and ripple. The associated radial electric field is also estimated.
80. z0rot3.m : simplified version of z0rot2 used in the public version of METIS. This version included only completely documented effects.
81. z0sectionh.m : cross-sections for H ionisation, charge exchange and recombination.

82. z0separatrix.m: this function handles the graphical interface and the calculations for the last closed magnetic surface.
83. z0signbi.m : this function computes the effective cross-section for neutral beam injection.
84. z0yield.m : function that computes impurities source for Z_{eff} law.
85. z0zeff.m: this function computes the effective charge profile by taking into account the neoclassical impurity accumulation.
86. zboot0diff.m : this function computes the main equilibrium quantities, such as Shafranov shift profile and elongation profile; calls the function to compute the Zeff, the resistivity, the bootstrap current, the LH current source, the current diffusion, and the ITB function. This function manage also the loop voltage and the associated controls.
87. zbpi0.m: this function computes the fusion power and neutron source due neutral beam interaction with the plasma.
88. zcall0d_fct.m : this function implements the callback of the METIS graphical interface
89. zcall0d.m : this function generates the main graphical interface window of METIS
90. zclear0dsepa.m: this is an auxiliary function that is used to manage the LCMS mode.
91. zdwdt0.m: this is an auxiliary function that is used to compute $\frac{dW}{dt}$ terms.
92. zeqie0prof.m: This function solves the stationary heat transport equations for ions and electrons including the equipartition term. It includes a convergence loop to determine the value of the equipartition flux. As a result, this function gives the T_e an T_i profiles and the equivalent equipartition source.
93. zero1t.m: this function performs a computation of all scalars and profiles of METIS without convergence. This function performs most of initialisations of the scalars and values at the first call.
94. zerodevolution.m : call of zerod in evolution mode where time slices can be added.
95. zerodfast.m: this function extracts the significant time of the shot and makes a subsampling of the input data in order to decrease the computation time.
96. zerodghost.m : ghost version of zerod to test genetic algorithms.
97. zerod_init.m: this function creates the data set for the METIS code. The data source can be a CRONOS data set, the Tore Supra data base, the JET data base or any user-defined data set.
98. zerod.m: this function is the main function of the METIS code, called to compute the results. This function implements the convergence loop and the plasma controls.
99. zerod_scalaire.m: this function creates a METIS data set from scalar value references. It is useful to study a steady-state shot.
100. zeta0.m: this function computes the plasma resistivity using the Sauter model
101. zfract0.m: this function implements an analytical formula giving the fraction of power heating ions for NBI.
102. zfus0tae.m: this function computes the fusion power deposition coming from the bulk plasma reaction (DT and DD) and the reactions between neutral beam and thermal plasma.

Additionally, as an option, the function can broaden the deposition profile to ensure that the TAE are not triggered.

103. zgeo0.m: this function computes the LCMS from moments when it is not given by points. This function also computes the plasma volume, surface, ...

104. zicd0.m: this function computes the current drive sources for LH, FWCD, NBICD, ECCD.

105. zjrun.m: this function computes the runaway current shape (for parallel electric field near the threshold of the runaway creation)

106. znalpha0.m: this function computes the plasma content in alpha particles

107. znbi_dd.m : this function computes alpha power due to beam/plasma interaction

108. zrad0.m: this function computes the radiative sources. The line radiative power is computed with the help of the Post radiative rate and/or the Matthews scaling law. The bremsstrahlung contribution is computed for each species including the relativistic correction. The cyclotron radiation is computed with the help of the Albajar scaling law.

109. zripts0.m: this function computes the ripple losses for Tore Supra with the help of scaling laws coming from experiments.

110. zsauter0d.m: this function computes the bootstrap current density using the Sauter model.

111. zscale0.m: this function implements the scaling law that are used in METIS for energy, L to H threshold and for impurity confinement time.

112. zsupra0.m: this function computes the supra-thermal energy content for fast ions generated by heating or fusion reactions.

113. ztf0.m: auxiliary function used to compute alpha particles density.

114. ztokcost.m : this function computes the tokamak cost and the electricity price on the basis of ITER scaling.

115. zuiacces0d.m : graphical interface to create CRONOS input files from METIS results.

10- METIS Application Program Interface for Simulink

116. flux_control_example.mdl : simulink model example using simmetis “sfunction”.

117. interface_simmetis.mdl : standard interface between simmetis and Simulink

118. library_simmetis.mdl : library implemented standard interface between simmetis and simulink. When components are used, the link between library and model must be suppressed.

119. simmetis.m : “sfunction” interfacing METIS and Simulink

120. z0intw.m : special integrator for METIS evolution

121. zerodevolution.m : version “time dependent” of METIS that can be implemented in a time evolution loop and that is called by simmetis.

11- References

[Albajar01] F. Albajar et al, Improved calculation of synchrotron radiation losses in realistic tokamak plasmas, Nucl. Fus., **41**, 2001, p 665-678

[Albajar02] F. Albajar et al, Electron cyclotron radiative transfer in fusion plasma, Nucl. Fus., **42**, 2002, p 670-678

[Artaud] J-F Artaud et al, Code de transport CRONOS : Equations gouvernant la rotation toroïdale du plasma et le champ électrique radial , 2003 (PHY/NTT-2003.001,CEA/DSM/DRFC) (2003)

[Asp1] E. Asp et al, 12th International Congress on Plasma Physics, 2004

[Asp2] E. Asp et al, Plasma Physics and Controlled Fusion **47**, 2005, p 505-519

[Basiuk03] V. Basiuk et al., Nucl. Fus., **43,**(2003), p 822-

[Basiuk04] V. Basiuk et al, Nucl. Fus. **55**, 2004, p 181-192

[Becker] G. Becker, Nucl. Fus. **30**, 1990, p 2285

[Beckurts] K. Beckurts et K. Wirtz , Neutron Physics, Springer-Verlay,1964

[Blank1] H.J. de Blank, plasma equilibrium in tokamaks, lecture note @ www.rijnh.nl

[Blank2] H.J. de Blank, Transactions of Fusion Science and Technology **49**, 2006, p 111-117

[Borrass] K. Borrass et al., Nucl. Fus. **44**, 2004, p 752

[Bosch] H.-S. Bosch and G.M. Hale , Nuclear Fusion, 32 , 1992, p 611-631

[Boucher] D. Boucher, CR Academie des Sciences, Tome 315, Serie 2, **9** 273, 1992

[Bracco] G. Bracco and K. Thomsen, Nuclear Fusion **37**,1997, p 759-

[Bush] C.E. Bush, Plasma Physics and Controlled Fusion 36, 1994, pp A153-A158

[Cohen] S.A. Cohen et al, Plasma Physics and Controlled Fusion **29** ,1987, p 1205-1217

[Cordey] J.G Cordey et al, Journal of Computational Physics, **28**, 1978, p 115-121

[CRONOS] CRONOS User's Guide, F. Imbeaux, V. Basiuk, J.F. Artaud, M. Schneider, 2006 (PHY/NTT-2006.002,CEA/DSM/DRFC)

[Devynck] P. Devynck, Influence of a boronisation on the radiated power and the effective charge on Tore Supra, 2007 (PHY/NTT-2007.012,CEA/DSM/DRFC)

[Dolan] T. J. Dolan, Fusion Research, **1**, Pergamon Press, 1980, p 29-

[Ejima] S. Ejima et al, Nuclear Fusion **22**, 1982, p1313-1319

[Erents1] S.K. Erents et al, Nuclear Fusion **40**, 2000, p 295-308

[Erents2] S.K. Erents et al, Nuclear Fusion **28**, 1988, p 1209

[Eriksson01] L-G Eriksson and F. Porcelli, Plasma Phys. Control. Fusion **43,** 2001, p R145–R182

[Eriksson93] L.G. Eriksson et al, Nucl. Fus. **33**,1993, p 1037-1048

[Eriksson03] L.G. Eriksson et al, Bulk plasma rotation in the presence of waves in the ion cyclotron range of frequencies, 15th Topical Conference on Radio Frequency Power in Plasmas, 2003

[Feng] Y. Feng et al, Comp. Phys. **88**, 1995, pp 161-172

[Fenzi] C. Fenzi et al ,Effect of Toroidal Rotation Generated by ICRF Waves on Core Energy Confinement, 31st EPS Conference on Controlled Fusion and Plasma Physics, 2004

[Fish] N.J Fish, Physical Review Letters **43,**1978, p 873-877

[Fonck] R. J. Fonck et al, Physical Review Letters **63**,1989, p 520-523

[Fu] G.Y. Fu Physics of Fluids B **1**,1989, p 1949-1952

[Garbet1] X. Garbet et al, Plasma Physics and Controlled Fusion 46, 2004, p B557-B574

[Garbet2] X. Garbet et al, Nuclear Fusion **43**, 2003, p 975-981

[Giruzzi87] G. Giruzzi, Nucl. Fus. **27**, 1987, p 1934-
and G. Giruzzi, private communication

[Giruzzi97] G. Giruzzi et al, Nuclear Fusion **37,**1997 ,p 673-680

[Giruzzi04] G. Giruzzi et al, Physical Review Letters **93**, 2004 , p. 255002-1 - 255002-4

[Goniche] M. Goniche et al, Lower Hybrid current drive efficiency on Tore Supra and JET, Sixteenth Topical Conference on Radio Frequency Power in Plasmas, 2005

[Helander1] P. Helander and D. J. Sigmar, Collisional transport in magnetized plasma, Cambridge university press, 2002, p 93.

[Helander2] P. Helander and D. J. Sigmar, Collisional transport in magnetized plasma, Cambridge university press, 2002, chapter 13.

[Hertout] P. Hertout, ALGORITHM FOR COST EVALUATION OF TOKAMAKS WITH COPPER OR SUPERCONDUCTING MAGNETS, private communication.

[Hoang1] G.T Hoang et al, 24th European Physical Society Conference on Plasma Physics,1997

[Hoang2] G.T. Hoang et al., Phys. Rev. Lett. **93**, 2004, p 135003-1 - 135003-4

[Huysmans1] G.T.A. Huysmans et al, CP90 Conference on Comp. Physics, World Scientific Publ. Co. 1991, p 371-

[Huysmans2] G.T.A. Huysmans et al, Physical Review Letters **87**, 2001, p 245002-1 - 245002-4

[Isichenko] M.B. Isichenko et al, Phys. Rev. Lett. **74,** 1996, p 4436-

[ITER1] ITER, Physics Guidelines, N 19 FDR 1 011-07-13 R 0.1, p 7-14

[ITER2] ITER, Physics Guidelines, N 19 FDR 1 011-07-13 R 0.1, annexe A1

[ITER3] ITER, Physics Guidelines, N 19 FDR 1 011-07-13 R 0.1, p 19

[ITER4] ITER,physics basis, Nuclear Fusion **39,** 1999, p 2226

[ITER5] ITER,physics basis, Nuclear Fusion **39,** 1999, p 2512

[ITER6] ITER,physics basis, Nuclear Fusion **39,** 1999, p 2514-2515

[ITER7] ITER, Physics Guidelines, N 19 FDR 1 011-07-13 R 0.1, p 44

[Janev] R.K, Janev et al, Nuclear Fusion **29**,1989, p 2125-2140

[Jaspers] R. Jaspers, Nuclear Fusion **33**, 1993, p 1775-1785

[Jayakumar] R. Jayakumar et al, Physics letters A **172** ,1993, p 447-451

[Joffrin1] E. Joffrin et al, 20th IAEA Fusion Energy Conference, 2004

[Joffrin2] E. Joffrin et al, Nuclear Fusion **43**, 2003, p1167-1174

[Kim] S.H. Kim et al, 34th European Physical Society Conference on Plasma Physics,2007

[Krivenski] Krivenski et al, Nuclear Fusion 25, 1985, p 127-

[Kukushkin] A. S. Kukushkin et al, Nuclear Fusion **43**, 2003, p 716-723

[Lao1] L.L. Lao et al, Phys. of fluids **24** (8) 1981 ,p 1436-

[Lao2] L.L. Lao et al, Nuclear Fusion **25**, 1985 , p 1421-1436

[Laporte] *P. Laporte,* Modélisation et analyse du transport des particules dans un plasma de tokamak, Thèse Doctorat, Université Aix-Marseille I, 1996

[Lin1] Y. R. Lin-Liu and F. L. Hinton, Phys. Plasmas **4,** 1997, pp 4179-

[Lin2] Lin-Liu and Miller, Phys. of Plasmas **2,** 1995, p 1666-1668

[Litaudon1] X. Litaudon et al, Nuclear Fusion **47**, 2007, p1285-1292

[Litaudon2] X. Litaudon, Plasma Physics and Controlled Fusion **48**, 2006, p A1-A34

[Lloyd] B. Lloyd et al, Nuclear fusion **31**, 1991, p 2031-2053

[Lukash] V.Lukash et all , Plamsa devices and operations **13** , 2005, p 143-156

[Maget] P. Maget et al, Nuclear Fusion **39**, 1999, p 949-962

[Maggi] C. F. Maggi, Nuclear Fusion **47 ,** 2007, p 535-551

[Mahdavi] M. Mahdavi et al, Physics of plasmas 10 ,2003, p 3984-

[Manini] A. Manini et al, Nuclear Fusion **46**, 2006, p 1047-1053

[Matthews97] G-F Matthews et al , Journal of Nuclear Materials **241-243**, 1997, pp 450-455

[Matthews99] G-F Matthews et al , Nuclear Fusion **39**, 1999, p 27-

[McDonald] D.C. McDonald et al, Nuclear Fusion **47,**2007, p 147-173

[Meo] F. Meo et al, Comparison of FWCD scenarios on ASDEX-Upgrade, JET, and DIII-D Tokamaks, 14th Topical Conference on Radio Frequency Power in Plasmas, 2001

[Mikkelsen1] D.R. Mikkelsen, Nuclear Fusion **29**, 1989 ,p 1113- 1115

[Mikkelsen2] D.R. Mikkelsen, Physics of fluids B **1**,1989, p 333-339

[Mineev] A.B. Mineev et al, Physics Conference IEEE 2003, St. Petersburg, Russia

[Mohr] Peter J. Mohr et al, CODATA Recommended Values of the Fundamental Physical Constants: 2006, arXiv:0801.0028v1 [physics.atom-ph] and http://physics.nist.gov/cuu/Constants/

[Neudatchin] S.V. Neudatchin et al, Nuclear Fusion 44, 2004, p 945-953

[Okano] K.Okano, 28 EPS conference on controlled fusion and plasma physic, 2001

[Onjun] T. Onjun, Phys. Plasmas **9**, 2002, p 5018-

[Pacher] G.W. Pacher et al, Proc. 19th IAEA Fusion Energy Conf. ,Lyon, France, 2002

[Peeters] A. G. Peeters, Plasma Phys. Control. Fusion **42,** 2000, pp B231–B242

[Peres] A. J. PERES, J. Nucl. Mater. 50 , 1979, p 5569-

[Petty] Petty et al, Fus. Science tech. **43** ,2003 , p 1-

[Peysson] Y. Peysson and J. Decker, submitted to Computing Physics Communication

[Pinches] S.D. Pinches et al, Plasma Physics and Controlled Fusion 46, 2004, p B187-B200

[Porter] G. D. Porter et al J. Nucl. Mater **266-269**, 1999, p 917-

[Post] D. E. Post et al, Atomic data and nuclear tables **20**, 1977, pp 397-439

[Rice] J.E. Rice et al, Nucl. Fusion **47**,2007, p 1618–1624

[Rosenbluth1] N.M. Rosenbluth, Physics of Fluids B **4**,1992, p 2189-2202

[Rosenbluth2] M.N. Rosenbluth, Nuclear Fusion **37**, 1997, p 1355-

[Rozhansky] V. Rozhansky and M. Tendler, Plasma Rotation in Tokamaks, Reviews of Plasma Physics **19**,1996.

[Rybicki] G.B. Rybicki and A. P. Lightman, Wiley interscience publication, 1979, p 156-159

[Ryter] F. Ryter, Plasma Phys. and Controlled Fusion **44**, 2002, p A415 -

[Sabbagh] S.A. Sabbagh, Physics of Plasma **9**, 2002 ,p 2085-2092

[Sauter] O. Sauter et al, Phys. Plasmas **6,**1999, p 2834- and Phys. Plasmas **9,** 2002, p 5140- (Errata)

[Schneider] M. Schneider et al, Plasma Phys. and Controlled Fusion **47,** 2005, p 2087-2106

[Simulink1] **http://www.mathworks.com/products/simulink/**

[Simulink2] http://www.mathworks.com/access/helpdesk/help/toolbox/simulink/sfg/f6-633.html

[Stangeby] P. C. Stangeby, The Plasma Boundary of Magnetic Fusion Devices, Institute of Physics Publishing, 2000

[Stix] T.H. Stix, Nuclear Fusion **15**, 1975, p 737-

[Stott] P.E. Stott, Plasma. Physics and Controlled Fusion **47**, 2005, p1305-1338

[Takizuka] Takizuka,Plasma Phys. Control. Fusion **46,** 2004, p A227-A233

[Tsitrone] E. Tsitrone, Contrôle des flux de particules dans un Tokamak au moyen d'une structure à évents, Thèse Doctorat, Université Aix-Marseille I, 1995

[Vlad04] G. Vlad et al, Plasma Physics and Control Fusion, **46**, 2004, p S81-S93

[Vlad06] G. Vlad et al Nuclear Fusion **48**,2006, p 1-16

[Wagner] Wagner et al , Plasma physics and controlled fusion **35**, 1993, p 1321

[Waltz] R. E. Waltz et al , Physics of Plasma **4,** 1997, p 2482-2495

[Ware] A. A. Ware ,Phys. Rev. Lett. **25**, 1970, p 15 - 17

[Weiland] J. Weiland et al , 31st EPS conference on plasma phys., London

[Weisen1] H, Weisen et al, poster EX/P6-31, 20th IAEA FEC, Vilamoura, Portugal, 2004

[Weisen2] H, Weisen et al, Nucl. Fus. **45,** 2005 , p L1-L4

[Weisen3] H. Weisen, et al., Plasma Phys. Control. Fusion **46**, 2004, p B557-B574

[Wesson1] J. Wesson, Tokamak, 3rd edition, Clarendon University Press, 2004, p 181

[Wesson2] J. Wesson, Tokamak, 3rd edition, Clarendon University Press, 2004, p 124-133

[Wesson3] J. Wesson, Tokamak, 3rd edition, Clarendon University Press, 2004, p 290-299

[Wesson4] J. Wesson, Tokamak, 3rd edition, Clarendon University Press, 2004, p 249

[Wesson5] J. Wesson, Tokamak, 3rd edition, Clarendon University Press, 2004, p 402-406

[Wesson6] J. Wesson, Tokamak, 3rd edition, Clarendon University Press, 2004, p 246-253

[Wesson7] J. Wesson, Tokamak, 3rd edition, Clarendon University Press, 2004, p 182

[Wesson8] J. Wesson, Tokamak, 3rd edition, Clarendon University Press, 2004, p 737

[Wesson9] J. Wesson, Tokamak, 3rd edition, Clarendon University Press, 2004, p 106-121

[Wolle] B. Wolle, Physics Reports **312**, 1999 , p 1-86

[Zabiego] M. Zabiego et al, Plasma Physics and Controlled Fusion **43**, 2001 , p 1625-1639

[Zerlauth] P. Zerlauth et al, note interne DRFC n° 1278

12- Acknowledgements

I am thankful to V. Basiuk, L.-G. Eriksson, J. Decker, R. Dumont, G. Giruzzi, G.T. Hoang, Ph. Huynh, G.T.A. Huysmans, F. Imbeaux, E. Joffrin, X. Litaudon, Y. Peysson and M. Schneider for providing contributions, sound advice, and useful discussions during the METIS development.

I thank especially G. Giruzzi and M. Schneider with careful reading of this document.